Winter 2012

Eukaryotic Microbes in the Deep Sea: Abundance, Diversity, and the Effect of Pressure

Danielle Morgan-Smith
Old Dominion University

EUKARYOTIC MICROBES IN THE DEEP SEA: ABUNDANCE, DIVERSITY, AND THE EFFECT OF PRESSURE

by

Danielle Morgan-Smith
M.S. May 2008, Old Dominion University
B.S. December 2005, College of William and Mary

A Dissertation Submitted to the Faculty of
Old Dominion University in Partial Fulfillment of the
Requirements for the Degree of

DOCTOR OF PHILOSOPHY

OCEANOGRAPHY

OLD DOMINION UNIVERSITY
December 2012

Approved by:

Alexander B. Bochdansky (Director)

Fred C. Dobbs (Member)

Margaret R. Mulholland (Member)

David T. Gauthier (Member)

ABSTRACT

EUKARYOTIC MICROBES IN THE DEEP SEA: ABUNDANCE, DIVERSITY, AND THE EFFECT OF PRESSURE

Danielle Morgan-Smith
Old Dominion University, 2012
Director: Dr. Alexander B. Bochdansky

The dark ocean is vast, high in pressure, cold, and scarce in resources, but has been shown to support a diverse and active microbial community wherever it is studied. Such studies, however, are scarce due to the difficulty of sampling at such depths, and are difficult to interpret due to compounding effects of pressure and temperature on physiology. Protists, functionally defined as the microbial portion of the domain Eukarya, are particularly neglected in studies of deep-sea microbiology. Here, I present three studies on microbial eukaryotes in the deep sea: first, a study of the abundance of microbial eukaryotes in the deep sea, second, a quantitative approach to study broad-scale diversity in the deep sea; and last, a series of experiments to explore the effect of deep-sea conditions on surface-isolated flagellates. In the deep sea, I found that eukaryote abundances decrease much more sharply than prokaryote abundances with depth, though most of this decrease occurs in the upper 1000 m, below which eukaryote abundance is relatively constant. In water masses below 1000 m, 50-70% of total eukaryotes detected by CARD-FISH can be attributed to one of the seven groups (six taxonomic using CARD-FISH and one by morphology when stained with DAPI). In the epipelagic 100 m samples, only 20% of total eukaryotes fall into one of these groups. This difference is driven largely by the morphotype I call the "split nucleus", which does not decrease in absolute abundance with depth, instead increasing in its proportion of the eukaryotic

population in deeper waters. Lastly, I found that eukaryotic microbes, typified by two heterotrophic flagellate species which appear to be ubiquitous in the world's oceans, can survive and even grow despite long-term exposure to the cold, high-pressure conditions of the deep sea, indicating that protists transported to the deep sea by advection or on particles can seed populations there.

This dissertation is dedicated to Muffin.

ACKNOWLEDGMENTS

Special thanks to my labmates Melissa Clouse, Cody Garrison, and Bonnie Bailey, my collaborator Gerhard Herndl, my committee members, and especially my advisor Alexander Bochdansky for making this dissertation possible. I'd also like to thank my wonderful husband Aaron Smith, my family, the BORG ladies, and my awesome friends for keeping me sane through the process.

TABLE OF CONTENTS

Page

LIST OF TABLES

LIST OF FIGURES

CHAPTER 1
INTRODUCTION

1.1 The deep sea environment

The deep sea below 200 m is a vast habitat, representing 80% of the ocean's total volume. This biome never sees the light of the sun and the only autotrophic processes that are present are mediated by chemoautrotrophs. Because of the remoteness of the habitat and the technical difficulty surrounding high pressure sampling and incubations, this huge and ecologically important habitat has been studied little in comparison to the more accessible surface ocean. Of the relatively few studies on microbial ecology in the deep ocean, most use samples from regions of hydrothermal activity, ignoring the vast majority of the deep ocean which is uniformly cold. This dissertation focuses on describing the microbiology of the cold, deep ocean, a habitat both extreme in conditions and grand in scale.

Before I can discuss the environment of the deep sea, it is important to first define the term. For the purpose of this document, "deep sea" will generally be used to describe the meso-, bathy- , and abyssopelagic realms of the ocean where no light is available for photosynthesis, hydrostatic pressure requires special adaptations, temperature is uniformly low, and utilizable organic carbon is sparse. All of these abiotic factors are important in shaping the microbial landscape of the deep sea. A practical depth of 200 m can be considered as the shallowest extent of this region. While the mesopelagic environment to a depth of 1000 m has some residual downwelling light, it is insufficient for photosynthesis and can be used for vision only in some low-light adapted organisms.

Beyond the mesopelagic layer, a completely dark ocean expands to more than 10,000 m depth at Challenger Deep in the Mariana Trench.

The physical environment of the deep sea is dominated by the effect of hydrostatic pressure. With every 100 m of descent through the ocean, pressure increases by 1 MPa, so that all biota in the bathypelagic realm experience 10-50 MPa. The deepest abyss, the Marianas Trench is home to both microbial and macrofaunal communities, despite pressures up to 110 MPa. This pressure has many effects on living cells, from protein denaturation to membrane solidification (Bartlett, 2002), which in turn have spawned a variety of adaptations to make life possible in the deep sea. In addition to high pressure, low temperature causes biological processes to slow and causes its own set of stress responses in deep sea organisms. Most importantly, this environment is starved in organic nutrient supply (Arístegui et al., 2009, Nagata et al., 2010) and no degree of pressure and temperature adaptation can make up for this lack of an energy source for heterotrophs. For metazoans, many adaptations for this hydrostatic pressure stress have been described (reviewed by Macdonald, 1997, Sebert, 2002), but adaptations of marine eukaryotic microbes to this environment are largely unknown.

The global conveyor of thermohaline circulation, although too slow to have a strong physical effect on microbes, defines the chemistry of the deep sea. Deep water masses are old compared to shallower waters, meaning it has been longer since they equilibrated to the atmosphere and were inundated with sunlight. Due to microbial respiration, oxygen levels decrease and inorganic nutrient concentrations increase as a water mass ages. Most organic matter available in the deep sea comes from the surface ocean through a steady rain of particles, including marine snow, fecal pellets, and

aggregates of dead phytoplankton (Steinberg et al., 2008). These particles are very difficult to study directly, because most collection methods cause them to break apart and mix into the ambient water.

In combination, the constant flux of particles from the surface ocean into the deep sea and the exceptional spatial scale of this environment make it incredibly important in the global carbon cycle. Old water masses with sparse and refractory organic compounds are characteristic of the deep sea, making particles all the more essential to deep-sea microbiota as sources of carbon and sites of enhanced biological activity.

1.2 Deep-sea microbiology

Although the deep sea is much more sparsely inhabited than the surface ocean, it is home to a microbial community which is diverse both in terms of taxonomy and function. In sunlit epipelagic waters, each ml of seawater is typically home to 8×10^5 prokaryotes, 6×10^6 viruses, and 2×10^3 heterotrophic flagellates, while in the mesopelagic there are 2×10^5 prokaryotes, 1×10^6 viruses, and 1.4×10^2 heterotrophic flagellates, and in the bathypelagic 6×10^4 prokaryotes, 5×10^5 viruses, and 1.3×10^2 heterotrophic flagellates ml^{-1} (meta-analysis by Arístegui et al., 2009). Water sampled from 4000 m depth in the North Atlantic contains an average of 2×10^6 prokaryotes, 2×10^6 viruses, and 12 heterotrophic protists ml^{-1} (Parada et al., 2007, Morgan-Smith et al., 2011, section 2.3), indicating large differences in the deep-sea microbial community in different locations. With increasing depth, the makeup of the prokaryotic community also changes, shifting from bacterial dominance in surface water to a more even split between Bacteria and Archaea in the deep sea (Karner et al., 2001, Herndl et al., 2005), although Bacteria are

much more diverse than Archaea in deep water (López-Garcia et al., 2001b). Within the domain Bacteria, a shift also occurs, with gamma-proteobacteria abundance increasing with depth (López-Garcia 2001b), while the Bacteroidetes, abundant in surface waters, are largely absent from the dark ocean (Arístegui et al., 2009). Processes, though much harder to measure in the deep ocean than abundance or diversity, also exhibit changes between the surface and deep ocean. For example, prokaryotic secondary production is 136 μmol C m^{-3} d^{-1} in the epipelagic, but only 24.4 and 4.0 μmol C m^{-3} d^{-1} in the meso- and bathypelagic, respectively (Arístegui et al., 2010). Globally, 20 - 33 Pg C is respired annually in the dark ocean (Arístegui et al., 2003). One process of particular interest is prokaryote mortality, and in particular, whether there is a shift from the protist-controlled prokaryote populations of the surface ocean (Fenchel, 1986, Jürgens and Massana, 2008) to viral-controlled populations in deep water masses (Parada et al., 2007, Arístegui et al., 2009).

Recent reviews of dark ocean microbiology have compiled data from disparate studies to paint a picture of the deep sea that is much more complex than previously assumed, despite the uniformly cold, dark, resource-poor environment (Arístegui et al., 2009, Nagata et al., 2010). Prokaryote communities in the deep sea exhibit 30% less diversity than surface waters (Herndl et al., 2008, Hewson et al., 2006), although heterogeneity between stations exists even within the bathypelagic (Agogué et al., 2011, Hewson et al., 2006). Metabolic complexity is also a factor of deep-sea ecology, with one study finding *in situ* chemoautotrophy and particle-derived carbon supporting prokaryote populations at different depths within the mesopelagic (Hansman et al., 2009).

1.3 Particles in the deep sea

Particles, including fecal pellets, decaying phyto- and zooplankton, and amorphous aggregates such as marine snow, are of great importance in the ecology of the deep sea, serving a dual role as hot spots of biological activity in an environment defined by scarce resources, as well as a vehicle to constantly deliver organisms and organic matter from the productive sunlit waters above (Steinberg et al., 2008). These particles are formed in the upper 100 m of the water column, and decompose below about 100 m (Boyd 1999), sinking at rates of approximately 100 - 1000 m d^{-1} (Berelson et al., 2002, Ploug et al., 2008), with speed increasing as a particle loses organic carbon during its descent (Berelson et al., 2002). In addition, buoyant and suspended particles are also present in the deep ocean, where they may be responsible for "missing" respiration in carbon budget calculations (Baltar et al., 2009, Bochdansky et al., 2010). In the deep sea, respiration has been found to correlate with particulate, but not dissolved, organic material (Baltar et al., 2009). Further, oxygen consumption is correlated only with macroscopic, rather than microscopic particle abundance (Bochdansky et al., 2010). Marine particles are rapidly colonized with large numbers of organisms, hosting 10^6 - 10^7 bacteria per aggregate, sometimes an enrichment up to four orders of magnitude greater than the abundance in ambient water, though more often close to 100x (Caron et al., 1982, Simon et al., 2002, Alldredge et al., 1986, Turley and Mackie, 1994). Flagellates are similarly enriched on particles in the surface ocean or laboratory, with abundances ranging from similar to ambient water to 1000x as great, and absolute abundances of 10^3 per aggregate, or 10^4 - 10^6 ml^{-1} of aggregates (Simon et al., 2002, Herndl and Peduzzi,

1988, Turley and Mackie, 1994). The protozoan community is not only increased in number, but exhibits shifts in diversity between particles and the ambient water (Artolozaga et al., 2000, Simon et al., 2002). This community contains many active bacterivores, which can graze particle-affiliated bacteria at a rate great enough to balance growth (Ploug and Grossart, 2000), and some species may require particles for survival where bacterial abundance in the ambient water falls below feeding thresholds (Caron et al., 1982). Protist species are able to preferentially colonize particles or remain in the surrounding water, depending on their feeding preferences (Artolozaga et al., 2000). Free viruses, on the other hand, are not thought to be transported readily on particles, where extracellular enzymes decompose them quickly (Simon et al., 2002).

Particles are not rare features of the marine environment, with densities of several macroscopic (>500 μm) particles per liter of water, sufficient to account for much of the observed oxygen consumption in the deep ocean (Bochdansky et al., 2010). Because of that abundance, along with the great enrichment of microbes on particles versus in the ambient water, particle-affiliated protists may channel three orders of magnitude more energy to higher trophic levels than freely suspended protists (Artolozaga et al., 2002).

1.4 High pressure biology

To study the deep sea, understanding the effect of pressure on microbes is of utmost importance. Traditionally, pressure effects are researched using vessels which can be subjected to high pressure over some period of time, then depressurized to study the organisms inside (e.g., ZoBell, 1950, Jannasch et al., 1973). This means that any incubation chamber can only yield one data point after depressurization, or else the

pressure vessel must be repeatedly be depressurized and repressurized, possibly confounding the effect of pressure itself on the organism with the effect of the repeated, rapid increases and decreases in pressure which would not be experienced in the environment. Another type of pressure vessel in use is the diamond anvil cell that contains a window to allow direct observation or analysis based on X-ray absorption spectroscopy (e.g. Sharma et al., 2002, Picard et al., 2011), but because only a small portion of the total volume is visible at any time, these chambers are much better suited to qualitative work on organismal behavior than quantitative study. Another alternative is a flow-through system for high pressure incubations, which allows only a subsample to be depressurized while maintaining pressure on the main culture vessel (Bianchi et al., 1999). This last example was the basic design of the high pressure system (HPS) used in this dissertation.

Despite the methodological limitations of studies using various types of pressure systems, much work has been done to study the effects of pressure, ranging from the level of intracellular processes to whole organisms and populations. The earliest pioneer of high pressure biology was Claude ZoBell, who found that bacterial multiplication, morphology, and metabolism are all affected by pressure (ZoBell and Oppenheimer, 1950). In the subsequent decades, a steady trickle of high pressure microbiology papers appeared, with findings of pressure effects on membrane structure (Allen et al., 1999, DeLong and Yayanos, 1985), membrane transporters (Vezzi et al., 2005), protein folding (Gross and Jaenicke, 1994) and function (Simonato et al., 2006), motility (Meganathan and Marquis, 1973, Welch et al., 1993), expression of proteins usually associated with

heat and cold stress (Welch et al., 1993) and accumulation of solutes to stabilize protein structures (Kelly and Yancey, 1999), among others.

Recent work has favored experimental approaches designed to mimic *in situ* conditions as closely as possible, for example by increasing pressure at the rate experienced by a sinking particle (Grossart and Gust, 2009, Tamburini et al., 2006) and by limiting the addition of organic material (Egan et al., 2012). These studies have found pressure effects not only on prokaryote abundance (Grossart and Gust, 2009, Winter et al., 2009), but also on community structure (Egan et al., 2012, Grossart and Gust, 2009), cell physiology (Winter et al., 2009), and metabolism (Grossart and Gust, 2009). Pressure effects can vary among taxonomic groups (Grossart and Gust, 2009) as well as strains isolated from different pressure environments (Tamburini et al., 2003). However, all of these effects have been studied in prokaryotes, with very little attention paid to pressure effects on microbial eukaryotes. The exception is the yeast *Saccharomyces cerevisiae*, which has been used in studies of metabolism at gigapascal pressures (Sharma et al., 2002) as well as the physiological, structural, and gene expression effects of more moderate high pressures (Brul et al., 2000, Marx et al., 2011, Miura et al., 2006, Shimada et al., 1993).

1.5 Microbial eukaryotes

1.5.1 Background

The ecology of microbial eukaryotes in the marine, freshwater, and terrestrial ecosystems has been the focus of much scientific work, but before I can introduce the historical advances in the field, it is first necessary to discuss the often-changing

terminology used to describe these organisms. To Leeuwenhoek (1632 - 1723), the first person to observe live protists under his early microscopes, they were animalcules, literally "tiny animals" (Dobell, 1932). Since that time, there has been periodic debate on how to describe these organisms which do not fit neatly into the taxonomy defined by plants, animals, and fungi (Corliss, 1992, Lahr et al., 2012). The most commonly used term, both historically and currently, is protist, based on the now defunct kingdom Protista, which included all eukaryotes except plants, animals, and fungi. However, with the advent of molecular biology, it has become obvious that the Protista are not a monophyletic group, leaving the term protist ill-defined in light of modern taxonomy. Another approach has been to characterize microbial eukaryotes based on morphology, giving rise to such groups as flagellates, ciliates, and amoebas. In particular, heterotrophic nanoflagellates, universally abbreviated to HNANs, are a commonly enumerated subset of the microbial eukaryotes, but it is important to note that neither phototrophic nor non-flagellated eukaryotes are included in counts of HNANs, so this term is not synonymous with protists or microbial eukaryotes, and care must be taken when comparing abundances from different sources. David Patterson, an eminent scholar in the field of protistology, has suggested doing away with flagellates as a grouping, as it has neither taxonomic nor ecological significance (Patterson, 1993). In more recent papers, the term microbial eukaryote, abbreviated mEuk (e.g., Finlay, 2002, Green et al., 2004, Lahr et al., 2012), has become preferred as a more descriptive term for single-celled eukaryotes. In this dissertation, the term protist will be used alongside the preferred, more modern descriptors microbial eukaryote, and its syntactical converse, eukaryotic microbe. The term flagellate, while also not describing a taxonomic group, is

also used in this document when only flagellated protists are being discussed, such as in chapter 4 involving cultured organisms, and in discussion of previous work in which solely flagellates were enumerated.

In addition to the naming of the broad group of microbial eukaryotes, the phylogenetic assignment of this group has changed many times, especially in the decades since sequencing technologies have allowed groups to be organized based on genetics, rather than structural characteristics; the latter led to many incorrect classifications due to convergent evolution as well as diverse morphologies within a species (Lahr et al., 2012). I will use the system of Adl et al. (2005), with six supergroups: Amoebozoa, Opisthokonta, Rhizaria, Archaeplastida, Chromalveolata, and Excavata making up the domain Eukarya as established by Woese et al. (1990). Minor changes to this phylogeny, including grouping the Stramenopiles, Alveolates, and Rhizaria into a new supergroup SAR, were published recently, but the general structure of the tree remains the same (Adl et al., 2012).

1.5.2 Ecology of microbial eukaryotes

Describing the ecology of an entire domain of microbial life is a task substantially beyond the scope of this dissertation or any single document, so this short review should not be considered comprehensive. Microbial eukaryotes are essential players in marine food webs, controlling bacterial abundance in surface water and transferring carbon from the microbial loop to the trophic system of larger organisms (Fenchel, 1986, Jürgens and Massana, 2008). Although HNAN and prokaryote abundance covary within systems (Gasol and Vaqué, 1993), the trend does not hold up across systems, suggesting different

controls on populations of both prokaryotes and microbial eukaryotes in marine, freshwater, and benthic environments (Gasol and Vaqué, 1993). Maximum growth and grazing rates vary over about an order of magnitude among species of heterotrophic nanoflagellates, suggesting different feeding strategies which allow many protist species to coexist, occupying slightly different niches even in the open ocean (Eccleston-Parry and Leadbeater, 1994). Moreover, culture experiments have shown that protistan predators can cause shifts in community structure of prokaryote assemblages, but not an overall decrease in richness (Massana and Jürgens, 2003).

The introduction of molecular methods has led to rapid evolution of the field of protist ecology, as it is now possible to identify organisms which are not cultivable and do not have easily recognized morphology, as is the case with many small eukaryotes. New clades belonging to the stramenopiles (Massana et al., 2002) and alveolates (López-Garcia et al., 2001a), although only discovered recently, are among the most abundant taxa in surface waters (Massana et al., 2002, López-Garcia et al., 2001a, Moon-van der Staay et al., 2001, Lovejoy et al., 2006, Not et al., 2008), and there is evidence of a broad rare biosphere (i.e., samples are dominated by a few abundant taxa, but also contain a large number of other taxa at low abundances, Sogin et al., 2006) among marine protists (Countway et al., 2005, 2007). The optimization of catalyzed reporter deposition fluorescence *in situ* hybridization (CARD-FISH) for protists allowed communities to be simultaneously characterized in terms of abundance and taxonomy (Beardsley et al., 2005, Not et al., 2002). Recently, unamended incubations in the dark have been used to select for yet uncultured protists (Weber et al., 2012).

1.5.3 Microbial eukaryotes in the deep sea

Within the deep sea, microbial eukaryotes have been studied in terms of two main properties: abundance and diversity. Abundance is often measured under epifluorescence microscopy using stains that bind a major cell component such as DNA or proteins, including DAPI, FITC, and Proflavine [4',6-diamidino-2-phenylindole, fluorescein isothiocyanate, and 3-6-diamino-acridine hemi-sulfate, respectively (Tanaka and Rassoulzadegan 2002, Paffenhöfer et al., 2003, Fukuda et al., 2007)]. Older papers, prior to the development of these stains, often report much lower abundances based on live counts or growth of cultures inoculated from a water sample (e.g. Arndt et al., 2003, Patterson et al., 1993). Diversity has been addressed historically using either live or fixed samples to classify microbial eukaryotes based on morphology or ultrastructure, with a skilled observer able to accurately assign individual organisms to broad taxonomic groups (Arndt et al., 2003).

Protist abundance decreases strongly between 100 and 1000 m; below this depth, HNANs and total eukaryotic microbes show no further decrease (Sohrin et al., 2010, Morgan-Smith et al., 2011, section 2.3, 3.3.1), while ciliate abundance continues to decline (Sohrin et al., 2010). Protist cell size does not vary with depth (Sohrin et al., 2010). In the subarctic Pacific, an active community of protistan grazers consumes 70% of prokaryotic production in the mesopelagic and nearly half in the bathypelagic (Fukuda et al., 2007), and in the mesopelagic East Sea, grazing by HNANs balanced prokaryotic production (Cho et al., 2000).

Community structure changes with depth among heterotrophic nanoflagellates (Arndt et al., 2003, Countway et al., 2007, López-Garcia et al., 2001a). Novel alveolate

and stramenopile lineages exist in both shallow and deep water masses (Countway et al., 2007), while Acantharea, Polycystinea, and Euglenozoa sequences are found in the bathypelagic but not euphotic zone (Countway et al., 2007). Alveolates and stramenopiles are both collected in the euphotic zone, but stramenopiles are absent from deep water (Not et al., 2007). In hydrothermal vent systems, kinetoplastids and alveolates are dominant (López-Garcia et al., 2003), while novel alveolate clades dominate the deep Antarctic waters (López-Garcia et al., 2001a). The first organisms to colonize experimental substrates in deep-sea hydrothermal vent fluids are kinetoplastids and ciliates (López-Garcia et al., 2003). A piezophilic isolate of *Bodo*, a kinetoplastid, grows readily at 450 atm (45 MPa, equivalent to 4500 m water depth) but not 1 atm (Turley et al., 1988), showing that piezophily exists within the microbial eukaryotes.

1.6 Description of the present work

In this dissertation, I address both abundance and broad-level diversity of eukaryotic microbes in the deep Atlantic Ocean. The methods I use include CARD-FISH, as well as staining with traditional fluorochromes. I compare the protist data to a broad array of environmental factors to shed light on the ecology of these organisms in the deep ocean. In addition, I present the results of a series of experiments in which surface-isolated flagellate cultures were subjected to the temperature and pressure conditions of the deep sea. The goal of these experiments was to identify possible transfer of live organisms from productive surface layers to the deep ocean and better understand whether deep-sea protist populations are primarily surface-derived or the result of *in situ* growth. *Cafeteria roenbergensis* and *Neobodo designis* were chosen for their contrasting

distributions, with *C. roenbergensis* common in surface water but not the deep sea, while *N. designis* appears in samples from all depths.

CHAPTER 2

ABUNDANCE OF EUKARYOTIC MICROBES IN THE DEEP SUBTROPICAL NORTH ATLANTIC

2.1 Introduction

The deep sea is the largest habitat on Earth, but is still relatively unexplored with respect to microbiology due to the difficulty of sampling such a distant and sparsely inhabited environment. In particular, small eukaryotes have only been examined and enumerated at depths below 1000 m in a few studies (Patterson et al., 1993, Fukuda et al., 2007, Countway et al., 2007, Tanaka and Rassoulzadegan, 2002, Sohrin et al., 2010). In the surface ocean, heterotrophic nanoflagellate abundances are 10^2-10^4 cells ml^{-1} and bacterial abundances are 10^5-10^7 cells ml^{-1} (Gasol and Vaqué, 1993) and flagellates are known to control bacterial densities through grazing (Fenchel, 1986). While in the mesopelagic flagellates may still be important grazers on bacteria (Fukuda et al., 2007), they may be of lesser role in the bathypelagic environment (Arístegui et al., 2009). Based on 18S rRNA sequences, Countway et al. (2007) found protistan communities in the deep sea distinct from those in the surface ocean. Fukuda et al. (2007) found that biomass of eukaryotic microbes dropped off more sharply with depth than prokaryotic biomass. In another study, a large diversity of diplonemids was reported in the deep sea (Lara et al., 2009). A recent review of deep-sea microbial oceanography included a comparison of eukaryote numbers between the Pacific and Atlantic Oceans, and the Mediterranean Sea (Arístegui et al., 2009). Most recently, protist numbers were reported for a large longitudinal transect from 10° S to 53° N at depths of 5 to 5000 m in the

Pacific Ocean (Sohrin et al., 2010), and protist diversity in the deep, anoxic Cariaco basin was reported (Edgcomb et al., 2011). Of the many available methods, only direct counts yield absolute numbers of protists in water samples, which is a critical piece of information to better understand microbial trophodynamics. Using samples collected on the same cruise used in this work, Parada et al. (2007) found abundances of picoplankton decreased exponentially from about 2.9×10^5 cells ml^{-1} at 100 m to 0.2×10^5 cells ml^{-1} at 4000 m. One may thus hypothesize that flagellates do not thrive in the deep sea because the abundance of prokaryote prey falls below their feeding threshold (ca. 10^5 cells ml^{-1}; Andersen and Fenchel, 1985, Wikner and Hagström, 1991), and that viruses, which maintain very high concentrations in the deep sea (Parada et al., 2007), are more likely to control prokaryotic abundance in deep water.

Three stains have been commonly used to obtain nanoflagellate counts in the ocean. These are 4',6-diamidino-2-phenylindole (DAPI), fluorescein isothiocyanate (FITC), and 3-6-diamino-acridine hemi-sulfate (Proflavine). Of these, DAPI stains the nucleus only, and is used in combination with FITC (Paffenhöfer et al., 2003, Fukuda et al., 2007) or Proflavine (Tanaka and Rassoulzadegan, 2002), which stain the entire cell body. Here we report cell abundances based on conventional DAPI-FITC staining and compare them with fluorescence in situ hybridization based on a probe considered universal to eukaryotes.

2.2 Methods

2.2.1 Sample collection

Water samples of 200-1250 ml were collected using Niskin bottles from 17 stations in the North Atlantic during the ARCHIMEDES-I cruise (Fig. 1) between November 13 and December 9, 2005. Samples were taken at depths of 100-5000 m, with most stations sampled at 900, 2750, and 4000 m, representing Antarctic Intermediate Water, North Atlantic Deep Water, and Antarctic Bottom Water, respectively (Tomczak 2003). Samples were fixed in 2% (final concentration) formaldehyde (stabilized with 10-15% methanol) overnight, then filtered onto 0.2 or 0.8 μm pore size white polycarbonate filters (Millipore GTTP and ATTP, respectively) at a vacuum of -200 mbar. The relatively long fixation at room temperature was necessary so that supersaturated gases were able to escape and thus not form bubbles on the filters, which would lead to non-uniform cell distributions. Filters were rinsed twice with 1X PBS, then with MilliQ water and immediately frozen at -80°C. They were transported from the Netherlands to Norfolk on dry ice via courier and subsequently stored in a -80°C freezer until CARD-FISH or direct staining was performed.

2.2.2 CARD-FISH

Prior to hybridization, pie-shaped pieces of approximately 1/8 filter were cut so that multiple analyses could be run on a single filter representing a single water sample. The CARD-FISH protocol (Pernthaler et al., 2002, Teira et al., 2004) was undertaken on each filter section, with 10-12 sections hybridized simultaneously from various filters.

Filter sections were embedded in warm 0.1% agarose to prevent cells from detaching from the filters during the hybridization and washing procedures. Permeabilization steps common for FISH with prokaryotes (Proteinase K or lysozyme treatment) were not used as they would damage the more fragile protist cell bodies. Probes labeled with horseradish peroxidase (HRP) were EUK516 (Amann et al., 1990) and KIN516 (Bochdansky and Huang, 2010) (Table 1), and competitor probes (probes not labeled with HRP displaying one central mismatch with the active probe, Table 1) were used for all hybridizations except for the depressurization tests (see below).

Hybridization took place at 35°C for 14-17 hours in hybridization buffer containing 55% formamide (1 g dextran sulfate, 1.8 ml 5M NaCl, 200 µl 1M Tris-HCl, 5 µl 100% Triton X-100, 5.5 ml formamide, 1 ml 10% blocking reagent, 1.5 ml Barnstead Nanopure water). Filters were then washed with washing buffer (30 µl 5M NaCl, 1 ml 1M Tris-HCl, 500 µl 0.5M EDTA, 50 µl 10% SDS, brought to 50 ml with Barnstead Nanopure water) for 15 minutes at 37°C, followed by PBS-T solution (5 ml 10x PBS, 25 µl Triton X-100, brought to 50 ml with Barnstead Nanopure water) for ten minutes at room temperature. Amplification was performed at 37°C for 15 minutes in the dark in amplification substrate B (493 µl amplification buffer, 5 µl Alexafluor 488, 5 µl amplification substrate A; amplification buffer: 2 g dextran sulfate, 8 ml 5M NaCl, 200 µl 10% blocking reagent, 11.8 ml 1X PBS; amplification substrate A: 1 µl H2O2, 200 µl amplification buffer), then washed at room temperature in PBS-T solution for ten minutes in the dark. After CARD-FISH, filters were mounted individually on microscope slides using Vectashield liquid mounting medium with DAPI as counter-stain, and stored horizontally at -20°C in the dark.

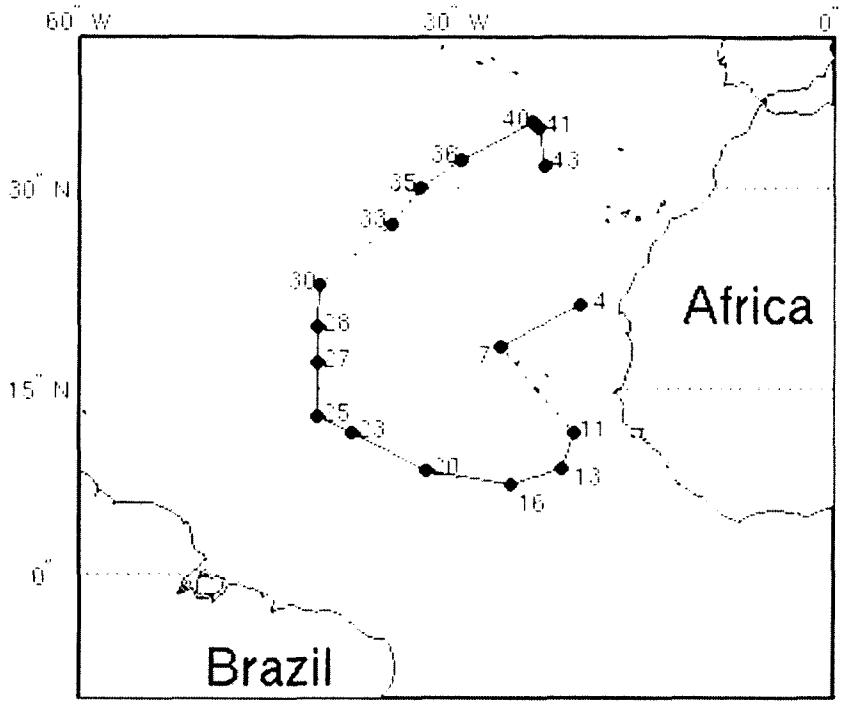

Fig. 1. Map of stations sampled in the North Atlantic. Station numbers are the same as in Parada et al. (2007). Stations along the western portion of the cruise track followed the North Atlantic Deep Water along the Mid Atlantic Ridge.

Table 1

The two horseradish peroxidase (HRP)-labeled probes used in this chapter. As there is only one central mismatch, unlabeled sequences of each probe were used as competitor probes to increase discriminatory power.

Name	Sequence	Reference
EUK516	5'-ACC AGA CTT GCC CTC C-3'	(Amann et al., 1990)
KIN516	5'-ACC AGA CTT GTC CTC C-3'	(Bochdansky and Huang, 2010)

2.2.3 Robotic microscopy

Samples were analyzed on a modified Olympus BX51 epifluorescence microscope with computer control of the stage in X, Y, and Z planes using a motorized stage with linear encoding (Prior Scientific). An X-Cite 120 (Exfo Inc.) light source provided highly consistent illumination. Band-pass filters (40 nm band at 360 nm, 15 nm band at 484 nm, and 25 nm band at 555 nm; Chroma Technology Corp.) in a Lambda 10-3 filter wheel (Sutter Instrument Co.) along with a multi-band beamsplitter (61000v2bs, Chroma Technology Corp.) and emission filter (20 nm band at 450 nm, 35 nm band at 520 nm, 45 nm band at 605 nm; 61000v2m, Chroma Technology Corp.) allowed scanning of the slide for both DAPI and the hybridization signal, with automatic shutters switching between the two excitation wavelengths at each image field. Images were taken with a QICam Fast 1394 (Qimaging) cooled charge-coupled device camera. Microscope

control and image acquisition were performed with Objective Imaging Ltd. software in combination with Image-Pro Plus software with customized macros for microscope operation.

Filter slices were scanned using a semi-automated process. First, the entire filter area was scanned in brightfield illumination at 40× total magnification. This allowed the area of the filter to be defined within the Image-Pro software as a custom scan area. The Z-stack for the scan was defined by noting the Z-plane of best focus for several points on the filter and setting a Z-range based on those values. The filter area was then scanned at 400× using the automated stage and the resulting images stitched into a mosaic of approximately 300-600 fields for display in Image-Pro, with images from the blue and green emission channels overlaid to create a single false-colored image on-screen. The Z-stack for each image in the mosaic, consisting of approximately 30 to 50 images for each stack, was assembled using an algorithm which combined areas of greatest contrast, to create focus across each image and the entire mosaic. The coordinates of each image pixel were stored so that the operator was able to return to any location on the filter to re-examine specific organisms and to take additional pictures at higher magnification. Organisms with positive hybridization signals as well as DAPI-stained nuclei were identified, counted, and individually photographed at 1000× total magnification in each channel. These photographs were sorted based on the morphotype of the nucleus in DAPI. Depending on the abundance of organisms in the sample, 5 to 446 protists were counted per sample using EUK516, and 0 to 232 kinetoplastids were counted using KIN516.

2.2.4 Nuclear morphology

Nuclear morphological categories as they appeared in DAPI were defined as "crescent", "long" (longest dimension at least three times greater than the shortest dimension), "kinetoplastid" (nucleus coupled with a distinctive kinetoplast), "donut" (round nucleus with a dark center), "bean" (one convex and one concave side), "split" (round nucleus with a distinctive dark line down the center), "round", and "miscellaneous" (all nuclei that do not fit into any of these groups). Figure 2 shows examples for each of these morphotypes.

2.2.5 Pressurization tests

This experiment was designed to determine whether there were any pre-fixation losses of cell numbers while the water samples were raised through the water column. Samples were collected from 2750 m and 4000 m depths at six stations in four 200 ml titanium chambers designed to retain in situ pressure. Pressure was released in two of the chambers before fixation with formaldehyde (2% final conc.). In the two other chambers, formaldehyde (2% final conc.) was injected through a high pressure liquid chromatography pump (Rainin Instrument, LLC) without loss of pressure. After 0.5 h of fixation to cross-link proteins and thus harden cells, pressure was released. All samples were filtered through 0.2 μm Millipore polycarbonate filters and hybridized with EUK516 probe as described above, but without the use of a competitor probe.

2.2.6 Methodological tests

In order to assess a variety of potential sources of error we performed a series of tests. We quantified each of them separately, then arrived at an overall correction factor. In this fashion, our results can be compared to many different methods and protocols employed in other studies.

2.2.6.1 Prokaryotes on hybridized and unhybridized filters

To determine whether material was lost from the filter surface during the hybridization procedure, 1/8 slices of 25 mm, 0.8 μm pore size polycarbonate filters were hybridized with the EUK516 or KIN516 probe, counterstained with DAPI and then analyzed under epifluorescence microscopy for DAPI signals of prokaryotes. These counts were compared with counts taken from 1/8 sections of the same filter stained with DAPI and not put through hybridization.

2.2.6.2 Pore size comparison

In order to determine whether any eukaryotic microbes were lost through the pores of 0.8 μm pore-size filters, paired deep-sea samples taken from a single Niskin bottle at each of eight stations were formaldehyde-fixed and filtered through 0.2 and 0.8 μm pore size polycarbonate filters at a vacuum of 200 mbar. Sample volumes were 250 ml for the 0.2 μm filters and 1000 ml for the 0.8 μm. Filters were stored at -80°C and 1/8 (for 0.8 μm) or 1/4 (for 0.2 μm, the larger portion necessary to count sufficient organisms given the smaller volume filtered) of the filter was mounted on a slide using Vectashield with DAPI mounting medium and counted using epifluorescence microscopy.

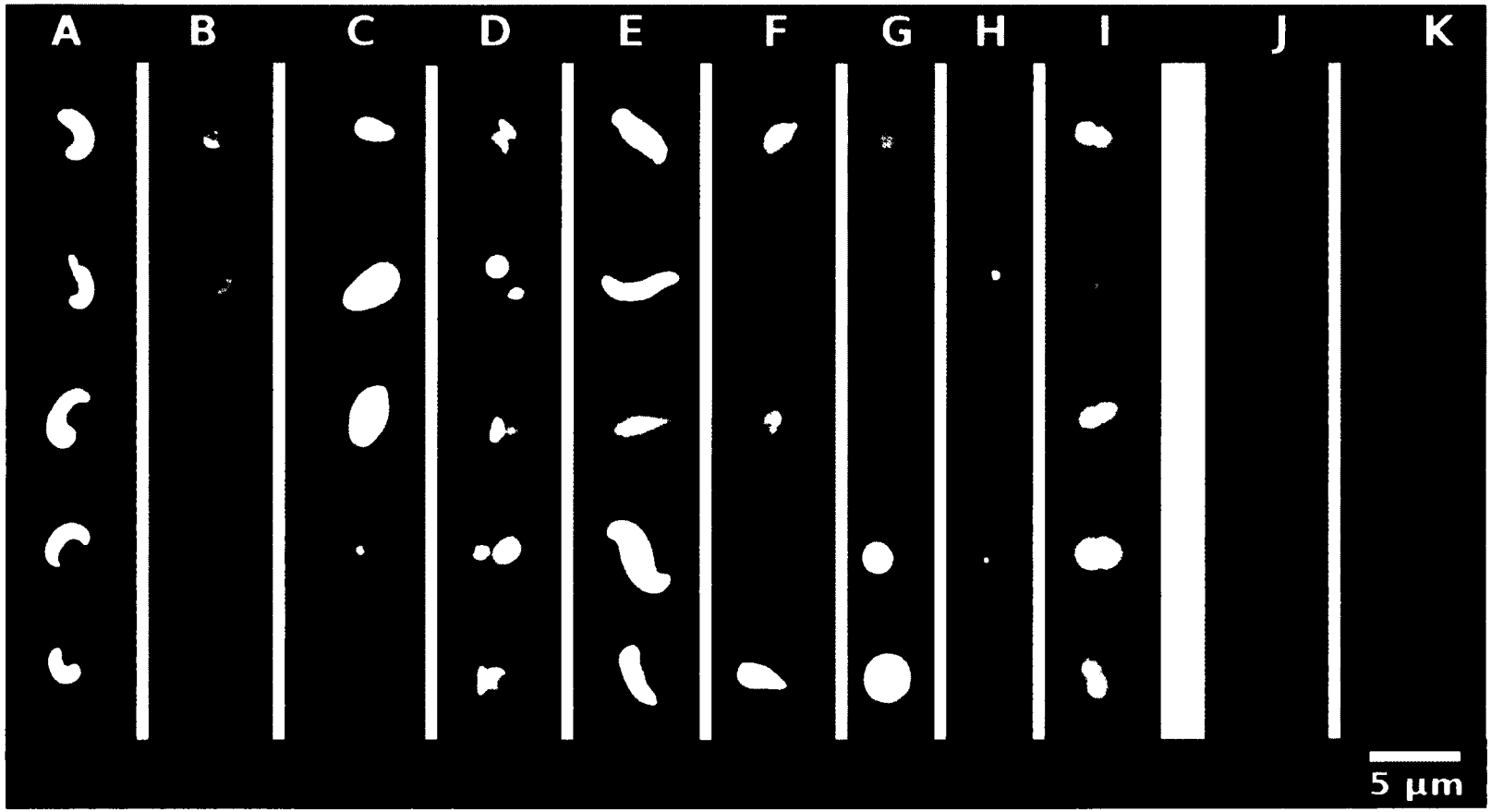

Fig 2. Five examples for each of the nuclear morphotypes

Fig 2 Continued. A – I: Five examples for each of the nuclear morphotypes. A: crescent, B: donut, C: bean, D: kinetoplastid (with the characteristically large mitochondrion), E: long, F: miscellaneous (non-round), G: round, H: tiny, and I: split. All photos show DAPI-stained nuclei of organisms from the deep sea with positive EUK516 hybridization, except for the kinetoplast morphotype, which were all positive with the KIN516 probe. J – K: examples of cultured diplomonads, to show similarity of morphology to split-nucleus type. J: *Hexamita pusilla* ATTC #50336, K: *Trepomonas agilis* ATTC #50337.

2.2.6.3 Test for detachment of organisms from filters

The purpose of this test was to determine whether material would fall off the filters during shipping and storage. Culture of *Cafeteria roenbergensis* was fixed with 2% formaldehyde and 10 ml aliquots were filtered through 0.8 μm polycarbonate filters. Five such filters were placed gently into PetriSlides (Millipore Corp.) and stored at -80°C for one week. The other five filters were placed into PetriSlides then shaken vigorously and knocked against the surface of the lab bench. These filters were then stored at -80°C in the Petrislides, removed several times to be shaken and dropped on the lab bench to simulate handling rougher than occurred with the deep-sea samples. At the end of one week, all filters were allowed to thaw then mounted on slides using Vectashield with DAPI mounting medium and counted using epifluorescence microscopy.

2.2.6.4 DAPI-FITC staining test

In order to compare the efficiency of DAPI and FITC staining procedures with each other, slices of 1/8 of a filter of cultured flagellates (*Neobodo designis, Paraphysomonas vestita,* and *Cafeteria roenbergensis*) were embedded in agarose, as in the CARD-FISH protocol, then soaked for ten minutes in 30% H2O2 to reduce background fluorescence. Filters were then soaked in FITC solution (2.5 ml sodium carbonate buffer, pH 9.5; 11 ml potassium phosphate buffer, pH 7.2; 11 ml 0.85% sodium chloride; 10 mg FITC) for ten minutes, and washed in sodium carbonate buffer (pH 9.5) for 20 minutes. Filter slices were mounted on microscope slides and counterstained using Vectashield with DAPI mounting medium. This FITC staining procedure was not performed on deep-sea samples, only on cultured flagellates, and

differs somewhat from the method used for deep-sea samples. Organisms were counted first in UV excitation for DAPI only, then in DAPI-FITC (i.e. a positive signal in both color channels was required for an organism to be counted).

2.2.6.5 DAPI versus EUK516+KIN516 in lagoon samples

Samples of ambient water, marine snow particles, and sediment were collected in Carrie Bow Cay, Belize, formaldehyde fixed and filtered through 0.8 μm polycarbonate filters. Sections of 1/8 filter each were hybridized with EUK516 and KIN516 probes. All filters were mounted on slides using Vectashield with DAPI mounting medium. Epifluorescence counts were done first counting protists in DAPI only, then counting organisms with both a positive hybridization signal and a visible nucleus in DAPI. This test was designed to account for organisms whose sequences do not match that of either probe. Details of this test can be found in Bochdansky and Huang (2010).

2.2.6.6 Manual counts

Slices of 1/8 filter mounted in Vectashield with DAPI medium were first counted robotically (see above), and then later recounted using the same microscope described above but with manual control of the stage without the aid of camera and imaging software over a minimum of 200 fields. This was performed on all EUK516 and KIN516 samples to assess whether the robotic scanning process introduces error.

2.2.6.7 DAPI-FITC counts

Sections of 1/8 of a 0.8 μm pore size polycarbonate membrane filter were taken from the same filters used for CARD-FISH. These were placed on top of a 3.0 μm pore size polycarbonate membrane backing filter on a glass filtration tower. The filter slices were flooded with 1 ml of FITC staining solution (10 mg FITC, 11 ml potassium phosphate buffer, 11 ml 0.85% NaCl, 2.5 ml sodium carbonate buffer; Sherr and Sherr 1983). After ten minutes of incubation in the dark, vacuum was applied to remove staining solution, then filters were rinsed twice with 10 ml cold (4°C) sodium carbonate buffer under ~200 mbar vacuum. Filters were mounted on slides using Vectashield with DAPI mounting medium, and stored at -20°C in the dark until they were counted on an Olympus BX50 epifluorescence microscope.

2.2.7 Prokaryotic size spectrum

To obtain prokaryotic counts, we scanned a random pattern of at least 100 fields per filter section at 1000× total magnification. This was performed on 0.2 μm pore size membrane filters from all stations. Minimum size and intensity cutoffs were set based on which objects appeared to be prokaryotes (i.e., those that would be counted as prokaryotes in DAPI), and image analysis was run using Image-Pro Plus to count such objects in each field. Concentrations of prokaryotes (cells ml^{-1}) were then calculated, accounting for the volume of water filtered and the proportion of the total filter area included in the scanned region.

2.2.8 Statistical analyses

Pearson correlation analyses were conducted to compare biological and environmental parameters, including total eukaryote, kinetoplastid and split nucleus abundances by CARD-FISH, depth, latitude, longitude, distance to nearest land, and measured nitrogen and phosphorus species. Pearson correlation analyses were also used to compare prokaryotic abundances obtained using image analysis to CARD-FISH abundances of total eukaryotes, kinetoplastids and the split nucleus organism. Linear regression of kinetoplastid abundance and kinetoplastids as a percentage of total CARD-FISH eukaryotes against depth were performed. Paired t-tests and Wilcoxon signed rank tests were conducted on groups 1, 2, 4, 5, 6, 7, and 8 of the methodological tests (Table 2). Student's t-tests and Wilcoxon rank sum tests were used for group 3, which did not have paired samples. All tests were performed using Matlab Statistics Toolbox.

Table 2

Results of statistics for methodological tests. Bold numbers indicate significant results at the α=0.05 level. Since the assumptions of parametric tests were not always fulfilled, the results of the non-parametric equivalents are shown as well. For test group 3 an unpaired Student's t-test and Wilcoxon rank sum test were used; for all other groups, paired Student's t-tests and Wilcoxon signed rank tests were performed. Group 1: counts of prokaryotes in DAPI on hybridized versus unhybridized deep-sea filters to determine whether material detaches from filters during the hybridization process; 2: eukaryotes counted in DAPI on 0.2 μm versus 0.8 μm pore size deep-sea filters to determine whether some eukaryotes were lost through the larger pores; 3: counts in DAPI of cultured *Cafeteria roenbergensis* on filters subjected to shaking to simulate the conditions during shipping and very rough handling versus filters which were left undisturbed; 4: eukaryotes counted in CARD-FISH on deep-sea samples maintained at in situ pressure until after fixation versus samples depressurized prior to fixation; 5: Counts of several flagellate cultures using DAPI versus DAPI-FITC staining techniques; 6: Eukaryotes from ambient and untreated lagoon waters of Carrie Bow Cay, Belize counted in DAPI versus using CARD-FISH (Details in Bochdansky & Huang, 2010); 7: Counts of the same deep-sea filter slices hybridized with the EUK516 and KIN516 probe pair using robotic versus manual control of the microscope stage; 8: Deep-sea samples using CARD-FISH with the EUK516 and KIN516 probe pair versus counts on different sections of the same filter using DAPI-FITC staining. Group 8 shows the overall difference between the DAPI-FITC and CARD-FISH methods.

Table 2 Continued.

Test group	Mean (cells ml^{-1})	SD	n	t	p	rank sum/ signed rank	p
1a. Prok. on hyb. filters	38775	20629	58	**11.3**	**<0.0001**	**5**	**<0.0001**
1b. Prok. on fresh filters	50828	25098	58				
2a. Euk. on 0.2 μm filters	37.1	16.6	8	**4.06**	**0.0048**	**0**	**0.0078**
2b. Euk. on 0.8 μm filters	26.5	10.9	8				
3a. Caf. on shaken filters	10964	1081	5	-0.409	0.703	28	>0.999
3b. Caf. on unshaken filters	11022	998	5				
4a. Pressurized samples	1.06	0.815	14	0.986	0.342	36	0.326
4b. Depressurized samples	0.782	0.554	14				
5a. Cultures in DAPI-FITC	6884	7649	12	0.381	0.710	33	0.677
5b. Cultures in DAPI	6666	6993	12				
6a. Protists in DAPI	1594	1195	11	**6.28**	**<0.0001**	**0**	**0.0009**
6b. EUK516+KIN516	1236	1327	11				
7a. EUK+KIN robotic	10.5	26.2	60	**-3.75**	**0.0004**	**109**	**<0.0001**
7b. EUK+KIN manual	15.8	32.8	60				
8a. Deep sea EUK+KIN	15.9	33.3	58	**3.50**	**0.0009**	**0**	**<0.0001**
8b. Deep sea DAPI-FITC	77.9	163.8	58				

2.3 Results

Abundances of eukaryotes counted using DAPI-FITC staining were an average of 228 cells ml^{-1} (SD = 248) in samples from the lower part of the euphotic zone (100 m), 25.7 cells ml^{-1} (SD = 19.6) in the Antarctic Intermediate Water (750-1000 m), 11.2 cells ml^{-1} (SD = 5.7) in the North Atlantic Deep Water (2400-2750 m), and 12.1 cells ml^{-1} (SD = 7.3) in the Antarctic Bottom Water (3500-5000 m) (Table 3). DAPI-FITC eukaryote abundance was significantly higher in the central water (100-500m) than in any of the lower water masses, none of which were significantly different (one-way ANOVA with Tukey-Kramer multiple comparison correction, $p < 0.0001$, $F = 9.91$; Table 3).

Similarly, we found overall eukaryote abundances counted by CARD-FISH decreased sharply from a mean of 109 (SD = 25, range = 76-149, n=6) cells ml^{-1} in samples from the lower part of the euphotic zone (100 m) to 4.3 (SD = 2.1, range = 1.6-8.4, n = 12) cells ml^{-1} in the Antarctic Intermediate Water (750-1000 m), then remained fairly constant through the North Atlantic Deep Water (2400-2750 m) with a mean of 2.6 (SD = 1.6, range = 0.68-6.4, n=16), and the Antarctic Bottom Water (3500-5000 m), with a mean of 2.0 (SD = 1.2, range = 0.77-4.7, n = 14) cells ml^{-1} (Fig. 3). Eukaryote distribution was strongly correlated with depth and therefore with other factors that were strongly depth-dependent, such as nutrient concentrations (Table 4). The same trends held for kinetoplastids, but not for the split-nucleus morphotype, which was not significantly correlated with depth or nutrients. No significant correlations existed with latitude, longitude, or distance to nearest land for any group (Table 4).

Table 3

Eukaryote abundances measured at various depth ranges. Mean (range) of eukaryote abundances, in cells ml-1. The first three columns are from this work, counted manually in CARD-FISH and in DAPI-FITC as described above. Literature values used DAPI and FITC staining (Fukuda et al. 2007, Sohrin et al. 2010), DAPI and Proflavine (Tanaka and Rassoulzadegan 2002) or live counts (Patterson et al. 1993). Data from Tanaka and Rassoulzadegan (2002) and Patterson et al. (1993) estimated visually from published figures. The abundance shown at 500m for Fukuda is an integrated value of 100-1000m.

	DAPI+FITC		FISH robotic		FISH manual		Fukuda		Sohrin		Tanaka		Patterson
0-100m							1400	(180-3300)	316	(210-738)	300	(20-900)	
100-110m	525	(269-725)	82	(47-111)	109	(76-149)			218	(177-262)	60	(13-170)	60
200-250m	89	(48-145)	12	(1.7-46)	16	(8.2-34)			42	(29-57)	25	(17-30)	60
500m	47	(27-68)	6.3	(0.44-28)	12	(3.5-34)	60	(5.7-260)	20	(12-24)	15	(6-20)	10
750-1000m	26	(6.6-82)	1.2	(0.09-4.8)	4.3	(1.6-8.4)			13	(10-19)	5	(2.5-10)	10
1500-3500m	12	(6.5-31)	0.50	(0.04-1.8)	2.6	(0.68-6.4)	6.6	(1.4-12)	8.9	(6.2-12)	2	(1.1-8)	20
3500-5000m	12	(6.4-32)	0.40	(0.16-1.1)	2.0	(0.77-4.7)			8.8	(5.5-9.9)			

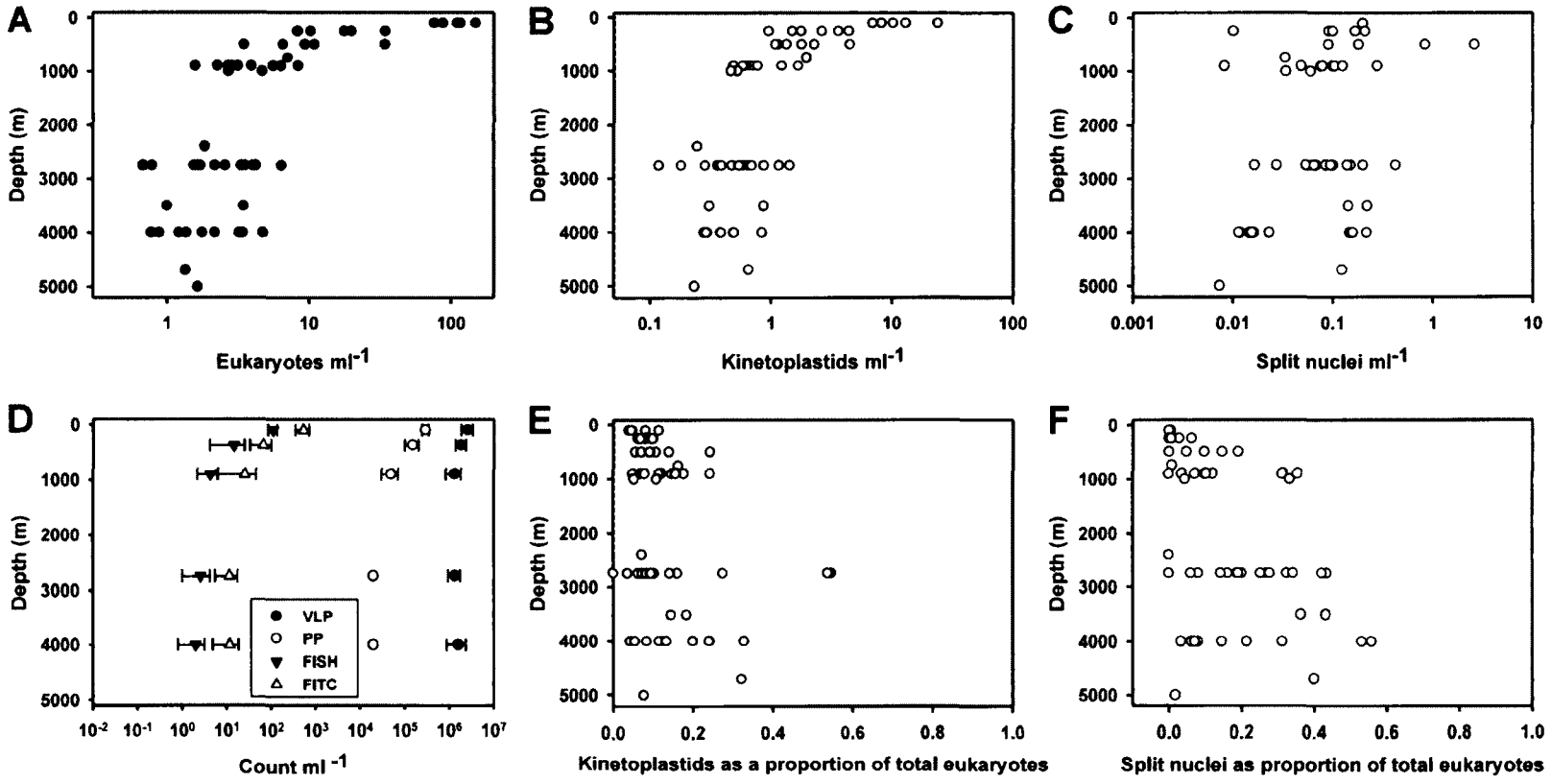

Fig 3. Counts of eukaryotes, kinetoplastids, split nucleus, virus-like particles and picoplankton.

Fig 3 Continued. A, B and C: counts in cells ml^{-1} of eukaryotes (EUK516 + KIN516 probes), kinetoplastids (KIN516 probe) and split nucleus (based on morphology), respectively. D: Mean values of virus-like particle (VLP), picoplankton (PP), CARD-FISH (FISH) eukaryote, and DAPI-FITC (FITC) eukaryote abundances. Error bars represent SD. Over the depths sampled, VLP abundances remain within a factor of two, PP decrease by about an order of magnitude, and EUK decrease by about two orders of magnitude with both methods. VLP and PP from Parada et al. 2007. E and F: Kinetoplastids and the split nuclear morphotype as a proportion of total eukaryotes (EUK516 + KIN516), respectively. All eukaryote and kinetoplastid graphs based on manually-counted CARD-FISH samples, except FITC portion of panel D. Split nucleus abundance in panels C and F are based on morphology observed in robotically-counted samples.

Table 4

Correlation analysis of cell abundances with geographic and chemical variables. Pearson correlation coefficients (r) between cell abundances measured by manual counting of CARD-FISH samples and geographic and chemical variables, with corresponding p-values, n = 57. Explanation and units of variables used: Depth (m), Latitude (°N), Longitude (°W), Distance to nearest land (km), PO_4 (µmol ml^{-1}), NH_4 (µmol ml^{-1}), NO_x (NO_2 + NO_3, µmol ml^{-1}), NO_2 (µmol ml^{-1}), TP = total phosphorus (µmol ml^{-1}), TN = total nitrogen (µmol ml^{-1}).

		Depth	Latitude	Longitude	Distance to nearest land
Eukaryotes	r	-0.487	0.223	-0.003	-0.047
(cells ml^{-1})	p	<0.0001	0.086	0.981	0.724
Kinetoplastids	r	-0.474	0.233	0.008	-0.062
(cells ml^{-1})	p	0.0001	0.073	0.954	0.639
Split nuclei	r	-0.135	0.068	-0.049	-0.019
(cells ml^{-1})	p	0.318	0.617	0.717	0.886

		PO_4	NH_4	NO_x	NO_2	TP	TN
Eukaryotes	r	-0.704	0.292	-0.718	0.904	-0.691	-0.697
(cells ml^{-1})	p	<0.0001	0.028	<0.0001	<0.0001	<0.0001	<0.0001
Kinetoplastids	r	-0.669	0.330	-0.681	0.882	-0.658	-0.659
(cells ml^{-1})	p	<0.0001	0.012	<0.0001	<0.0001	<0.0001	<0.0001
Split nuclei	r	-0.055	-0.061	-0.027	-0.010	-0.052	-0.023
(cells ml^{-1})	p	0.687	0.653	0.842	0.461	0.702	0.862

Because of an apparent discrepancy between counts obtained by DAPI-FITC and CARD-FISH methods, we undertook the series of methodological tests described above. These tests led us to several sources for the difference, which are summarized in Table 2. Significant differences were found in groups 1, 2, 6, and 7 (i.e., losses due to hybridization procedure, filter pore size, staining method, and robotic control of the microscope stage). These comparisons all showed that our method underestimated protist abundance, with 76.3%, 71.4%, 76.1%, and 66.7%, respectively, as many organisms as in the control. Compounding the errors for factors that differed between our two methods (i.e. losses due to hybridization, staining method, and robotic stage control), the CARD-FISH method should count 38.7% of protists in a sample, a 2.6-fold difference on average. This is approximately half of the 4.9-fold difference shown in Table 2, group 8 comparing DAPI-FITC and CARD-FISH estimates of eukaryotes in deep-sea samples. Factors tested that did not contribute to the observed discrepancies were detachment of cells from filters (3), depressurization of samples before fixation (4), and differences between independent DAPI and DAPI-FITC counts (5) (Table 2). Factors we did not investigate which could contribute to the other half of the discrepancy include differences in the rRNA and protein content of eukaryotic cells, counting of dead eukaryotic cells, or inclusion of some large prokaryotes in the DAPI-FITC counts.

Based on manual CARD-FISH counts, kinetoplastid abundance averages were 5.7 (SD = 6.1) cells ml^{-1} in the upper water column (100-500 m), decreasing sharply to 0.84 (SD = 0.50) cells ml^{-1} in the Antarctic Intermediate Water, 0.56 (SD = 0.39) cells ml^{-1} in the North Atlantic Deep Water, and 0.44 (SD = 0.21) cells ml^{-1} in the Antarctic Bottom Water. Using the empirical correction factor of 4.9 as assessed above, the kinetoplastid

abundances change to 27.9 cells ml^{-1} for 100- 500 m, 4.1 cells ml^{-1} for the Antarctic Intermediate Water, 2.7 cells ml^{-1} for the North Atlantic Deep Water, and 2.2 cells ml^{-1} for the Antarctic Bottom Water. The abundance of kinetoplastids decreased significantly with depth (linear regression on semi-log transformed data Fig. 3; $F = 106$, $p < 0.0001$, $n = 60$). As a percentage of total CARD-FISH eukaryotes, however, kinetoplastids increased with depth (linear regression on semi-log transformed data, Fig. 3; $F = 05.87$, $p = 0.019$, $n = 60$). Kinetoplastid percentage averages of total eukaryotic microbes were 15.9% (SD = 7.4) at 100-500 m, 21.5% (SD = 9.0) in the Antarctic Intermediate Water, 24.0% (SD = 20.3) in the North Atlantic Deep Water, and 27.1% (SD = 13.3) in the Antarctic Bottom Water.

Community composition based on nuclear morphotype changes with depth. Images of DAPI-stained nuclei for all FISH-positive organisms were sorted into nine categories and labeled as crescent, long, kinetoplastid, donut, bean, split, tiny, round and miscellaneous. Round and miscellaneous made up the majority of nuclei at all depths, but became less dominant in deeper samples due to an increase in the relative abundance of the "split" morphotype (Fig. 3, Fig. 4). The "split" morphotype was remarkably constant in absolute abundance throughout the water column from 100 m to 5000 m, which consequently increased their relative abundance from 0.07% of total CARD-FISH eukaryotes in the lower euphotic zone (100 m) to 24% in deep water masses (3500 – 5000 m) (Fig. 4).

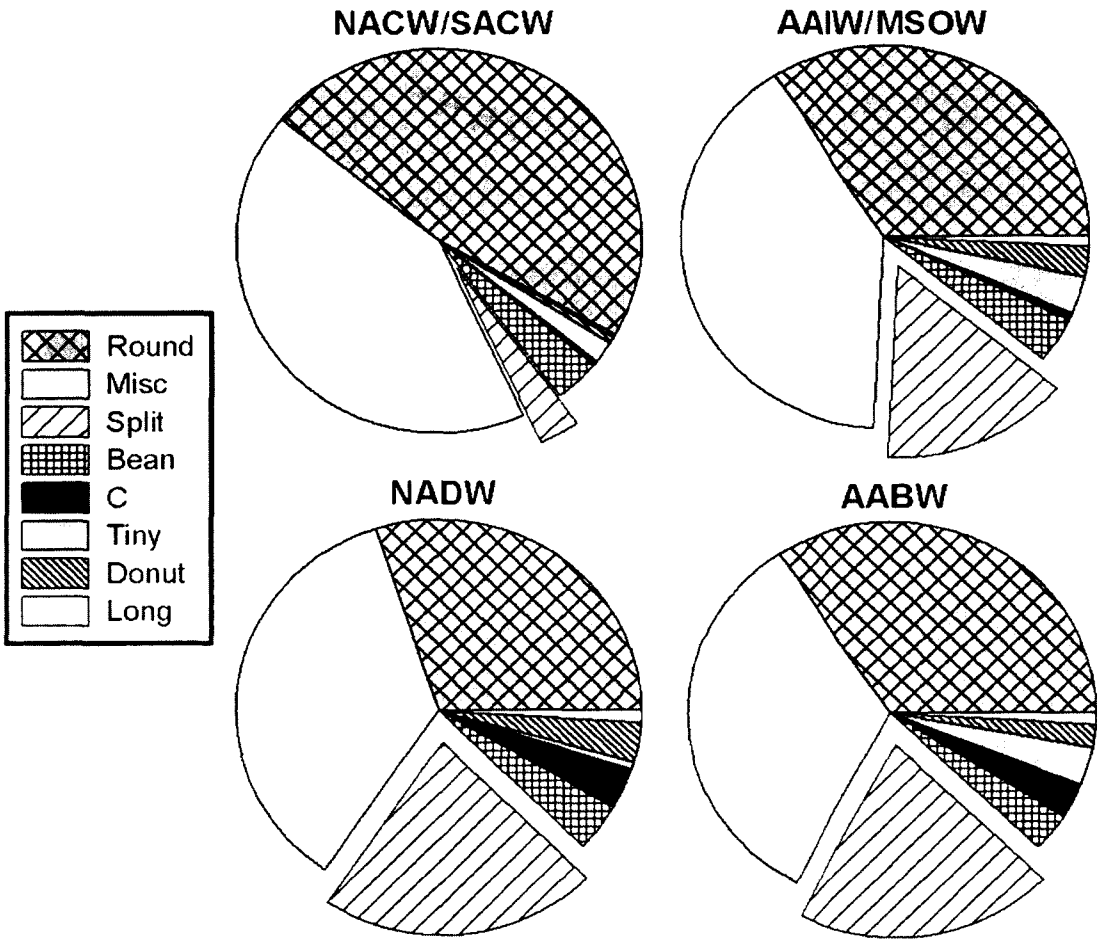

Fig. 4. Relative abundance of morphotypes in various water masses. Note the increase in the split morphotype with increasing depth, which is due to a constant absolute abundance of this morphotype as total eukaryotes declined. NACW/SACW: North/South Atlantic Central Water (samples taken between 250 and 500 m), AAIW/MSOW: Antarctic Intermediate Water/ Mediterranean Sea Outflow Water (samples taken between 750 and1000 m), NADW: North Atlantic Deep Water (samples taken between 2400 and2750 m), AABW: Antarctic Bottom Water (samples taken between 3500 and 5000 m). Sample depth varied in order to target the center of each water mass.

Automated counts of prokaryotes using DAPI staining showed that prokaryotic abundance correlates negatively with depth ($r = -0.734$, $p < 0.0001$ $n = 59$), positively with total flagellate abundance ($r = 0.630$, $p < 0.0001$ $n = 59$), and positively with kinetoplastid abundance ($r = 0.338$, $p = 0.0089$ $n = 59$), but not with split nucleus abundance ($r = 0.065$, $p = 0.627$ $n = 59$). Image analysis of the size of DAPI signals on these filters showed a continuum, with no clear demarcation between prokaryotes and eukaryotic nuclei, rendering a cutoff based on size arbitrary (Fig. 5).

2.4 Discussion

Protist abundance decreased exponentially from 100 to 900 m, then did not decrease further between 900 and 5000 m. This result is consistent with previous studies which have shown low but relatively stable numbers for heterotrophic nanoflagellates (the primary eukaryotes in deep-sea samples) below 1000 m [Fig. 6 in (Sohrin et al., 2010)]. Using picoplankton and virus-like particle abundances from the same expedition (Parada et al., 2007), eukaryote abundances decrease by more than two orders of magnitude over the depths sampled, compared to one order of magnitude for picoplankton, and less than one for virus-like particles (Fig. 3). This suggests that viruses are relatively more important and small eukaryotes less important in the control of bacterial numbers in the bathypelagic region than in surface waters, which is also consistent with the conclusions reached by Arístegui et al. (2009).

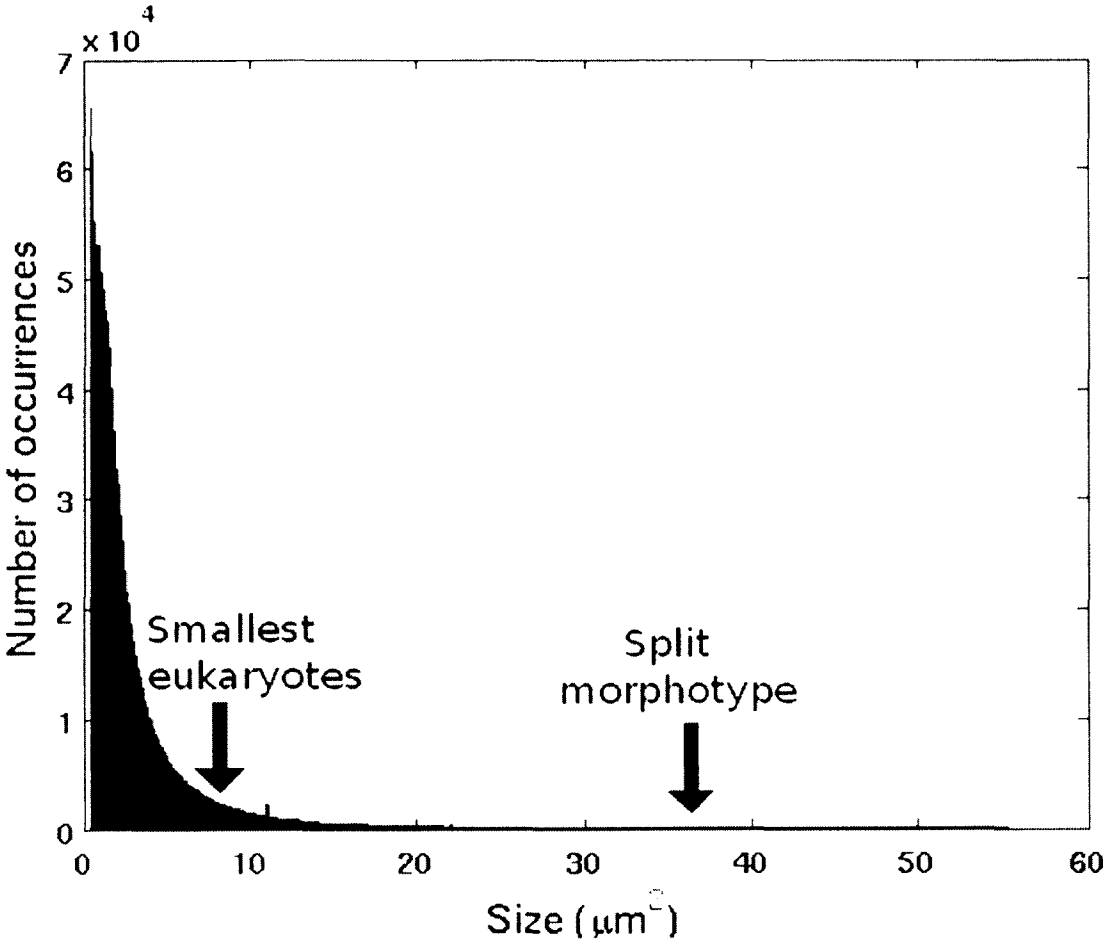

Fig. 5. Frequency distribution of size of DAPI signals on 0.2 μm filters. Measurements were made using the automated microscope and Image-Pro Plus image analysis software. At least 100 random fields per filter from 60 filters (total signals = 1995252, fields = 6502) representing all stations and depths sampled were analyzed. The size of nuclei of two eukaryotic microbes (i.e., tiny and split morphotypes, arrows) demonstrates the size overlap between prokaryotes and eukaryotes.

Counts obtained using FITC staining were higher than those using CARD-FISH for all samples. There are several possible reasons for this discrepancy, and we tested for such effects including loss of material from filters during the hybridization process, rough handling of filters, depressurization of samples, and the robotic scanning process of the microscope. Other factors we were not able to test directly include eukaryotes which have too few copies of rRNA to show a positive CARD-FISH signal, which may be due to low activity levels of living cells (i.e. CARD-FISH could undercount) or to faster degradation of rRNA compared to the proteins and DNA which bind DAPI and FITC in dead cells. Conversely, a source of error in the DAPI-FITC counts could be the inclusion of a small fraction of prokaryotes in the tally that appear like eukaryotes because of very thick cell walls and DNA concentrated inside a nucleoid. Given the much higher abundance of prokaryotes in the samples, even the inclusion of a very small percentage of prokaryotes could make a big difference (Fig. 5). Although the scanning process of the robotic microscope introduced a significant error into counts of our samples (Table 3), it is nonetheless a useful tool for the quantification of very rare events, where the errors in manual counting would be at least as high due to the large number of empty fields to be assessed. By comparison, our counts of eukaryote abundances using the DAPI-FITC protocol are very similar to those of other workers despite the fact that they were collected at many different locations ranging from the Pacific (Sohrin et al., 2010) to the Mediterranean (Tanaka and Rassoulzadegan, 2002). These data suggest that differences in the abundances of eukaryotic microbes do not primarily arise among ocean basins but are rather due to latitudinal differences (Sohrin et al., 2010) and due to different methodology employed (Table 5 in Nagata et al., 2010).

In our samples, depressurization pre- versus post-fixation did not significantly affect the number of eukaryotes counted by CARD-FISH in deep-sea samples. This finding is consistent with previous work, which has shown that many eukaryotes can be isolated from the deep sea after depressurization (Arndt et al., 2003, Atkins et al., 1998) and that eukaryotes cultured under pressure can survive and continue dividing after repeated depressurization (Turley et al., 1988). It is also consistent with the finding that protists do not burst due to intracellular bubble formation during pressure loss, and have nearly 100% survival when samples are depressurized over 0.5-1 hour (Hemmingsen and Hemmingsen, 1979). This validates the common practice of collecting samples for protist counts in non-pressurized samplers such as Niskin bottles, which allow for collection of the large volumes of water necessary for accurate counts, but do not maintain these samples at *in situ* pressure. It is important to emphasize, however, that while cells may not disappear due to depressurization, their physiology may be greatly impacted by changes in pressure. Any measurements to that effect (e.g., respiration, growth, feeding) may thus need to be performed under in situ pressure and temperature to obtain accurate results.

We used nuclear morphology to quantify certain types of organisms without knowing their taxonomic affiliation. The most striking example of this was the "split" morphotype (Fig. 2), in which the nucleus appears divided into two equal halves, which could be due to a double nucleus such as that found in the diplomonads (Lee et al., 2000, Fig. 2) or possibly some feature of the cell blocking the center of the nucleus from view. These organisms were distinctive in the size, shape, and the relative brightness of their nucleus as viewed with DAPI staining and they readily hybridized with the EUK516

probe but not with KIN516. In individual deep-sea samples, the "split" nucleus type sometimes made up more than 50% of positive organisms using the EUK516 probe and robotic counting method, thus making this morphotype the most abundant in the deep sea where we sampled (Fig. 3). It showed no correlation with prokaryotic abundance, which was strongly correlated with depth while the split nucleus remained constant over the depth range sampled. The high abundance and consistent appearance of the nucleus mean that it would be impossible for the cells be arranged on the filter in random orientations and we therefore propose that these organisms have cells which are flattened or are otherwise forced to land on the filter in a consistent orientation, similar to what we observed in diplomonads (Fig. 2).

We have not yet resolved the taxonomic affiliation of the "split" nucleus organism. It appears most similar to the twin nuclei of diplomonads, though it does not match precisely with the shape of the nuclei of cultured *Hexamita pusilla* ATTC #50336 or *Trepomonas agilis* ATTC #50337 (Fig. 2). Interestingly, the appearance of "split" nucleus type from our ocean samples had much less variation in appearance than that found in monocultures of both *Hexamita* and *Trepomonas* (Fig. 2). As we suspect for the split-nucleus type, *Hexamita* and *Trepomonas* are dorso-ventrally flattened and come to rest on the filter surface at a preferred orientation exposing their peculiar 2-nucleus feature to view in the majority of individuals counted in our test (65.6% in *Hexamita*, 81.5% in *Trepomonas*). Most diplomonads are parasitic or live in anoxic, high nutrient environments (Lee et al., 2000), which makes them unlikely candidates for the most abundant eukaryote in the oxygenated, oligotrophic deep sea. However, microenvironments with anoxic and high-nutrient conditions exist in marine snow

particles (Alldredge and Cohen, 1987), which could provide a niche for diplomonads in the deep sea. Diplomonads are not currently known to exist in the deep sea, and are not to be confused with the diplonemids, reported to be very diverse in deep water (Lara et al., 2009).

Our examination of community composition based on nuclear morphotype shows that distinctive shifts occur between shallow and deep water samples, which independently validates the observations by Countway et al. (2007) based on 18S rRNA sequences. The abundance of organisms with recognizable nuclear morphologies means that a simple DAPI stain and visual inspection of a filter can be used as a first rough assessment of its eukaryotic community, allowing rapid characterization of some eukaryote types without fluorescence in situ hybridization or sequencing. Classifying organisms based on morphology, including that of the nucleus, is an important tool of classical protist ecology. For example, the permanently condensed chromosomes typical for dinoflagellates and Diplonema have long been used to recognize these organisms (Lee et al., 2000, Lukeš et al., 2009). Given the abundance of the unusual "split" morphotype in our samples, we suggest that this simple tool can be used as a first step in the classification of some morphologically identifiable organisms from environmental samples prior to molecular characterization.

No correlation was found between eukaryote abundance by CARD-FISH and geographical factors such as latitude, longitude, or distance to nearest land, which may affect organic carbon input to the deep sea (Rowe, 1983, Table 4). This suggests a decoupling between surface water conditions and eukaryote abundance in the deep water. This decoupling may be due to the disconnect between the upper water masses with

wind-driven circulation and the deep waters where thermohaline circulation dominates. In this data set, however, the apparent decoupling may also be due to the high between-sample variability and statistical type II errors, which are an inherent problem with any quantification of rare events. Some of the high between-sample variability (Table 4, Fig. 3) may also be attributable to the presence of aggregates in the deep sea. Recently, Bochdansky et al. (2010) found that macroscopic aggregates are found in high numbers in some layers of the deep sea, particularly below 2000 m. If protists of the deep sea are primarily located on aggregates because numbers of freely-suspended prey items fall below threshold feeding levels (Wikner and Hagström, 1991), much of the observed variability may be the result of this spatial heterogeneity.

Using the six supergroups proposed by Adl et al. (2005), Not et al. (2007) found the dominant eukaryotes in the deep Sargasso Sea to be Chromalveolata and Rhizaria, represented primarily by alveolate and radiolarian sequences, respectively. Another study in the Sargasso found Chromalveolata and Rhizaria to dominate as well, but also found the supergroup Excavata represented by euglenozoan sequences (Countway et al., 2007). The taxonomic details within the euglenozoan sequences in that study was unclear, but Euglenazoa includes the kinetoplastids which we found to be important numerically in our deep sea samples, as well as the diplonemids which have recently been discovered to be highly diverse in the deep sea (Lara et al., 2009). More studies using FISH probes targeted at apparently abundant groups such as the alveolates and radiolarians need to be undertaken on deep sea samples to establish whether these groups are actually the dominant deep-sea eukaryotes or if biases inherent in PCR-based methods have led to this conclusion.

The kinetoplastids should be included in any future quantification of eukaryotes from the deep ocean, and care must be taken to include them in studies using molecular techniques. In water mass averages of our samples, their contribution to total CARD-FISH eukaryotes ranged from 15.9 to 27.1%. Kinetoplastids are a diverse branch of the eukaryotic tree (Simpson et al., 2006), and are as important in deep waters as in surface waters and sediments (Arndt et al., 2003, Atkins et al., 2000, Bochdansky and Huang, 2010). Some kinetoplastids such as *Bodo* are barotolerant (Turley et al., 1988) or even barophilic (Turley and Carstens, 1991). They have been collected from both the water column and sediments of the deep sea and successfully cultured in pressure vessels (Patterson et al., 1993). The kinetoplastids *Neobodo saliens* (formerly *Bodo saliens,* Simpson et al., 2006) and *Rhynchomonas nasuta* as well as an unknown kinetoplastid have been isolated from deep-sea hot vent sites (Atkins et al., 1998, Atkins et al., 2000). Kinetoplastids have generally not been recorded specifically in sequences from the deep sea, but they are part of the Euglenozoa, whose sequences are more abundant in deep water than in the euphotic zone (Countway et al., 2007). Kinetoplastids and euglenids, both members of the Euglenozoa, have also been found to be abundant in live counts and enrichment cultures from the deep sea (Arndt et al., 2003). Also, the recent discovery that diplonemids, another member of the Euglenozoa, are highly diverse in the deep sea (Lara et al., 2009) suggests that deep branches of the eukaryotic tree comprise a significant portion of deep-sea eukaryotes.

CHAPTER 3

DIVERSITY AND DISTRIBUTION OF MICROBIAL EUKARYOTES IN THE DEEP TROPICAL AND SUBTROPICAL NORTH ATLANTIC

3.1 Introduction

The ecological role of microbial eukaryotes, which are important in controlling prokaryotic populations and mediating major biogeochemical cycles in the surface ocean (Fenchel, 1986), is poorly understood in the meso- and bathypelagic ocean. Their enumeration is complicated by the fact that some eukaryotes are as small as many prokaryotes and may easily be missed in counts using traditional fluorochromes (Morgan-Smith et al., 2011). Use of fluorescence in situ hybridization (FISH) may exclude organisms with sequences that do not match universal probes and total eukaryote abundance may thus be underestimated. Methods of studying microbial diversity are therefore prone to biases whether they are based on traditional fluorochromes or modern molecular biology. Several studies have quantified microbial eukaryotes in the meso- and bathypelagic realms (Countway et al., 2007; Fukuda et al., 2007; Morgan-Smith et al., 2011; Patterson et al., 1993; Sohrin et al., 2010; Tanaka and Rassoulzadegan, 2002), while others have used genetic methods to study their diversity (Countway et al., 2007; Edgcomb et al., 2011; Eloe et al., 2011; Lara et al., 2009), but none have combined these approaches to quantify diverse taxonomic groups. In this study, we used catalyzed reporter deposition fluorescence in situ hybridization (CARD-FISH) with several probes representing important taxonomic groups to simultaneously examine diversity and abundance of eukaryotic microbes in the deep North Atlantic. Total eukaryotes were also

enumerated by using dual staining with 4',6-diamidino-2-phenylindole and fluorescein isothiocyanate (DAPI-FITC).

Previous studies of eukaryotic diversity in the deep ocean have primarily employed PCR-based methods. These methods allow a broad view of community structure, but are generally not quantitative and may suffer from biases inherent to PCR including chimera and heteroduplex formation, differences in binding energy between primers, and bias toward one-to-one product ratio (Kanagawa, 2003). Using a PCR-based approach, Countway et al. (2007) found radiolarians to be the most abundant groups in deep-water (2500 m) samples. Other studies have used PCR-based methods to analyze the diversity within certain taxa such as diplonemids, which are highly diverse in the deep ocean (Eloe et al., 2011; Lara et al., 2009), and stramenopiles (Massana et al., 2002). In this study, we enumerated groups which have featured prominently in previous studies of eukaryotes in the marine environment, including stramenopiles (MAST 4; Massana et al., 2002), diplonemids (Eloe et al., 2011; Lara et al., 2009) alveolates (Group II; Massana, 2011), and the split-nucleus morphotype (Morgan-Smith et al., 2011). In addition, we targeted eukaryotic taxa likely to be favored in the food-limited deep sea due to their behavior, such as saprotrophic feeding by fungi and labyrinthulomycetes (Ragukhumar, 2002) and particle-affiliation in the deep-branching kinetoplastids (Bochdansky and Huang, 2010).

3.2 Methods

Samples were collected aboard the R/V Pelagia on the Archimedes III and Archimedes IV cruises (Fig. 6); both expeditions were aimed at studying deep-water microbiology in relation to basin-scale oceanographic features. A particular focus was placed on fracture zones, deep trenches across the Mid-Atlantic Ridge where significant exchange of deep water between the eastern and western basins of the Atlantic occurs within the North Atlantic Deep Water and Antarctic Bottom Water.

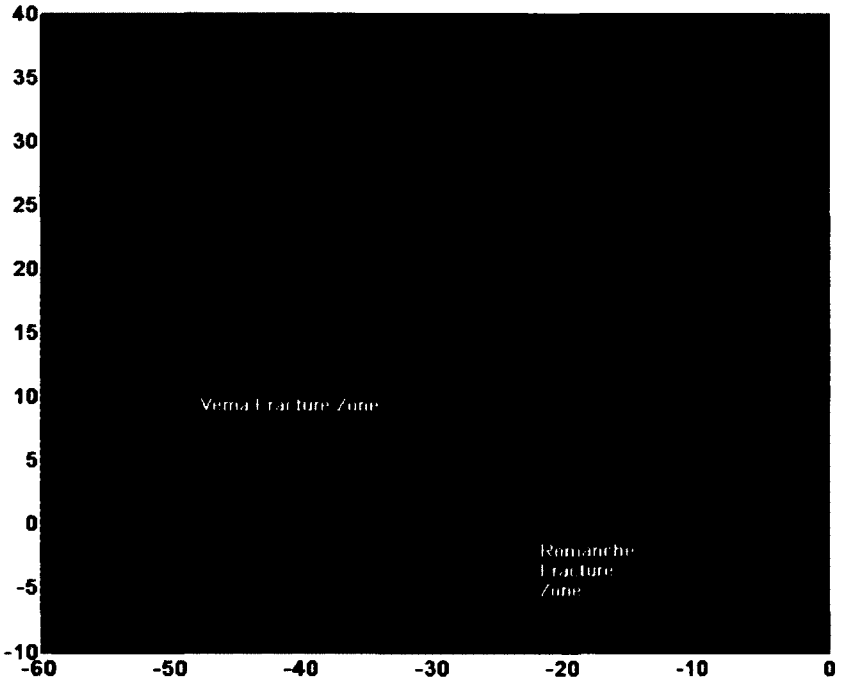

Fig. 6. Map of stations sampled during the Archimedes III and IV cruises. Archimedes III (red) left Fortaleza, Brazil, crossed the Brazil Basin and sampled within the Romanche Fracture Zone to a maximum depth of 7000 m at Vema Deep, then turned northwest to

Fig. 6 Continued

cross the Sierra Leone and Cape Verde basins, placing a final station at the TENATSO time-series site near the Cape Verde islands. Archimedes IV (green) ported out of the Canary Islands, sampling across the Madeira Abyssal Plain to the Vema Fracture Zone, then northward along the eastern flank of the Mid-Atlantic Ridge before crossing the Madeira Abyssal Plain again toward the Canary Islands.

The Archimedes III cruise (17 Dec 2007-17 Jan 2008) began in Fortaleza, Brazil, crossed the Brazil Basin and sampled within the Romanche Fracture Zone to a maximum depth of 7000 m at Vema Deep, then turned northward to cross the Sierra Leone and Cape Verde basins, with a final station at the Tropical Eastern North Atlantic Time-Series Observatory (TENATSO) site near the Cape Verde islands (Fig. 6). Several distinct water masses were sampled, defined by their neutral density and temperature characteristics, including upper thermocline water, South Atlantic Central Water, Northeast Atlantic Central Water, Antarctic Intermediate Water, South Atlantic Intermediate Water, Northeast Atlantic Deep Water, upper North Atlantic Deep Water, middle North Atlantic Deep Water, lower North Atlantic Deep Water, Lower Deep Water, and Antarctic Bottom Water (Tomczak and Godfrey, 2003). For most of the analyses performed, these were grouped into (sampling depth ranges in brackets): Central Water (100-470 m, including an oxygen minimum zone near 250 m), Intermediate Water (500-750 m), upper Deep Water (1750 m), middle Deep Water (2700-3750 m), lower Deep Water (3500-4500 m), and Bottom Water (4350-7000 m). Samples from the Oxygen Minimum Zone

and Romanche Fracture Zone were separated from their water masses only for analyses comparing these samples to others taken in the same water mass.

During the Archimedes IV cruise in the tropical north Atlantic (9 Oct-4 Nov 2010), samples were collected for total eukaryote enumeration (no CARD-FISH analysis). This cruise embarked from the Canary Islands, sampled across the Madeira Abyssal Plain to the Vema Fracture Zone (different from the Vema Deep within the Romanche Fracture Zone, Fig. 6), then traced the eastern flank of the Mid-Atlantic Ridge northward against the flow of the North Atlantic Deep Water (i.e., against a time series of ventilation ages), before crossing the Madeira Abyssal Plain again toward the Canary Islands (Fig. 6). As with the previous cruise, samples were taken based on physical water mass characteristics, rather than at pre-determined depths, within the upper thermocline water, lower thermocline water, Subtropical Mode Water, Antarctic Intermediate Water, Labrador Sea Water, North Atlantic Deep Water, and Antarctic Bottom Water (Tomczak and Godfrey, 2003). Water masses used for analysis were Central Water (sample depth ranges: 100-380 m), Intermediate Water (319-1069 m), Labrador Sea Water (1964-2400 m), North Atlantic Deep Water (2750-3900 m), and Antarctic Bottom Water (4200-5200 m). Where it was present, the Oxygen Minimum Zone was also sampled (between 319 and 795 m) though these samples were grouped with the water mass from which they were collected except when the effect of oxygen was being tested.

These two cruises provided a marked contrast in oceanic regimes, with Archimedes III sampling below the relatively productive equatorial upwelling and the coastal upwelling area adjacent to west Africa, whereas Archimedes IV visited oceanic sites in the oligotrophic North Atlantic Gyre.

Samples were collected using a rosette sampler fitted with eighteen 12 L Niskin bottles during Archimedes III and sixteen 25 L Niskin bottles during Archimedes IV. Depressurization of deep-sea samples retrieved in Niskin bottles has been shown not to affect eukaryote abundance estimates (Morgan-Smith et al., 2011). Samples were collected within approximately 30 min of rosette arriving on deck. Seawater was dispensed through silicone tubing previously soaked in 1.2 N HCl, then rinsed twice each with Milli-Q water and sample water prior to use. Water was collected in 1.75 L sample bottles which had been rinsed twice with ultra-pure water and twice with sample water, and filled gently from the bottom either to 1 L (Central Water samples) or 1.5 L (all other water masses), leaving a headspace for gas exchange. Samples were immediately fixed overnight with 0.2 μm-filtered formaldehyde solution (final concentration ~2%) at room temperature to allow outgassing and prevent bubble formation on filters. Subsamples of 100-250 ml were then filtered under gentle vacuum (-200 mbar) onto Millipore 0.2 μm white polycarbonate filters for DAPI-FITC and 500-1000 ml onto 0.8 μm white polycarbonate filters for CARD-FISH. A pore size of 0.2 μm is preferred for enumeration of total eukaryotes because some smaller eukaryotes are lost through the pores of 0.8 μm filters, leading to underestimation of eukaryote abundance (Morgan-Smith et al., 2011), but 0.8 μm filters allowed processing of the larger volumes necessary to enumerate rare taxa. Filters were washed with phosphate buffered saline (PBS) and ultra-pure water, then immediately stored at -80°C. Water samples were also collected for oxygen, PO_4, NH_4, NO_3, NO_2, Si, dissolved organic carbon (DOC), dissolved organic phosphorus (DOP), and dissolved inorganic carbon (DIC) using standard methods for the analysis of seawater.

CARD-FISH was used to survey a subset of major groups of eukaryotes (Morgan-Smith et al., 2011, modified from Pernthaler et al., 2002, Teira et al., 2004). Briefly, each filter was cut into eight approximately equal-size pieces. Ten to 12 of these sections from various filters representing different water samples were embedded in warm 0.1% agarose, and hybridized at 35°C for 14 to 17 h in hybridization buffer containing 40% (for LabY probe) or 55% (all other probes) formamide. All probes were initially tested for optimal stringency (i.e., formamide concentration) using cultured representatives from each of the probes' target groups, or using natural samples in cases where no cultured representative was available. All probes were labeled with horseradish peroxidase (HRP), except for EUK516 and KIN516 hybridizations, where unlabeled versions of the alternative probe (i.e., unlabeled EUK516 for KIN516 hybridization and unlabeled KIN516 for EUK516 hybridization) were used as competitor probes to prevent non-specific binding (Bochdansky and Huang, 2010). Washing with washing buffer (30 µl 5 M NaCl, 1 ml 1 M Tris-HCl, 500 µl of 0.5 M EDTA, 50 µl 10% sodium dodecyl sulfate, brought to 50 ml with Milli-Q water) and phosphate buffered saline (PBS) with Triton X-100 (PBS-T) were followed by amplification (493 µl amplification buffer, 5 µl Alexafluor 488, 5 µl amplification substrate A; amplification buffer: 2 g dextran sulfate, 8 ml 5 M NaCl, 200 µl 10% blocking reagent, 11.8 ml 10× PBS; amplification substrate A: 1 µl H2O2, 200 µl amplification buffer) at 37°C for 15 min in the dark, and a further washing step with PBS-T. Filters were mounted on slides using Vectashield mounting medium with DAPI and stored at -20°C until enumeration. Probes used were EUK516 (general eukaryote), KIN516 (kinetoplastids), LabY (labyrinthulomycetes), PF2 (fungi), Alv01 (Group II alveolates), NS4 (MAST 4 stramenopiles), and DiploR1792

(diplonemids). Probe sequences and stringencies, as well as their initial references are summarized in Table 5. EUK516 and KIN516 probes were not enumerated for all samples due to a shortage of filter sections after a failed hybridization. One unique DAPI-morphotype was characterized and represents an abundant taxonomic group in the deep ocean (Morgan-Smith et al., 2011).

Double staining with DAPI-FITC was used to enumerate total eukaryotes (modified from Fukuda et al., 2007, Sherr and Sherr, 1983). Pie-shaped slices of approximately 1/8 of filter were cut, and 3-4 of these slices representing different water samples were placed atop a 25 mm diameter, 0.2 μm pore size polycarbonate filter on a glass frit and covered with a 10-ml filter tower, which was then flooded with 1 ml FITC staining solution (2.5 ml 0.5 M sodium carbonate buffer, pH 9; 11 ml 0.01M potassium phosphate buffer, pH 7.2; 11 ml 0.85% sodium chloride; 10 mg FITC), and incubated for 10 min in the dark. Then vacuum was applied (-200 mbar) and filters were washed twice with 10 ml ice-cold carbonate buffer (0.5 M, pH 9). Filter sections were mounted on slides using Vectashield mounting medium with DAPI and stored at -20°C until analysis. CARD-FISH and DAPI-FITC samples were analyzed on Olympus BX51 and BX50 epifluorescence microscopes, respectively.

Table 5

Oligonucleotide probes used in this chapter. Percent formamide determines the stringency of CARD-FISH hybridizations, with higher concentrations leading to higher specificity. For each probe, the highest formamide concentration that did not lead to a decrease in the number of labeled target cells was used (Daims et al., 2005). Unlabeled EUK516 was used as a competitor probe in all KIN516 hybridizations and unlabeled KIN516 in all EUK516 hybridizations, as these two probes contain a single central mismatch. No competitors were used in hybridizations with other probes.

Probe Name	% Formamide	Target group	Sequence (5'-3')	Reference
EUK516	55	General eukaryote	ACC AGA CTT GCC CTC C	(Amann et al., 1990)
KIN516	55	Kinetoplastids	ACC AGA CTT GTC CTC C	(Bochdansky and Huang, 2010)
LabY	55	Labyrinthulomycetes	AAC CCG AAA TGT CCC TCT AAG AAG	(Stokes et al., 2002)
PF2	40	Fungi	CTC TGG CTT CAC CCT ATT C	(Kempf et al., 2000)
Alv01	55	Alveolates, group II	GCC TGC CGT GAA CAC TCT	(Guillou et al., 2008)
NS4	55	Stramenopiles, MAST 4	TAC TTC GGT CTG CAA ACC	(Massana et al., 2002)
DiploR1792	55	Diplonemids	GCA TTC CTC ATT CAA GGA	(Lara et al., 2009)

Statistical analyses (ANOVA, ANCOVA, regression, rank sum, and PCA) were performed in Matlab using the Statistics Toolbox. Figures were created in Matlab (Fig. 6, 8, 10, 12) and Ocean Data View (Fig. 7, 9, 11; Schlitzer, 2012). Surface chlorophyll and primary productivity values were calculated using NASA's SeaDAS software based on MODIS Aqua imagery (SeaDAS Development Group, 2012) and the Behrenfeld-Falkowski model of primary productivity (Behrenfeld and Falkowski, 1997; Behrenfeld and Falkowski, 2010), respectively. For both chlorophyll and primary productivity, 8-day composite values were used to minimize data loss due to cloud cover and specular reflection of sunlight (sun glint). To represent the time it takes for surface-produced material to arrive in the deep ocean, imagery from previous 8-day composites was used when comparing surface values to measurements from samples taken at depth. For the upper 1000 m, the 8-day composite immediately preceding sampling was used, and for each 1000 m below that, the prior 8-day composite was used, such that data collected between 3000 and 4000 m were compared to imagery taken four 8-day intervals prior to sampling at that station. This lag time was chosen to represent a typical sinking rate of particles, based on published estimates of in situ (664-2648 m per 8 days; Berelson, 2002) and laboratory (408-5856 m per 8 days; Ploug et al., 2008) settling velocities of marine snow particles, fecal pellets, and phytoplankton aggregates.

3.3 Results

3.3.1 Abundance

As estimated via DAPI-FITC staining, average eukaryote abundance during Archimedes III was 384.7 cells ml^{-1} in the Central Water (SD = 185.9, n = 18), and

decreased sharply below that, with a mean of 72.9 cells ml^{-1} in the Intermediate Water (SD = 24.1, n = 12), 35.3 cells ml^{-1} in the Deep Water (SD = 10.3, n = 33), and 20.5 cells ml^{-1} in the Bottom Water (SD = 10.1, n = 12). During Archimedes IV, lower abundances were measured in all water masses, with a mean of 72.2 cells ml^{-1} in the Central Water (SD = 35.5, n = 21), 13.0 cells ml^{-1} in the Intermediate Water (SD = 11.1, n = 44), 3.6 cells ml^{-1} in the Deep Water (SD = 1.4, n = 29), and 2.8 cells ml^{-1} in the Bottom Water (SD = 0.7, n = 22). Eukaryote abundance based on CARD-FISH followed a similar pattern, but at lower abundances than those measured via DAPI-FITC staining (for a thorough comparison of the two methods see Morgan-Smith et al., 2011), with means of 57.3 (SD = 52.3) cells ml^{-1} in the Central Water, 4.4 (2.3) cells ml^{-1} in the Intermediate Water, 3.6 (2.8) cells ml^{-1} in the Deep Water and 3.3 (3.2) cells ml^{-1} in the Bottom Water, respectively, during Archimedes III (Fig. 7, Table 6). No CARD-FISH analysis was performed on samples from Archimedes IV.

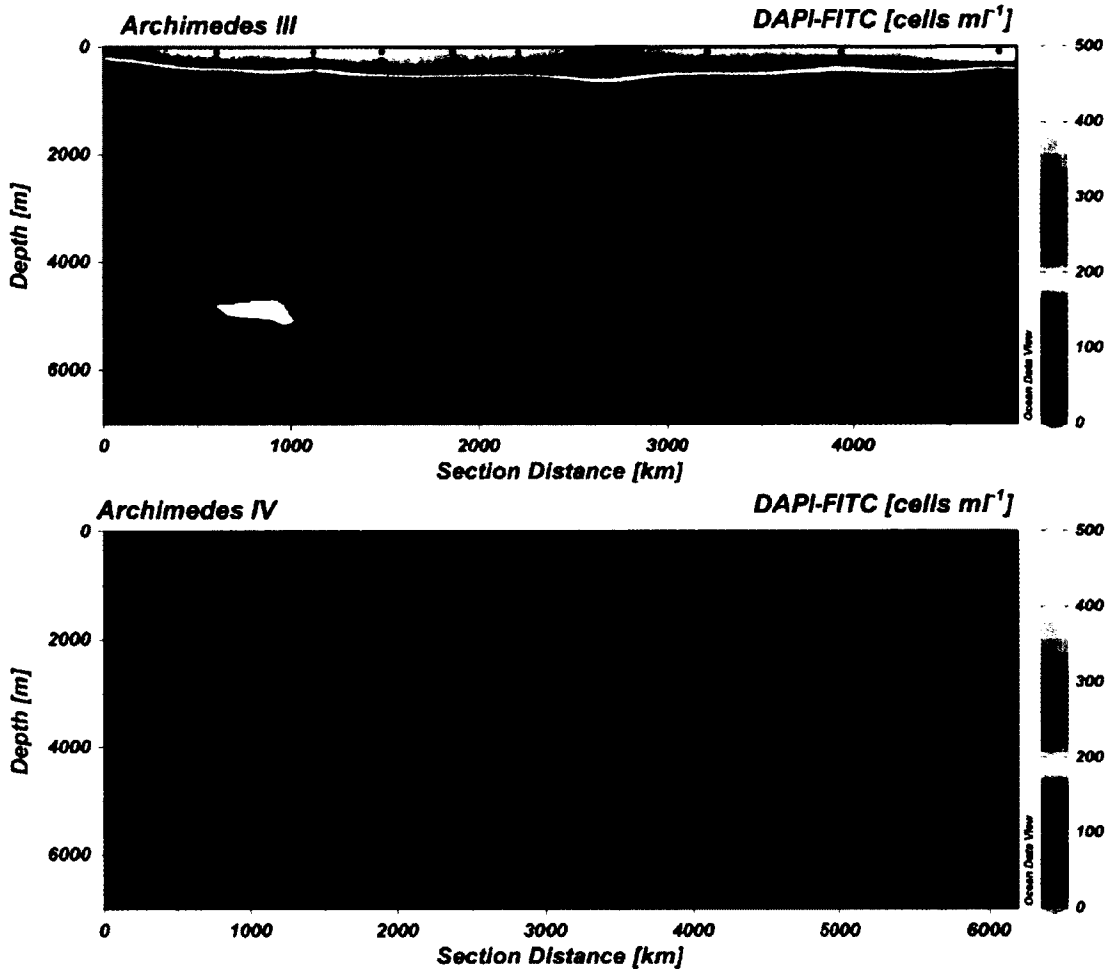

Fig. 7. Abundance of total eukaryotes as measured by DAPI-FITC staining. Higher abundances were recorded throughout the water column during the Archimedes III cruise, which sampled in areas of relatively high productivity including the equatorial upwelling, African coastal upwelling, and the TENATSO time-series station near the Cape Verde islands, whereas lower abundances were found during the Archimedes IV cruise which sampled within the oligotrophic North Atlantic gyre. Along-transect trends in total eukaryote abundance did not exist for either cruise. Bottom topography (taken from General Bathymetric Chart of the Oceans) is only approximate, and does not exactly

Fig. 7 Continued.

match our transects. Consequently, some sample locations appear below the sea floor. All samples were taken at least 90 m above the ocean floor.

3.3.2 Diversity

While the proportion of the total eukaryotic organisms identified using universal CARD-FISH probes that could be assigned to one of the seven groups varied greatly between Central Water masses and deeper water masses, the composition of deep-sea eukaryote communities determined by CARD-FISH did not change with depth below the Central Water. In total, 19% of eukaryotes identified by CARD-FISH in the Central Water, 67% in the Intermediate Water, 65% in the upper North Atlantic Deep Water, 50% in the middle North Atlantic Deep Water, 51% in the lower North Atlantic Deep Water, and 53% in the Antarctic Bottom Water belonged to one of the seven groups quantified (Fig. 8). Kinetoplastids were important throughout the water column, accounting for, on average, 7-12% of FISH-labeled eukaryotes in each water mass.

Table 6

Abundance of total eukaryotes and taxonomic groups in deep-sea samples. Only DAPI-FITC staining was conducted on samples from the Archimedes IV cruise, whereas DAPI-FITC and CARD-FISH analyses were performed on Archimedes III samples. All values are presented as cells ml^{-1}. EUK+KIN: combined abundance of EUK516 and KIN516 probes, representing the total eukaryote abundance as measured by CARD-FISH. Target groups of probes are EUK516: eukaryotes excluding kinetoplastids, KIN516: kinetoplastids, LabY: labyrinthulomycetes, PF2: fungi, Alv01: group II alveolates, DiploR1792: diplonemids, NS4: MAST 4 stramenopiles. Overall eukaryote abundance and most taxonomic groups decreased approximately 20-fold over the depth range sampled, with the notable exception of the split nucleus morphotype, which remained nearly constant at all depths.

		Archimedes IV		Archimedes III									
Water Mass		DAPI-FITC	Split nucleus	DAPI-FITC	Split nucleus	EUK+KIN	EUK516	KIN516	LabY	PF2	Alv01	Diplo-R1792	NS4
Central Water	Mean	72.2	2.2	384.7	6.0	57.2	52.9	4.35	0.89	1.04	1.31	0.47	0.71
	SD	35.5	1.3	185.9	3.5	52.3	51.6	3.85	1.11	1.53	1.91	0.58	0.72
Intermediate Water	Mean	13.0	1.3	72.9	4.4	4.4	3.8	0.53	0.15	0.24	0.35	0.12	0.25
	SD	11.1	0.8	24.1	2.2	2.3	2.1	0.21	0.11	0.23	0.58	0.08	0.14
Deep Water	Mean	3.6	0.5	35.3	4.2	3.6	3.3	0.23	0.10	0.11	0.17	0.06	0.07
	SD	1.4	0.3	10.3	1.6	2.8	2.7	0.14	0.07	0.09	0.14	0.05	0.09
Bottom Water	Mean	2.8	0.5	20.5	4.2	3.3	3.1	0.23	0.05	0.15	0.12	0.06	0.03
	SD	0.7	0.2	10.1	2.0	3.2	3.1	0.10	0.03	0.31	0.10	0.05	0.03

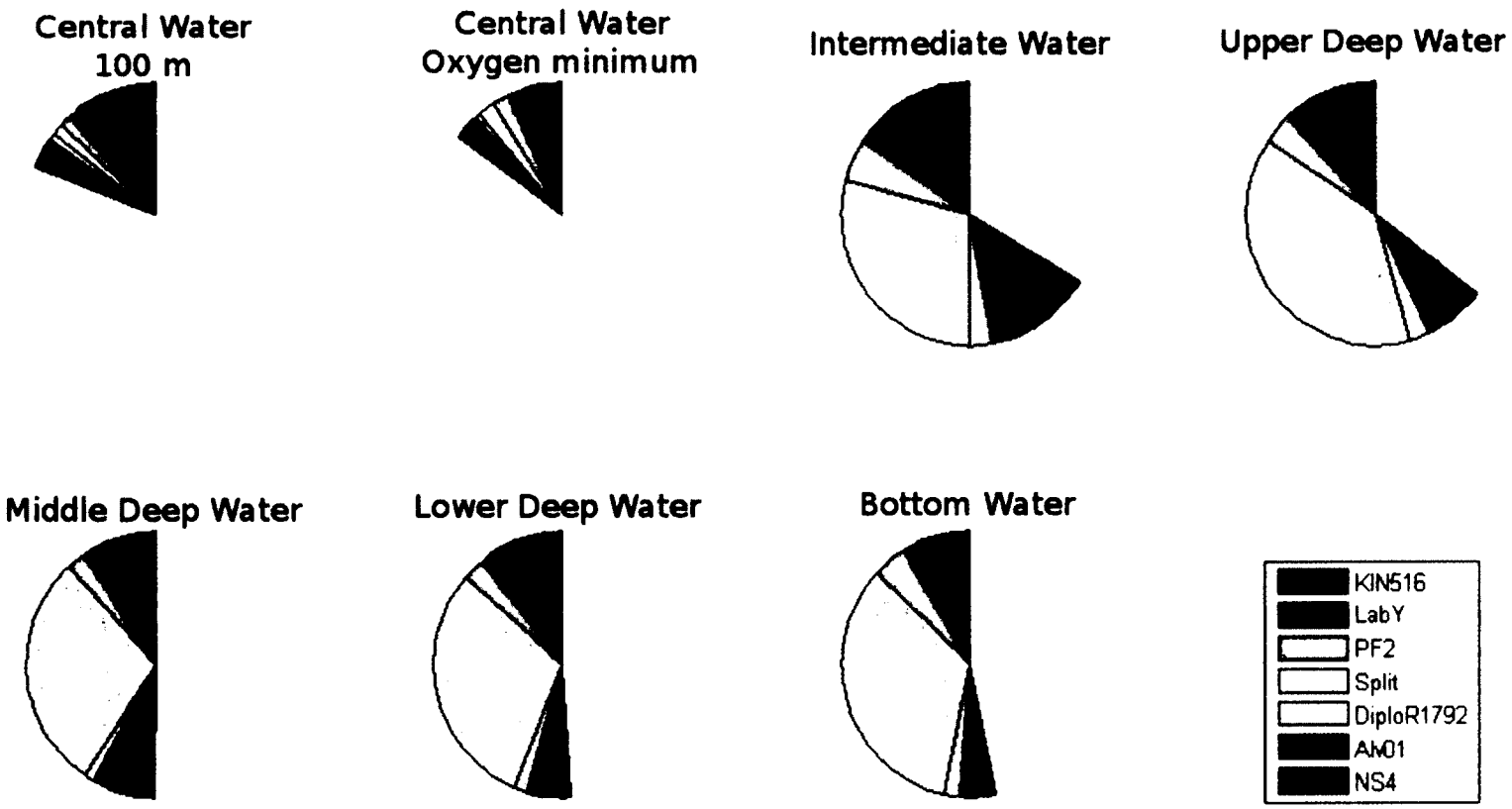

Fig. 8. Proportion of organisms identified using CARD-FISH and morphology.

Fig. 8 Continued. Proportion of organisms identified using CARD-FISH and morphology as a proportion of total eukaryotes as determined by the sum of organisms hybridizing with the probes EUK 516 and KIN 516 (Chapter 2). A full circle represents the mean of total EUK516+KIN516 counts in each water mass. KIN516, LabY, PF2, DiploR1792, Alv01 and NS4 correspond to probes listed in Table 1. The split morphotype was identified based on its appearance using DAPI stain. The Central Water, including the 100 m samples and the oxygen minimum zone had much lower proportions of identified eukaryotes than deeper water masses, driven primarily by an increase in the relative abundance of the split nucleus morphotype in deep water. The Central Water had much higher total eukaryote abundance due to the presence of phototrophic eukaryotes which are absent in deep water. The largest proportion of eukaryotes was identified in the Intermediate Water, where kinetoplastids, fungi, group II alveolates, and MAST 4 stramenopiles were all represented in greater proportions than in either shallower or deeper water masses.

Labyrinthulomycetes, fungi, diplonemids, Group II alveolates, and MAST 4 stramenopiles were small but consistent contributors to eukaryotic communities at all depths (Fig. 8). Averaged within each water mass, 1.6-3.4% of total FISH-identified eukaryotes were labyrinthulomycetes, and there was no significant difference among water masses (ANOVA, $n = 35$, $F = 0.10$, $p = 0.75$). Similar to the labyrinthulomycetes, fungi made up 1.8-5.5% of FISH-identified eukaryotes, and showed no significant difference in relative abundance among water masses (ANOVA, $n = 35$, $F = 0.09$, $p = 0.76$). Diplonemids accounted for 0.8-2.7% of eukaryotes with no difference among water masses (ANOVA, $n = 35$, $F = 2.45$, $p = 0.14$). Group II alveolates made up 2.3-8.0% with no difference among water masses (ANOVA, $n = 35$, $F = 0.20$, $p = 0.66$), and MAST 4 stramenopiles accounted for 0.9-5.7% of eukaryotes with no difference among water masses (ANOVA, $n = 35$, $F = 0.15$, $p = 0.72$). Because the normality assumption of the ANOVA was violated using these proportion data, the p-values were calculated using a custom F-distribution based on 10,000 randomizations of the present data.

The unidentified split nucleus morphotype (Morgan-Smith et al., 2011) was the most abundant group in deep water samples, and showed a marked increase in abundance as a proportion of total eukaryotes with increasing depth. It readily hybridized with EUK516 but not with any of the other probes. In the Central Water, 2.3% (SD = 2.1) of FITC-labeled eukaryotes were the split nucleus morphotype, increasing to 6.1% (SD = 2.2) in the Intermediate Water, 12.5% (SD = 5.0) in the North Atlantic Deep Water, and 22% (SD = 10) in the Antarctic Bottom Water. Significant differences in the split nucleus as a proportion of total eukaryotes existed among all water masses except the Intermediate and Deep Water masses (ANOVA, $n = 33$, $F = 43.2$, $p < 0.0001$).

3.3.3 Abundances of eukaryotic microbes in relation to abiotic factors

While different in magnitude (ANCOVA comparison of elevation on log-transformed abundance data, $n = 204$, $F = 409$, $p < 0.0001$), the abundance of eukaryotic microbes during the two cruises showed the same rate of decrease with depth (ANCOVA test for homogeneity of slopes on log-transformed eukaryote abundance, $n = 204$, $F = 1.1$, $p = 0.296$). Samples collected within the Romanche Fracture Zone showed no significant difference in eukaryote abundance from other Antarctic Bottom Water samples (Fig. 7; one-way ANOVA, $n = 34$, $F = 2.58$, $p = 0.083$).

Trends in deep-water abundance along the cruise transect differed among taxonomic groups (Fig. 9). Labyrinthulomycetes (LabY), fungi (PF2), and Group II alveolates (Alv01) all had their highest deep-water abundance in the region of the equatorial upwelling, which coincides with the Romanche Fracture Zone. MAST 4 (NS4) and diplonemids (DiploR1792) both showed patchiness in their deep-water distribution, but no discernible geographic trend. The split nucleus morphotype (Split) was the only group with no significant difference in abundance between shallow and deep water masses, but it was significantly higher at stations east of the Mid-Atlantic Ridge (one-way ANOVA, $n=45$, $F=3.87$, $p=0.029$), with peak abundance at the station closest to the African coast (Fig. 9).

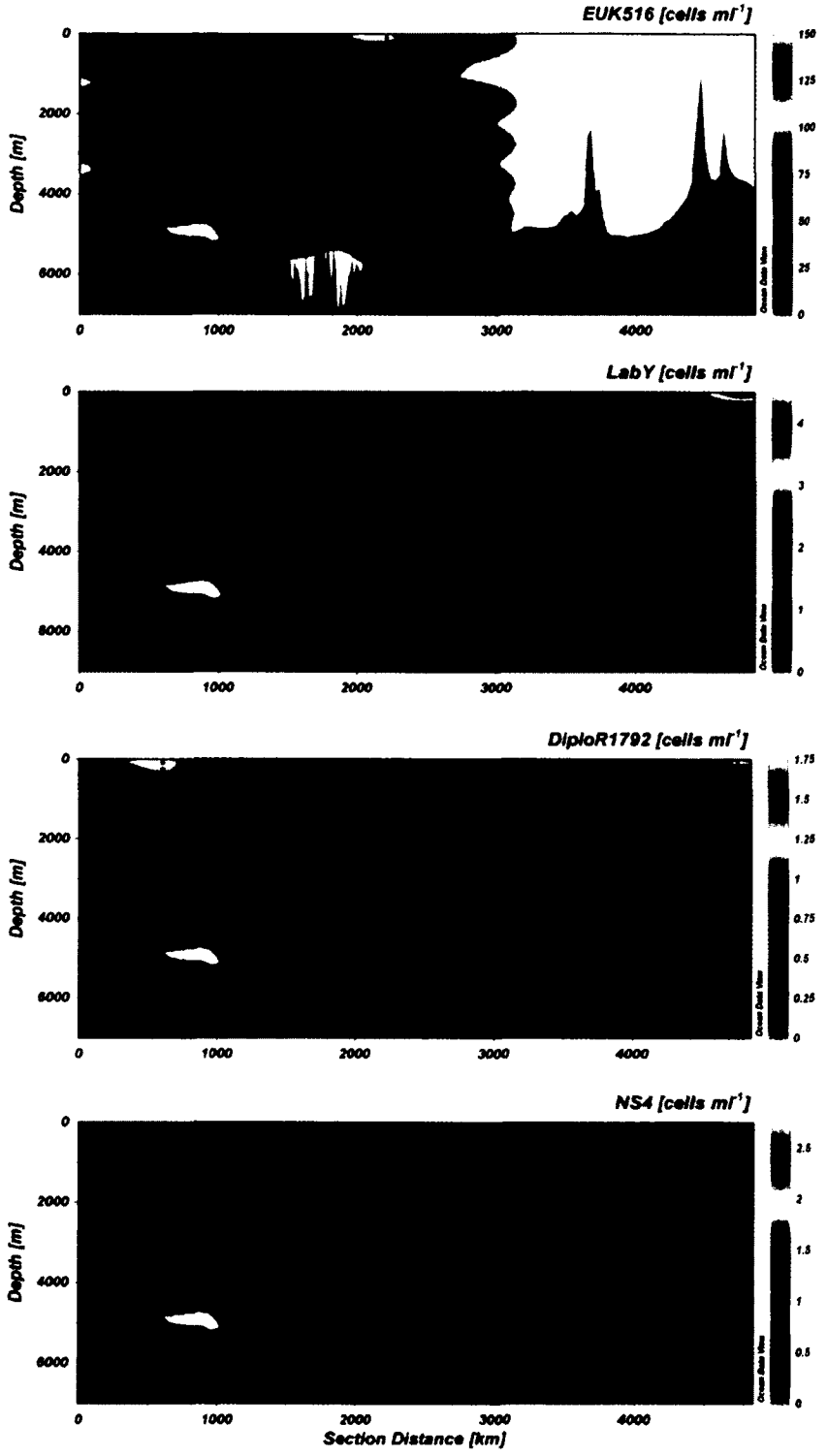

Fig. 9. Along-transect patterns in abundance of groups during Archimedes III.

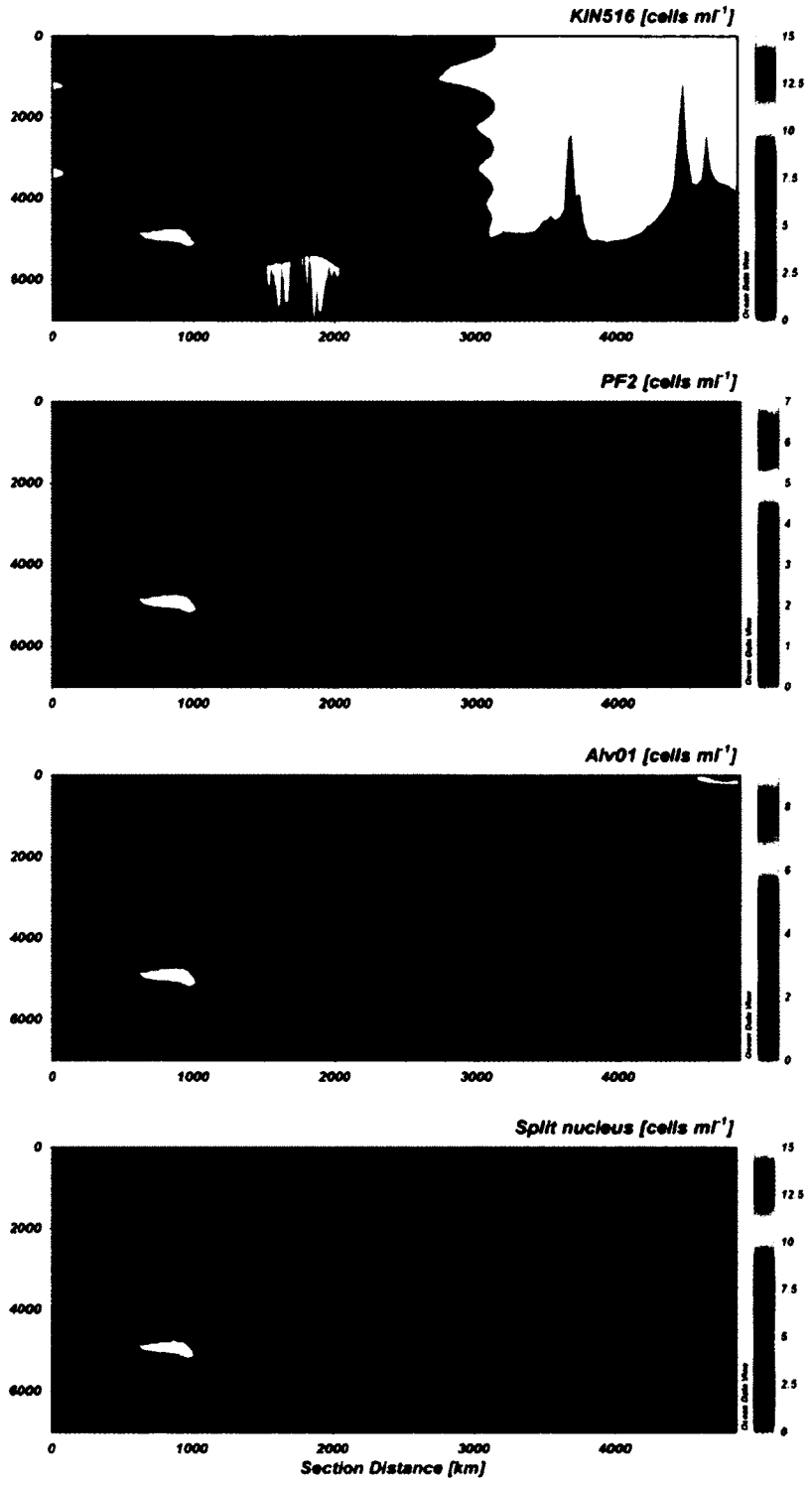

Fig. 9 Continued.

Fig. 9 Continued. Section begins near Brazil coast, crosses the Mid-Atlantic Ridge at the Romanche Fracture Zone (1500-2000 km), then turns northwest to follow the African coast (2500 km) (red triangles in Fig. 6). EUK516 and KIN516 hybridizations were not performed on all samples. Both saprotrophic groups, the labyrinthulomycetes (LabY) and fungi (PF2) showed an increase in abundance at all depths in the region of the equatorial upwelling and Romanche Fracture Zone (1500-2000 km), as did Alv01. DiploR1792 and NS4 showed a patchy distribution in deep water that does not appear to be tied to geographic factors. Split nucleus, unlike any other group, did not generally decrease in abundance with increasing depth, though it did show an increase in stations near the African coast (after 2500 km) versus those in the transect across the Atlantic basin (prior to 2500 km).

Principal component analysis showed that the first component, driven largely by depth, accounted for 48% of the variability among samples, and the second component, which was tied most strongly to latitude, accounted for another 17% (Fig. 10). Abundances of all taxonomic groups and total eukaryotes correlated negatively with depth, and therefore with Component 1. The groups were divided on whether they correlated positively (split nucleus, Alv01) or negatively (DiploR1792, NS4, PF2, and LabY) with Component 2, representing latitude (Fig. 10). Total eukaryote counts based on DAPI-FITC staining did not correlate with Component 2 (Fig. 10).

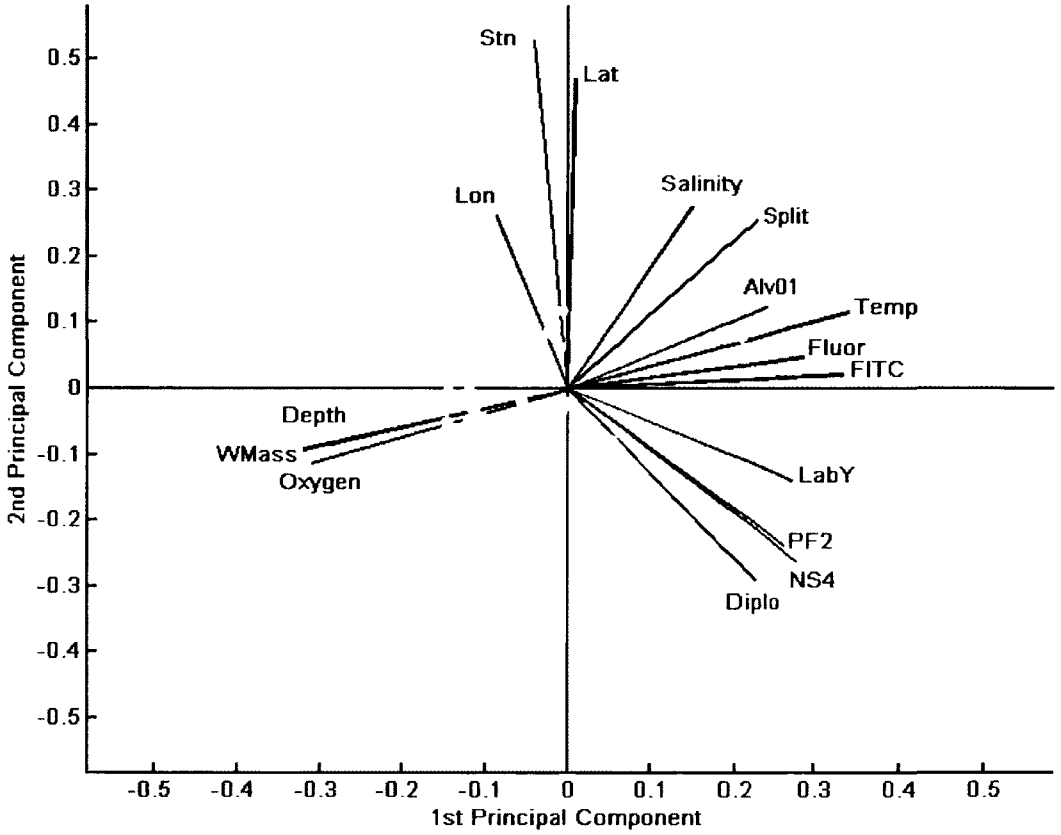

Fig. 10. Bi-plot of Principal Component Analysis on samples from Archimedes III. Gray points represent individual water samples (i.e. a specific station and depth), and black lines are variables measured for each sample. Points that fall near each other correlate with the same variables; points that fall near a line correlate positively with that variable, and points in the opposite quadrant of the graph from a line correlate negatively with that variable. Component 1 is strongly tied to depth, and explains 47.8% of the variability among samples. All taxonomic groups tested, as well as temperature and chlorophyll fluorescence, were negatively correlated with depth, having a positive loading in component 1 while depth and water mass have a strongly negative loading in this component. Oxygen shows a strong positive loading in Component 1. Component 2,

Fig. 10 Continued.

which correlates most strongly with geographic factors (Station, Latitude, and Longitude), explains 16.6% of the sample variability.

Surface water primary productivity, calculated based on satellite data, showed a strong positive regression with eukaryote abundance in all water masses when data from both cruises were combined and a time lag was applied to account for the transport of material to a given depth (Table 7, Fig. 11, 12). Because samples taken on different cruises are not directly comparable, and the residual pattern was unacceptable, a combined regression between cruises must be treated as invalid. No significant trend existed for the individual cruises, except for the Intermediate and Labrador Sea Water in Archimedes IV (Table 7). However, protist abundance was significantly different between the two cruises in every water mass (Table 7A, Fig. 12). Sea-surface chlorophyll obtained from MODIS Aqua imagery, with the same time lag applied, showed no significant relationships within individual cruises (Table 7, Fig. 12). To compare productivity, chlorophyll, and eukaryote abundance between cruises, ANOVA and Wilcoxon rank sum analyses were performed (Table 7B). Significant differences were found between cruises in every water mass where productivity or eukaryote abundance were analyzed, and the only non-significant result was for the chlorophyll estimates for the Intermediate Water using the rank sum test (Table 7B).

Table 7

Regression, ANOVA, and rank sum analysis of sea-surface chlorophyll and primary productivity against deep-sea eukaryote abundance. Cruise 3: Archimedes III, 4: Archimedes IV, 3&4: combined data from Archimedes III and IV cruises. Productivity: Behrenfeld-Falkowski model primary productivity (mg C m^{-2} d^{-1}), Chlorophyll: sea-surface chlorophyll (mg m^{-3}) from MODIS Aqua imagery, FITC: total eukaryote abundance measured with DAPI-FITC staining. For both primary productivity and chlorophyll, 8-day composite values were used with a lag of 8 days per 1000 m water depth to account for the sinking time of particulate matter from the surface to reach deep water masses. Bold font indicates significant results at the $\alpha = 0.05$ level. Panel A: Regression analysis showed that a relationship between productivity or chlorophyll at the surface and eukaryotes at depth rarely existed within individual cruises. Panel B: ANOVA showed significant differences between the two cruises, but failed to meet the assumption of normally distributed residuals (Kolmogorov-Smirnov test, data not shown), so in addition, the non-parametric Wilcoxon rank sum test was used for inter-cruise comparison.

Table 7 Continued.

A

Cruise	Water Mass	X	n	R^2	P
3	Central	Productivity	18	0	1
3	Intermediate	Productivity	12	0.056	0.45
3	Deep	Productivity	33	0.0078	0.64
3	Bottom	Productivity	12	0.0053	0.82
3	Central	Chlorophyll	18	0	1
3	Intermediate	Chlorophyll	12	0.022	0.71
3	Deep	Chlorophyll	33	0.016	0.55
3	Bottom	Chlorophyll	12	0.18	0.22
4	Central	Productivity	21	0	0.70
4	Intermediate	Productivity	44	**0.095**	**0.042**
4	Labrador	Productivity	29	**0.49**	**0.0073**
4	Deep	Productivity	22	0.11	0.080
4	Bottom	Productivity	13	0.10	0.16
4	Central	Chlorophyll	21	0	0.50
4	Intermediate	Chlorophyll	44	0.033	0.25
4	Labrador	Chlorophyll	29	0.041	0.53
4	Deep	Chlorophyll	22	0.018	0.54
4	Bottom	Chlorophyll	13	0.11	0.23

B

Cruise	Water Mass	X	n	F	p	rank sum	p
3 & 4	Central	Productivity	39	**17.1**	**0.0002**	**525**	**<0.0001**
3 & 4	Intermediate	Productivity	56	**23.6**	**<0.0001**	**494**	**0.0025**
3 & 4	Deep	Productivity	75	**31.3**	**<0.0001**	**1704**	**<0.0001**
3 & 4	Bottom	Productivity	34	**14.2**	**0.0007**	**297**	**0.0018**
3 & 4	Central	Chlorophyll	30	**13.1**	**0.0011**	**215**	**0.0088**
3 & 4	Intermediate	Chlorophyll	52	**9.4**	**0.0035**	306	0.105
3 & 4	Deep	Chlorophyll	61	**21.3**	**<0.0001**	**1089**	**<0.0001**
3 & 4	Bottom	Chlorophyll	26	**68.2**	**<0.0001**	**215**	**<0.0001**
3 & 4	Central	FITC	38	**57.1**	**<0.0001**	**502**	**<0.0001**
3 & 4	Intermediate	FITC	56	**156.7**	**<0.0001**	**602**	**<0.0001**
3 & 4	Deep	FITC	72	**383.4**	**<0.0001**	**1767**	**<0.0001**
3 & 4	Bottom	FITC	33	**65.4**	**<0.0001**	**330**	**<0.0001**

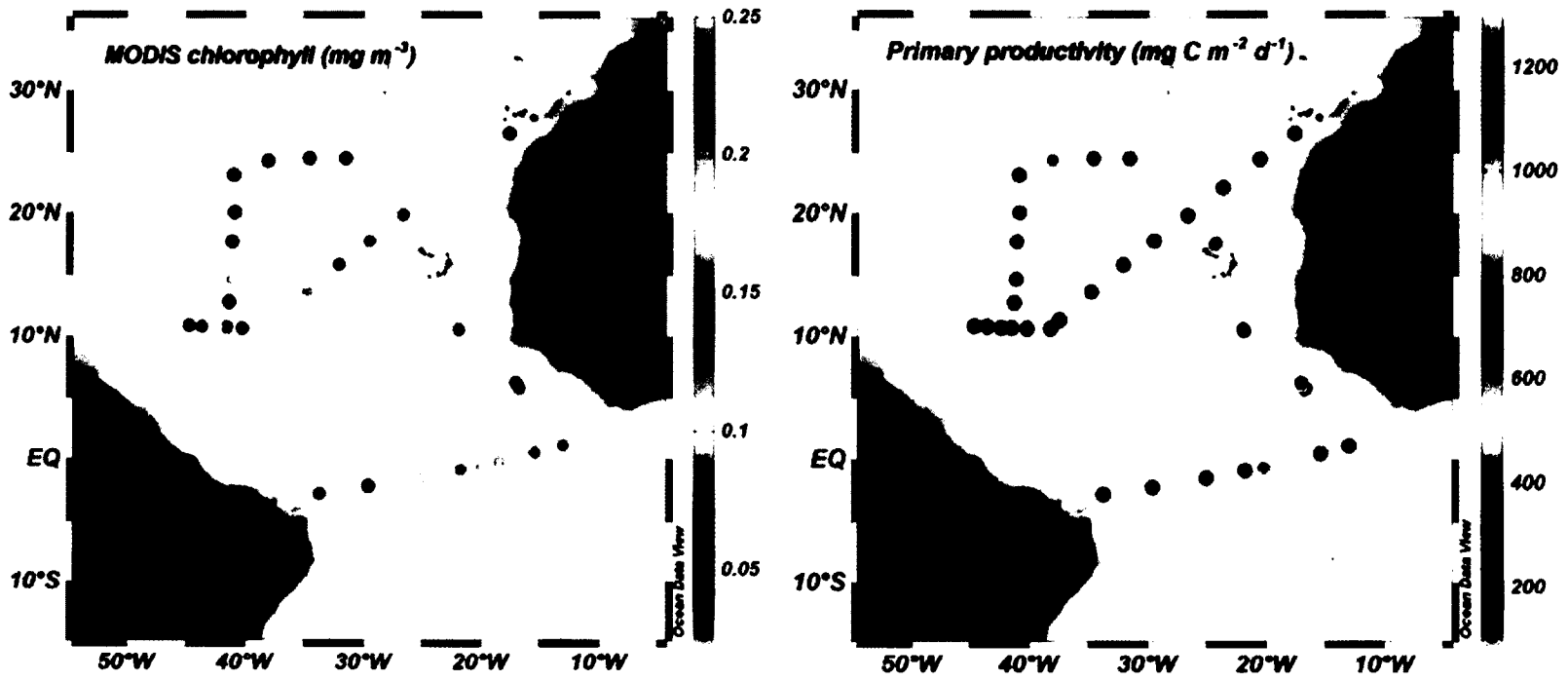

Fig. 11. Surface chlorophyll and primary productivity at sampling locations.

Fig. 11 Continued. Chlorophyll (left panel) values are from MODIS Aqua, mg m^{-3}; figure draws from several eight-day composite images during and immediately prior to sampling so that all stations would be represented despite missing data due to cloud cover and sun glint. Primary productivity (right panel) using Behrenfeld and Falkowski model, mg C m^{-2} d^{-1}, with each point representing the value from the eight-day average immediately preceding our visit to the station, i.e. the productivity value used in comparisons with protist abundance in the upper 1000m.

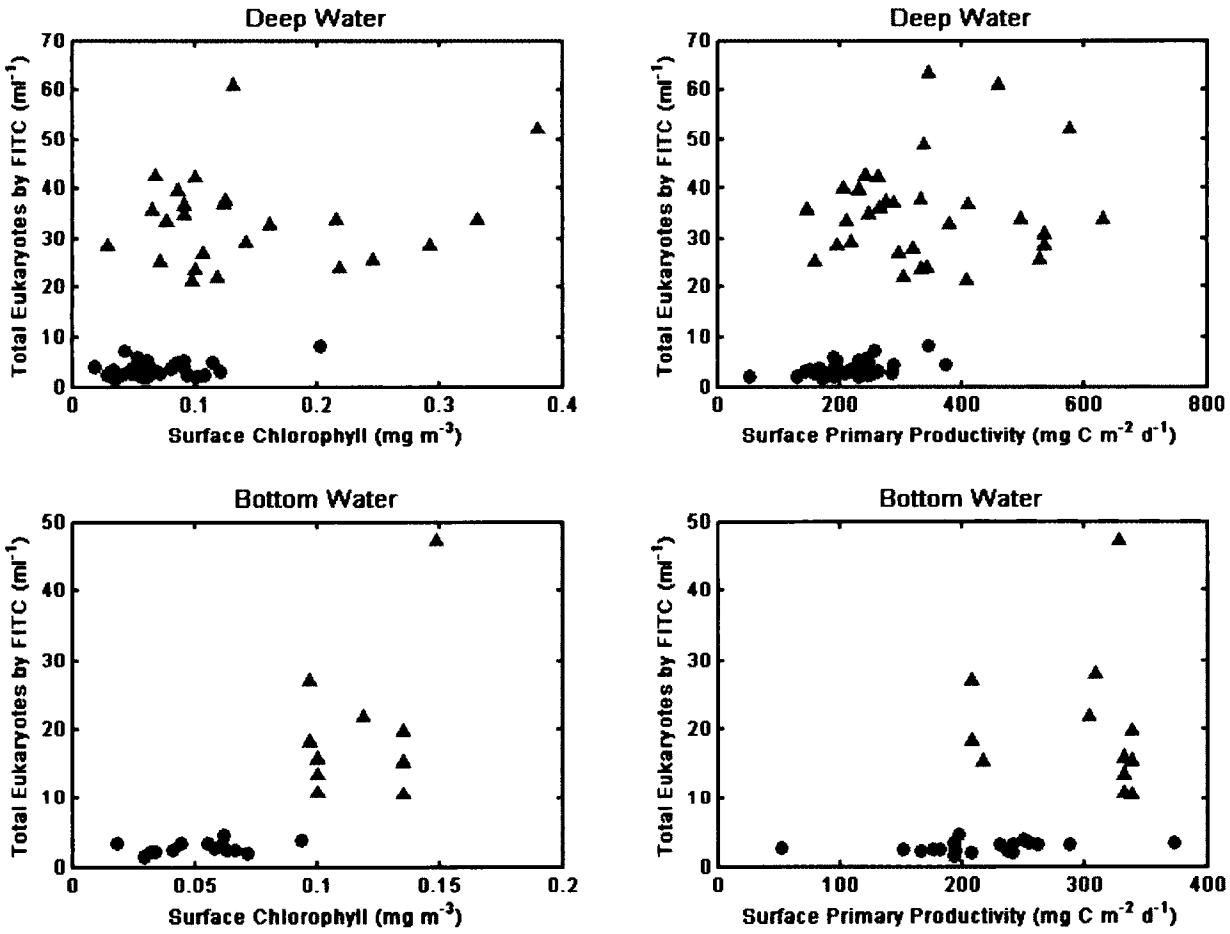

Fig. 12. Eukaryote abundance in deep water and surface productivity.

Fig. 12 Continued. Data from Archimedes III (red triangles) and Archimedes IV (green circles) cruises combined. Chlorophyll (left panels) values are from MODIS Aqua; primary productivity (right panels) using the Behrenfeld and Falkowski (1997) model, with a time lag applied to account for delivery of surface material to the deep ocean on particles at a rate of 1000 m per 8 days.

Labyrinthulomycete abundance significantly correlated with dissolved organic phosphorus (DOP; n = 68, Pearson's r = 0.259, p = 0.039) and carbon (DOC; n = 62, Pearson's r = 0.298, p = 0.025) and were the only group to show such a correlation. However, a Type I error is a possible cause of this association, given that many correlations between taxonomic groups and environmental variables were tested. Although the abundance of labyrinthulomycetes did not correlate with oxygen, two samples from the oxygen minimum zone contained this taxon in approximately five-fold higher abundance than other samples collected at similar depths (data not shown). There were no significant correlations between eukaryote abundance or diversity measures (DAPI+FITC, EUK516+KIN516, or any of the individual probes) and abundance of particles as measured by video observation (particle data from Bochdansky et al., 2010). Kinetoplastids, many of which are particle affiliated, showed no relationship with particle abundance (n = 31, Pearson's r = 0.017, p = 0.93).

3.4 Discussion

3.4.1 Abundance

The overall abundance of eukaryotes measured by CARD-FISH was approximately ten-fold lower than that estimated using DAPI-FITC staining (Table 6), consistent with our previous work (Morgan-Smith et al., 2011). There was also a significant difference between the two cruises, a finding which is not surprising given the regional differences in surface productivity overlying the water masses sampled. This finding suggests a possible connection between the microbial productivity at depth and

surface productivity. Assuming that most protists are bacterivores, organic carbon transported to the deep ocean on sinking particles may cascade to microbial predators through higher prokaryotic productivity (see section 4.3).

3.4.2 Diversity

Seven groups within the eukaryotes were quantified, six using CARD-FISH probes for taxonomic groups of interest, and one based on morphology, which we call the split nucleus morphotype. In combination, 50-67% of all eukaryotic organisms were attributable to these groups in the deep water masses, but only 19% in the Central Water mass. Kinetoplastids made up 7-12% of the FISH-identified eukaryotes averaged within each water mass. Kinetoplastids, which were identified with the KIN516 probe (Bochdansky and Huang, 2010), are a deep branch in the eukaryote tree with sequence mismatches to the most commonly used general eukaryote probes (EUK516 and EUK1209; Bochdansky and Huang, 2010), leading to their exclusion in FISH-based enumeration of eukaryotes. Kinetoplastids are well-known from live counts of deep-sea protists (Arndt et al., 2003), and are also readily identified in DAPI-stained samples due to the presence of the kinetoplast, a single large mitochondrion characteristic of this group. There was no significant correlation between kinetoplastids and the abundance of particles as measured by video observation. This result is surprising given that the kinetoplastids, the most abundant taxon determined by CARD-FISH in this study, are frequently particle-affiliated and because particles are an important source of organic carbon in the deep ocean (e.g., Bochdansky et al., 2010).

Labyrinthulomycetes, which includes the labyrinthulids and thraustochytrids, is a taxon primarily made up of saprotrophic protists, with a few bacterivorous and parasitic members (Raghukumar, 1992). The thraustochytrids are obligately marine, feed by expelling an ectoplasmic net which can penetrate particles, are known to break down refractory carbon sources such as pine pollen (Raghukumar, 2002), and have been recorded as a small portion of sequences in deep-sea clone libraries (López-Garcia et al., 2001a). No culture-independent quantification of this group in the deep sea has previously been made. Labyrinthulomycete abundance was positively correlated with DOP and DOC, a relationship also recorded for thraustochytrids in the coastal ocean (Kimura et al., 2001), although the latter group is not known to consume dissolved organic matter directly, feeding instead on organic particles (Raghukumar, 2002).

We quantified fungi, another saprotrophic group, using the PF2 probe (Kempf et al., 2000). Fungi have often been used as model organisms in experimental work of pressure effects, where they maintained metabolic activity at pressures up to 1 GPa (Sharma et al., 2002) despite damage to cell structures including the nuclear membrane and mitochondria at pressures of 100 MPa (Shimada et al., 1993). Marine yeasts have been grown in culture at pressures of 40 MPa (Lorenz and Molitoris, 1997) and have been recovered from the deep sea using cultivation-dependent methods (Raghukumar and Damare, 2008) as well as sequence-based methods (López-Garcia et al., 2001a). Neither saprotrophic taxon increased in deep water masses, where the available carbon is increasingly refractory (Bauer et al., 1992).

Diplonemids, like kinetoplastids, form a basal branch of the eukaryotic tree. They have been identified by sequence analysis in the deep sea (López-Garcia et al., 2001a),

where they exhibit high diversity (Lara et al., 2009). In our samples, diplonemids made up a very small proportion (0.8-2.7% of total eukaryotes), and were the least abundant group in all water masses. However, this group's low abundance does not preclude the high diversity recently reported in deep-sea diplonemids (Lara et al., 2009). The combination of high diversity and low abundance places diplonemids within the eukaryotic rare biosphere (*sensu* Sogin et al., 2006).

Alveolates (Group II) and stramenopiles (MAST 4) were not as dominant in this study as we expected given their abundance reported in previous studies based on 18S rRNA sequences (e.g. Countway et al., 2007; López-Garcia et al., 2001a; Massana et al., 2002). Group II alveolates made up approximately 2-8% of FISH-identified eukaryotes, while López-Garcia et al. (2001a) found Group I and II to account for most of the diversity and 67-75% of sequences recovered from 250-3000 m in Antarctic waters, with Group II being more highly represented in the 2000-3000 m samples. The MAST 4 stramenopiles are abundant in surface waters in all ocean basins except in polar regions (Massana et al., 2006), making up on average 19% of the heterotrophic flagellates in surface samples taken over a seasonal cycle (Massana et al., 2002). In contrast, this group represented only 1.9% of FISH-labeled eukaryotes in our shallowest samples (100 m, which fell within the Central Water and the photic zone). One reason for this discrepancy is that total eukaryote counts by CARD-FISH comprise phototrophs as well as heterotrophs, increasing the total count by which the abundance of each taxon is divided and thus giving lower proportional abundances for heterotrophic taxa when compared to studies that only enumerated heterotrophic nanoflagellates. Although MAST 4 stramenopiles may be sensitive to the low temperature of the deep sea, as evidenced by

their absence in polar regions (Massana et al., 2006), temperature would not explain their low abundance in Central Water samples, where the temperature was 10-12 °C.

The split nucleus morphotype remained constant in absolute abundance throughout the water column, therefore becoming more dominant in deep samples, as overall eukaryote abundance declined with depth. Although this morphotype was identified using morphology rather than a FISH probe, it hybridizes readily with the EUK516 general eukaryote probe. This organism, which has not yet been identified taxonomically, has been previously recorded with a similar distribution pattern in the deep sea (Morgan-Smith et al., 2011). The most striking basin-scale distribution feature is its increase from the western to the eastern basins of the Atlantic by approximately 1.4-fold at depths below 1000 m (Fig. 9)

3.4.3 Abundances of eukaryotic microbes in relation to abiotic factors

The proportion of eukaryotes identified in the seven groups was lower in the oxygen minimum zone than in the other water masses. Previous work has found unusual eukaryotic communities in low-oxygen environments, including clades at the base of the eukaryotic tree that appear to be unique to anoxic environments (Dawson and Pace, 2002). These clades have been found in environments as disparate as the water column of the Cariaco Basin (Stoeck et al., 2003) and a Danish fjord (Zuendorf et al., 2006). Anoxic marine environments also contain deep branches within established clades, including subsets of the alveolates and stramenopiles different from those quantified in this study (Stoeck et al., 2003; Zuendorf et al., 2006). Saprotrophic groups, including the fungi and Labyrinthulomycetes, were consistently represented in clone libraries from anoxic water

columns (Edgcomb et al., 2011; Stoeck et al., 2003; Zuendorf et al., 2006). The thraustochytrids, a subset of the Labyrinthulomycetes, reach a similar biomass as bacteria in the pronounced oxygen minimum zone of the Arabian Sea (Raghukumar et al., 2001). Although we found no significant correlation between oxygen and labyrinthulomycete abundance, two samples from the oxygen minimum zone were highly enriched with labyrinthulomycetes, with approximately five-fold higher abundance than well-oxygenated samples. Because the oxygen levels measured in our samples were never as low as those in the Arabian Sea or Cariaco Basin, the increase in labyrithulomycetes in these two samples may be due to suboxic microniches within particles, which support different prokaryotic and eukaryotic communities than the surrounding water (Artolozaga et al., 2000; DeLong et al., 1993), and which may be important in oxygen consumption in the deep sea (Bochdansky et al., 2010).

The eukaryotic taxa identified in this study showed different trends of abundance in deep water along the cruise track (Fig. 9). Several groups (i.e., fungi, labyrinthulomycetes, and Group II alveolates) increased in the region of the equatorial upwelling, which is directly above the Romanche Fracture Zone. These taxa are likely influenced by the high surface productivity of this region relative to adjacent areas providing an elevated particulate organic matter supply to deep waters. Specifically, the saprotrophic labyrinthulomycetes and fungi, both of which can use decaying phytoplankton as a food source (Raghukumar et al., 2001), increased in abundance in the equatorial upwelling area. Previous work has found labyrinthulomycete biomass comparable to that of bacteria during the decay phase of some phytoplankton blooms (Raghukumar et al., 2001). Another factor may be an increase in particulate or dissolved

organic matter within the Romanche Fracture Zone due to leaching or resuspension from the canyon walls, an idea supported by an increase in macroscopic particles in this region (Bochdansky et al., 2010). Group II alveolates also showed an increase in abundance in this region despite not being known to be particle-affiliated or saprotrophic, suggesting that their relationship with the productive waters above must be indirect, likely through an increase in bacterial prey compared to other deep-sea regions. Neither MAST 4 (stramenopiles) nor diplonemids showed a consistent geographic or productivity-related trend along the cruise track (Fig. 9). The split nucleus morphotype showed no consistent difference in abundance between shallow and deep waters, albeit lower abundances were found in the deep water at in the western basin and within the Romanche Fracture Zone than in the eastern basin, where the cruise track followed the African coastline (Fig. 9). In addition, the highest split nucleus abundances throughout the water column occurred at the stations near the African coastal upwelling. In this region, satellite-derived chlorophyll concentration and primary productivity showed strong local gradients in both space and time, with stations exhibiting extremely high and extremely low productivity in close proximity (Fig. 11) as currents and eddies transport rich upwelled waters (see also Arístegui et al., 1997). Thus, a given location in the region likely exhibits a pulsed or sporadic transport of particles into the deep sea. Since the lifestyle of the unidentified split nucleus organism is not known, it is impossible to explain the increase in cell abundance at those stations, however, it might be linked to oceanographic features.

Depth is the most important factor in the variability among samples, as shown by Principal Component Analysis (Fig. 10). Abundance of eukaryotes in all taxonomic groups correlated negatively with depth, and the loading in this component was high for

all taxa, indicating that these correlations are strong. Geographic factors including latitude and longitude, representing the different oceanic regimes sampled during the two cruises, formed a second component, which had a positive correlation with some groups (split nucleus, Alv01) and a negative correlation with others (DiploR1792, NS4, PF2, and LabY).

Regional differences in primary productivity and surface chlorophyll sometimes correlate with the abundance of microbial eukaryotes even in the deepest water masses (Table 7). However, significant differences in all measurements (i.e. productivity, chlorophyll, and eukaryote abundance) between cruises make regression analysis across the full data set invalid. (Fig. 12). In this study, we compared data from two cruises which were conducted in very different productivity regimes within the tropical and subtropical Atlantic Ocean. Archimedes III passed through the equatorial upwelling and African coastal upwelling, and also sampled the TENATSO time-series station, close to the Cape Verde Islands. All these locations exhibited greater surface chlorophyll and primary productivity as derived from satellite data when compared to the gyre stations sampled during Archimedes IV (Fig. 11), and Archimedes III also exhibited higher abundances of eukaryotes at all depths sampled (Fig. 7). It should be noted that no surface samples were taken on either cruise, with the shallowest sample at each station collected at 100 m depth, so no direct validation of the satellite data is possible. Uncertainty in the satellite derived chlorophyll levels arise from cloud cover, sun glint, and the exclusion of chlorophyll below the uppermost layer of the ocean. To establish a relationship between surface production and deep-water eukaryote abundance is outside the scope of this study, but the interaction between surface productivity and eukaryote

abundance in deep waters warrants further investigation, with samples taken from more disparate environments. If such a relationship is found to exist, it could be due to increased export of particulate material which provides a food source either directly to saprotrophic eukaryotes or indirectly by supporting bacterial populations which are grazed upon by bacterivorous eukaryotes. These particles may also act as "hot spots" of biological activity, concentrating organic substrates and prokaryotic prey so that eukaryotes can thrive in the deep ocean where prey or substrate concentration in the ambient water otherwise would be too low to support them (Bochdansky et al., 2010).

3.5 Conclusion

The deep-sea eukaryotic community is made up of a few dominant and a large number of much less abundant taxa, many of which are not yet taxonomically identified. This finding broadly supports the idea of a rare biosphere among eukaryotic microbes in the ocean. The abundance and diversity of deep-water eukaryotes reflect surface ocean productivity conditions when compared across different oceanic regimes. This observation suggests a strong coupling between the microbial food webs of the surface and deep ocean, driven by sinking particles which carry organic matter and bacterial prey to deep-sea eukaryotic communities.

CHAPTER 4

INCUBATION OF FLAGELLATE CULTURES UNDER SIMULATED DEEP-SEA CONDITIONS

4.1 Introduction

The aphotic zone of the deep ocean accounts for 95% of the marine habitat by volume (Arístegui et al., 2009), but has not been studied to the same extent as surface waters due to the difficulties of sampling such a distant and sparsely inhabited environment. Therefore, to provide insights regarding life in the deep sea, the physiological and population-level effects of high pressure and low temperature were examined using organisms isolated in surface waters and subjected to conditions of the deep sea for one to two weeks. This time scale replicates the time it would take an average particle to reach the bathypelagic after forming and being populated with protists in the surface ocean, to answer the question of whether surface-adapted flagellates can seed populations in the deep sea.

Many studies of pressure effects have been undertaken to understand specific cell processes. Cell morphology, membrane structure, flagellar motility, protein function, and gene expression are all influenced by high pressure (reviewed by Bartlett, 2002, Simonato et al., 2006). At the same time, high-pressure environments have been suggested as the habitat where life began (Daniel et al., 2006), making studies of organisms in this habitat particularly important. Pressure effects, and the adaptation to high pressures known as piezophily, have been studied in all three domains of life. Most

work has focused on bacteria, with many piezophilic strains isolated and maintained in laboratory high pressure vessels (Bartlett, 2002). In addition, pressure effects on specific cell components and processes have been examined in bacteria (reviewed by Bartlett, 2002, Simonato et al., 2006). Among the Archaea, only a few piezophilic organisms have been isolated, but these few organisms represent a broad diversity within the domain, as compared to the fairly narrow taxonomic representation of piezophilic bacterial isolates (Bartlett, 2002, Kato and Qureshi, 1999). Most of the eukaryotes that have been studied are metazoans, especially the crustaceans and fish that inhabit the deep ocean, as well as hydrothermal vent fauna (reviewed by Sebert, 2002). An important exception is the yeast, *Saccharomyces cerevisiae,* which has been used as a model organism in several studies of pressure effects on metabolism (Sharma et al., 2002) and gene expression (Miura et al., 2006). Mortality of *S. cerevisiae* under high pressure has been attributed to damage to intracellular membranes (Brul et al., 2000), cell membranes and the cell wall (Marx et al., 2011), though metabolic processes continued at pressures above 1 GPa (Sharma et al., 2002), a pressure an order of magnitude greater than that in the deepest ocean trench.

Membrane structure is affected by pressure, as mono- and poly-unsaturated fatty acid content is increased in order to maintain the fluidity of membranes in deep-sea organisms (Allen et al., 1999, DeLong and Yayanos, 1985). Changes in the distribution of structural membrane proteins, respiratory chain trans-membrane proteins, and transporters has also been observed in response to high pressure (Vezzi et al., 2005) and protein folding has been shown to be inhibited at 400 MPa (Gross and Jaenicke, 1994). While these pressures are much higher than those experienced in the deep sea, function has also been shown to be affected at pressures less than 110 MPa, which exist in the

ocean's deepest regions (Simonato et al., 2006). The effect of pressure on proteins is caused by changes not only in protein conformation, but also in interactions with water molecules, which are necessary for protein function (Balny et al., 1997). Bacterial motility can also be reduced, as both formation and function of bacterial flagella are degraded under high pressure (Meganathan and Marquis, 1973, Welch et al., 1993). Enzymes can lose their function at pressures characteristic of deep sea environments, including mitochondrial and chloroplast F_1F_0 ATP-synthases, which are inactivated at 50MPa (Dreyfus et al., 1988, Souza et al., 2004). Pressures characteristic of ocean depths of 1000 - 5000 m can lead to physiological responses, including expression of heat and cold stress proteins when temperature stress is not present (Welch et al., 1993) and accumulation of osmolytes which may be used to stabilize proteins against pressure effects or reduce the energetic cost of osmoregulation under pressure (Kelly and Yancey, 1999).

Most previous studies of pressure effects on marine microbes are from short-term incubations, sometimes under pressures much higher than those observed in the deep ocean, using axenic cell cultures or isolated cell components (e.g. Miura et al., 2006, Welch et al., 1993). While these studies are necessary for understanding physiological responses to pressure, they do not replicate the conditions faced by organisms which are transferred from the surface to the deep ocean via advection or riding on sinking particles, which is an equally important objective. Studies in which natural particle-affiliated prokaryote communities were subjected to increasing pressure over several days showed that function but not taxonomic structure of prokaryote communities was affected by pressure (Tamburini et al., 2006). In particular, degradation of fecal pellets by

prokaryotic communities was inhibited by high hydrostatic pressure (Tamburini et al., 2009). However, this work was limited to bacteria, and one cannot assume that the effects on eukaryotes will be the same, because the details of cell membrane structure, biochemical makeup, cell physiology, and reproduction differ among the three domains (Woese et al., 1990), and all of these factors can be affected by the temperature and pressure of the deep sea (Bartlett et al., 2002, Rivalain et al., 2010). Another important difference between previous work and this study is the length of time that organisms were incubated at high pressure. Most previous studies investigated acute effects of pressure on cells or cell components in short-term incubations (one to several hours) (e.g. Miura et al., 2006, Welch et al., 1993). However, longer timescales are important for studying population growth due to the slow rates of respiration and reproduction exhibited by deep-sea organisms (reviewed in Arístegui et al., 2009, Morita, 1984). In this study, we incubated flagellate cultures under simulated deep-sea conditions for one to two weeks in order to examine not only immediate effects of pressure but also the longer-term recovery from the initial stress response.

We subjected two model flagellates, *Cafeteria roenbergensis* Fenchel et Patterson (Fenchel and Patterson, 1988) and *Neobodo designis* (Skuja) Vickerman (Moreira et al., 2004), both isolated from surface water, along with a mixed community of bacterial prey, to incubations lasting one to two weeks and measured the population-level response to temperature and pressure conditions representative of the deep ocean. These organisms were chosen because *Cafeteria roenbergensis*, although cosmopolitan in surface waters, is generally absent from the deep sea, while *Neobodo designis* is common in both surface and deep waters. We used a semi-continuous flow-through system, which allowed daily

subsampling without loss of pressure to the main culture chamber. Cultures were not acclimated to the experimental temperature and pressure conditions prior to the start of each experiment, so this work represents a perturbation experiment and not a study of steady-state conditions.

4.2 Methods

4.2.1 Pressure system

The high-pressure system (HPS) used in these experiments consisted of a 200-ml titanium culture vessel attached to a 14-ml stainless steel subsampler, with pressure maintained by a high-pressure liquid chromatography (HPLC) pump (Fig. 13). All components that came into contact with the culture medium or cultured organisms upstream of the subsampler were made of titanium or non-reactive plastics to prevent iron contamination, which can lead to overgrowth of iron-oxidizing bacteria in the pressure vessel. Medium used in these experiments was Instant Ocean brand artificial seawater at 34 ppt, autoclaved and cooled to 15°C, with a metal-free filter (Alltech) fitted to the inflow tubing to prevent any particles from entering the HPS (Fig. 13). Medium was held in a non-pressurized flask connected to the HPLC pump by 1/16" PTFE tubing.

The HPLC pump (Rainin HPXL) pressurized the media, and routed it via 1/16" titanium tubing to deliver the inflowing seawater to the bottom of the chamber (i.e. the opposite end of the outflow). Continuous washing of the HPLC pump head was maintained using a peristaltic pump (Fisher) and deionized water. During all experiments, the needle remained lowered, so that medium was delivered into the bottom of the culture

vessel. Outflow from the top of the pressure vessel was directed through 1/8" titanium tubing (inner diameter 0.094") to the subsampler, with flow controlled by needle valves at both the top and bottom of the subsampler (Jannasch et al., 1973). The subsampler contained a piston with distilled water above it, to maintain pressure during sampling.

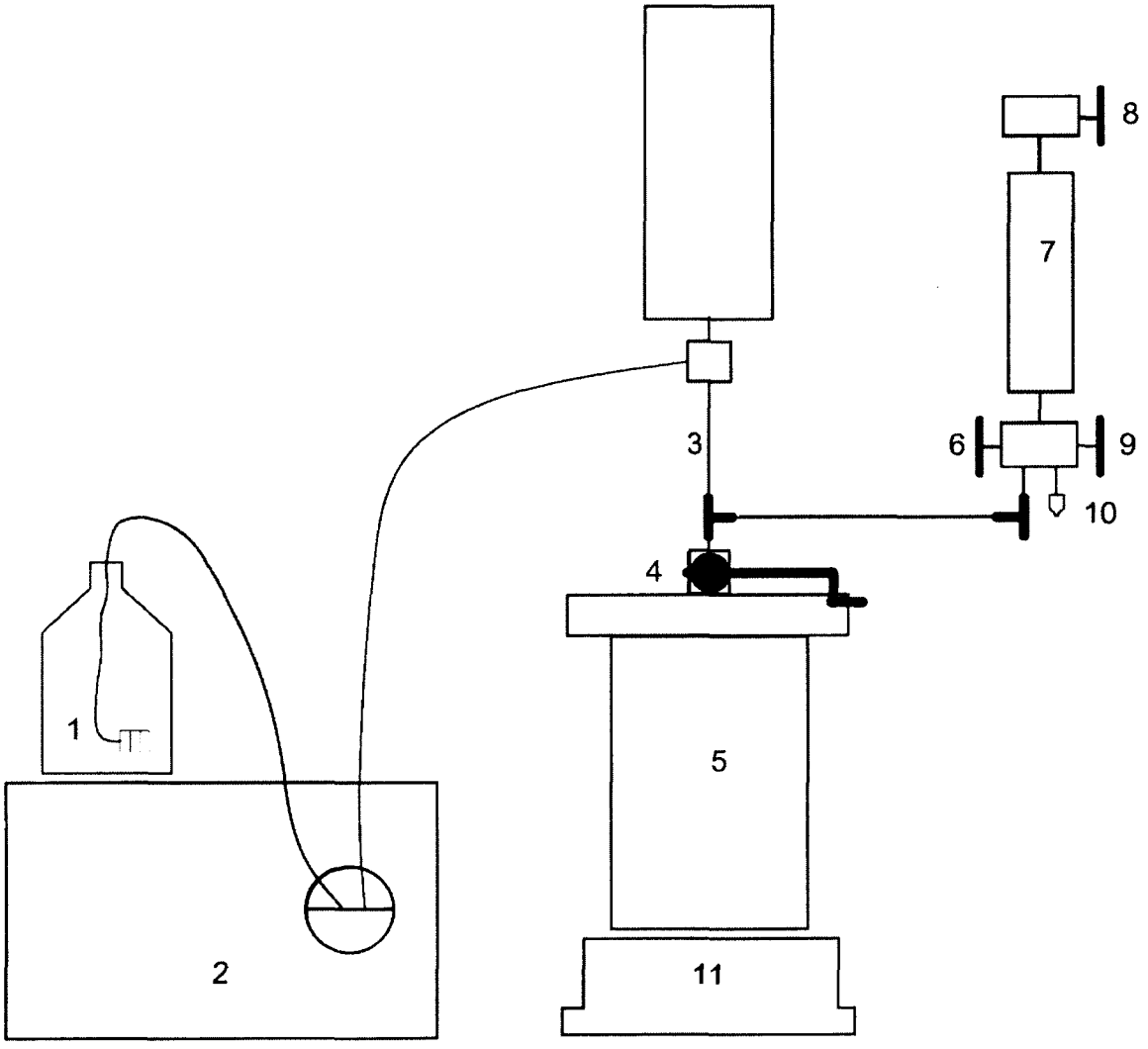

Fig. 13. Schematic of HPS system. 1: media flask, 2: high-pressure liquid chromatography (HPLC) pump, 3: titanium tubing to deliver artificial seawater to the

Fig. 13 Continued.

bottom of the chamber (inflow), 4: outflow at top of chamber, 5: culture vessel, 6: needle valve to subsampler, 7: subsampler, 8: needle valve to hydraulic pump, 9: needle valve to outflow, 10: outflow nozzle, 11: magnetic stirring plate. The subsampler assembly was constructed according to Jannasch et al. (1973).

The subsampler could also be bypassed through the use of the needle valves to send culture directly to the outflow nozzle when pressure release was desired. A small autoclaved PTFE-coated stir bar was placed in the bottom of each pressure vessel prior to filling, and gentle stirring (60 rpm) was maintained during experiments to prevent cultures from settling and ensure that subsamples were representative of the vessel contents. The culture vessel was surrounded by a PVC sleeve connected at the top and bottom via 3/8" inner diameter vinyl tubing to a recirculating chiller (Brinkmann Lauda RM6) filled with 25% Ethylene glycol in water, which maintained a temperature of 2 ± 0.1 °C in the culture vessel. Tubing connecting the cooling sleeve to the chiller was surrounded with foam pipe insulation to prevent warming and buildup of condensation.

4.2.2 Experimental organisms

Two flagellate cultures were used in experiments, the bicosoecid *Cafeteria roenbergensis* Fenchel et Patterson (Fenchel and Patterson, 1998) and the kinetoplastid *Neobodo designis* (Skuja) Vickerman (previously *Bodo designis*; Moreira et al., 2004). *Cafeteria roenbergensis* is ubiquitous in surface waters globally, and occasionally

appears in cultures inoculated from deep ocean water (Arndt et al., 2003, Patterson et al., 1993). In one study, *Cafeteria sp.* was isolated from 2500 m at the site of a hydrothermal vent (Atkins et al., 2000) where water temperature was elevated, which suggests that temperature rather than pressure may be the more important factor in its absence from the deep sea. *Neobodo designis*, and other *Bodo*-type species on the other hand, are regularly identified in live counts and isolations from deep-sea environments (Arndt et al., 2003, Patterson, 1993, Turley et al., 1988). Both flagellates are culture opportunists, and both organisms used in this study were isolated from surface environments. Stock cultures were maintained in well plates in artificial seawater (Instant Ocean, 34 ppt) with a portion of an autoclaved rice grain as an organic carbon source for the heterotrophic bacteria on which the flagellates feed. To grow the large volume of flagellates required for experiments, a continuous-flow chemostat was used. First, a 2 L flask was filled with 600 ml of artificial seawater (Instant Ocean, 34 ppt) amended with 0.05 g L^{-1} peptone and 0.01 g L^{-1} yeast extract (Difco Marine Broth 2216) and inoculated with 3 ml of stock culture of either *C. roenbergensis* or *N. designis*. As these were not axenic cultures, associated heterotrophic bacteria grew in the 2 L flask and provided food for the protists. The cultures were allowed to grow for one week before flow was started. Medium for the chemostat was artificial seawater with 0.1 g L^{-1} peptone and 0.02 g L^{-1} yeast extract, added at a flow rate of 80 ml d^{-1}. The outflow tube of the chemostat was placed at a height such that outflow began when the culture volume reached ~1400 ml, and after that time, inflow and outflow were maintained at the same rate. Once outflow began, culture was sampled daily using a sterile pipette, and an experiment was started when cell densities reached sufficiently high levels (generally above 10,000 cells ml^{-1}). Due to

predator-prey interactions within the flagellate cultures (Massana and Jürgens, 2003; Fig. 14), cell densities of both flagellates and bacterial prey followed a pattern of peaks and crashes. An attempt was made to start experiments during net flagellate population growth near the peak flagellate abundances, but timing of crashes was not always predictable, and consequently led to widely variable starting abundances among experimental runs.

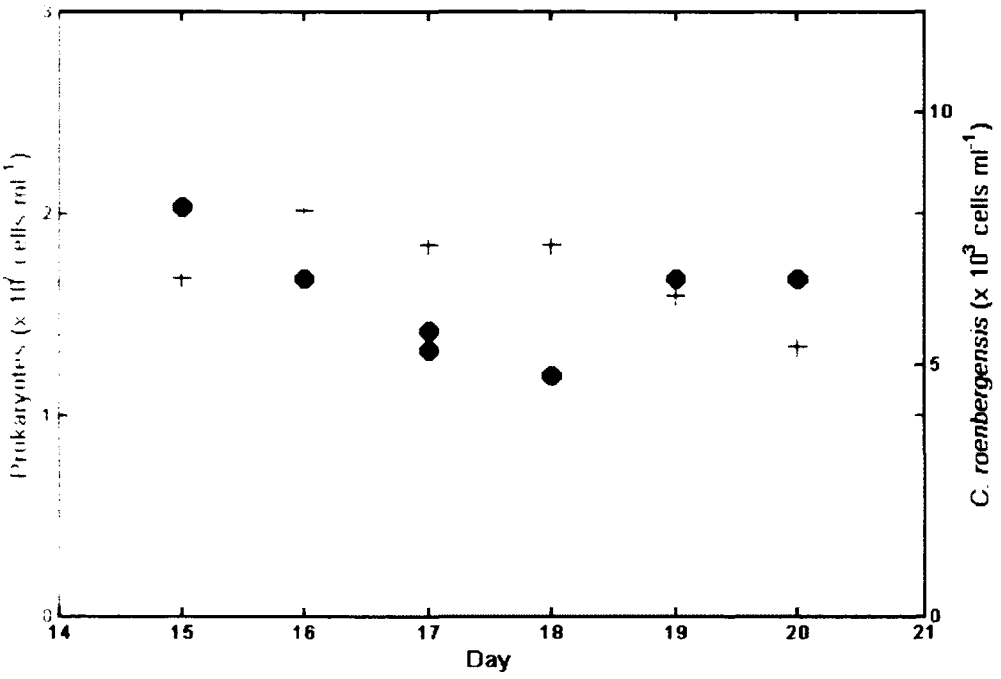

Fig. 14. Chemostat cell abundances for *Cafeteria roenbergensis* and prokaryotes. In general, flagellate abundance (blue circles) increased after a peak in prokaryote abundance (red + symbols), showing predator-prey cycling. An example of this is visible

Fig. 14 Continued.

near the right side of the figure, with prokaryote abundance peaking on day 16 and *C. roenbergensis* increasing from day 18-20 in response. In this case, experiment was initiated on day 20.

4.2.3 Sampling protocol

Experiments were sampled daily, beginning with a time-zero sample collected immediately after the system was assembled and pressurized. This system did not operate as a chemostat because no new carbon was added during incubation. Therefore, the high pressure system can be considered as a batch culture with dilution, and which was repeatedly sampled. Growth rate was not strictly controlled by flow rate as in a typical chemostat system. For sampling, the HPLC pump was turned on to "prime" mode, which allowed a high flow rate of medium into the bottom of the culture vessel. The needle valve between the culture vessel and subsampler was opened slowly to minimize pressure loss, then opened fully once the subsampler had been pressurized, so that shear stress through the valve was minimized. Next, the needle valve at the top of the subsampler was opened slightly, allowing a slow release of the deionized water in the top of the subsampler so that the piston in the subsampler rose and the bottom of the subsampler was filled with culture. When the subsampler was filled, the valve connecting the chamber and subsampler was closed, the HPLC pump priming was stopped, and the valve between the subsampler and the outflow nozzle was opened, depressurizing the subsampler. A hydraulic hand pump was then used to slightly pressurize (maximum

pressure ~1.5 MPa) the water in the top of the subsampler, pushing the piston down and forcing the sample out through the outflow nozzle into a 15-ml polypropylene tube.

After sample collection, oxygen was measured immediately using a microprobe (Unisense, Aarhus, Denmark). The probe was calibrated daily, using air-saturated artificial seawater at the same salinity as culture medium for 100% saturation, and a 0% oxygen standard made by removing the oxygen from artificial seawater with a solution of 0.1M ascorbic acid and 0.1M NaOH through a silicone membrane which is permeable to oxygen but not water or salts. After samples from all vessels were collected (maximum time ~30 minutes), each was mixed gently by inversion and two 5-ml aliquots were removed then fixed with 37% formaldehyde solution to a final concentration of ~2%. Samples were fixed at room temperature overnight, then filtered onto 0.2 μm white polycarbonate filters (type GTTP, Millipore, Billerica, MA, USA) at a pressure of -200 mbar and mounted on microscope slides using Vectashield with 4',6-diamidino-2-phenylindole (DAPI) mounting medium (Vector Laboratories, Burlingame, CA, USA). Slides were stored horizontally at -20°C until analysis.

All slides from *C. roenbergensis* experiments were counted using epifluorescence microscopy (Olympus BX50 microscope, excitation 330-385 nm, emission >420 nm) and both flagellates and bacteria were enumerated. For *N. designis* experiments, only flagellate abundance was measured, as the population of bacteria was so dense that accurate counting was not possible when a large enough sample volume was filtered to allow quantification of flagellates. Most experiments with *N. designis* were run for 9-15 days and for *C. roenbergensis* for 7-8 days. One *N. designis* run lasted only 5 days, as a hurricane led to the closure of the university. At the end of most experiments (four of the

six runs for each organism), a 12-well plate with sterile artificial seawater and a portion of a rice grain in each well was inoculated with serial 10-fold dilutions of culture from each vessel. This allowed an assessment of survival of a small population of cells using the most probable number (MPN) method (Cochran, 1950, Blodgett, 2010) when counts by epifluorescence microscopy were below the detection threshold.

4.2.4 Data analysis

In order to compare experimental runs in which the starting abundance of flagellates was different, each abundance measurement was divided by the abundance in that chamber at the beginning of the experiment (time zero) and multiplied by 100 to give a percentage of the initial cell count. The resultant values are presented throughout the paper as "normalized cell counts". Epifluorescence counts below the detection limit were treated as zero values. Statistical analyses were performed in Matlab, using the Statistics Toolbox.

4.3 Results

4.3.1 Cafeteria roenbergensis

Abundance of *C. roenbergensis* decreased in all chambers, but the decline was steeper under high pressure with an average of 1.6 (SD = 3.8)% of the initial count after seven days versus 8.4 (SD = 21.3)% in the control chambers (Fig. 15). To linearize the data of the time series, cell numbers were natural log transformed over days 0-5, when exponential decrease in abundance occurred, for ANCOVA analysis. The slope of decrease in cell numbers with time was significantly greater in high pressure chambers

(ANCOVA test for homogeneity of slopes, $F = 11.2$, $p = 0.0011$, $n = 138$), using data pooled from all six runs. In one of the six experiments, cell counts apparently increased after day five in both high and low pressure treatments (Fig. 15, Run 3), but not enough data were available to determine whether or not this increase was statistically significant.

Repeated measures ANOVA was performed to compare the two pressure treatments over the entire study period, which could not be simply transformed to meet the linearity requirement of ANCOVA. Because this was not a crossover design (i.e., the same organisms were not measured under high and low pressure conditions), subject matching was used (Davis, 2010) and found to be significant ($F = 4.0$, $p < 0.0001$, $n = 324$), allowing the assumptions of the test to be met (Davis, 2010). Although time had a strong effect on abundance ($F = 85$, $p < 0.0001$, $n = 324$), neither the pressure ($F = 3.6$, $p = 0.07$, $n = 324$) nor pressure-time interaction ($F = 0.75$, $p = 0.64$, $n = 324$) were significant using this analysis over the entire period of incubation.

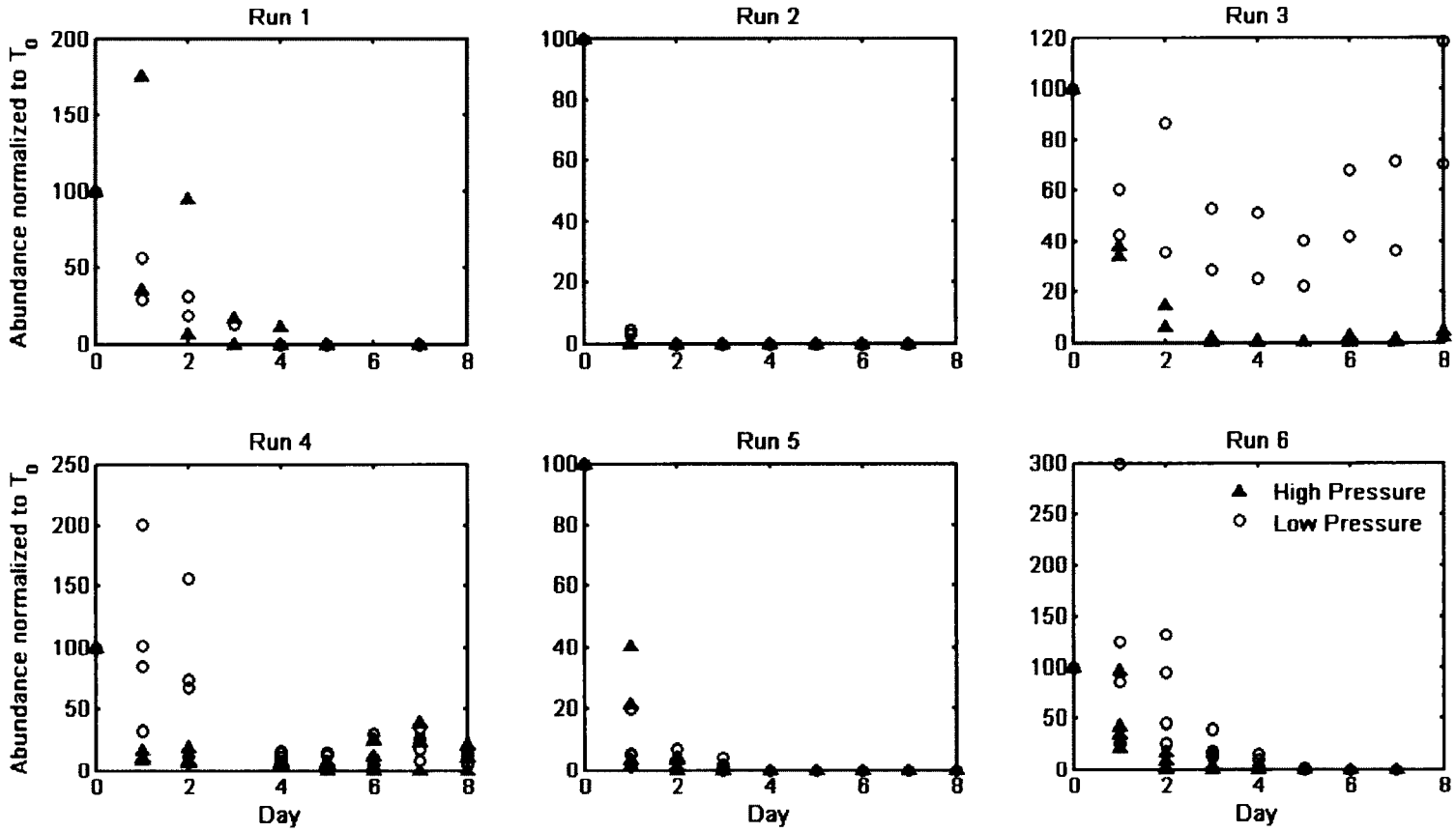

Fig. 15. *Cafeteria roenbergensis* abundance normalized to time zero for six experiments.

Fig. 15 Continued. High pressure treatments shown with red triangles, low pressure with blue circles. Each experimental run consisted of two high pressure and two low pressure chambers, with either single (runs 1-3) or duplicate (runs 4-6) subsamples taken from each chamber daily. In most experiments, abundance in both high and low pressure treatments decreased rapidly below detection by epifluorescence microscopy. In runs 3 and 4, a population increase occurred after several days, but this was not seen in other experiments.

In the *C. roenbergensis* experiments, prokaryote abundance declined slowly over the study period in all chambers. Rather than the exponential decrease seen in *C. roenbergensis* counts, prokaryote abundance decreased only at the rate of dilution due to daily sampling. This means that no net growth or mortality of prokaryotes occurred during the experiments. After subtraction of the rate at which a passive particle would be removed (Fig. 16), the slope of prokaryote abundance over time was not significantly different from zero (ANCOVA, $n = 281$, $F = 2.65$, $p = 0.10$). The rate of decrease of prokaryote abundance was not significantly different between high and low pressure treatments (ANCOVA test for homogeneity of slopes, $n = 281$, $F = 0.19$, $p = 0.66$).

Dissolved oxygen fell in all chambers during the study period. Although fresh medium was air-saturated at 15°C and atmospheric pressure, this input was not enough to replace the oxygen consumed by respiration within the culture vessels. Minimum oxygen saturation reached ~20% in some chambers.

Serial dilution cultures inoculated at the end of most experiments showed that some *C. roenbergensis* cells survived in all chambers, even when their abundance was too low to count accurately using epifluorescence microscopy. Most probable number (MPN) estimates showed no difference between low and high pressure treatments (Student's paired t-test, $n = 8$, $t = -0.64$, $p = 0.57$; Fig. 17).

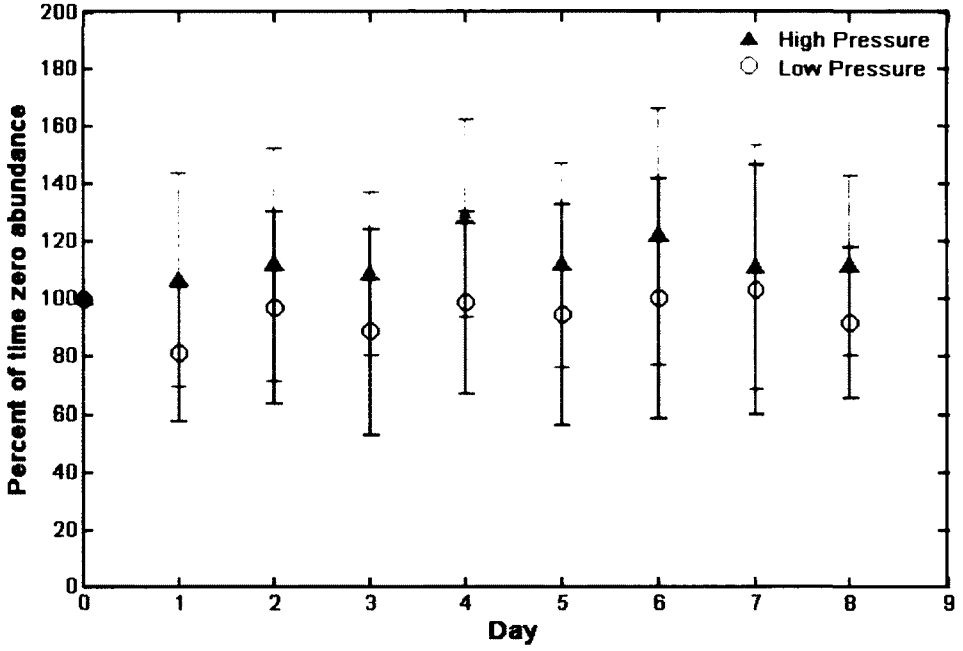

Fig. 16. Prokaryote abundance during *Cafeteria roenbergensis* experiments. Abundance (mean ± SD) has been normalized to time zero and corrected for passive removal of cells during daily sampling. Abundance did not change over the course of the experiments although high and low pressure treatments were significantly different in terms of absolute numbers.

4.3.2 Neobodo designis

Abundance of *N. designis* decreased sharply after time zero, then leveled after about five days (Fig. 18). The average final abundance was 10.0 (SD = 6.1)% of the initial abundance in high pressure treatments, and 31.4 (SD = 31.2)% in low pressure

chambers, with high variability among experiments. The rate of decrease in cell abundance was compared between high and low pressure treatments using ANCOVA on normalized, ln-transformed cell abundances over days 0 - 5 of each experiment (the time period during which exponential decrease in abundance occurred), pooled for all six runs. The slopes did not differ between the two treatments ($F = 0.01$, $p = 0.94$, $n = 286$), but the elevation of the intercept was significantly different ($F = 102$, $p < 0.0001$, $n = 286$), with higher cell abundances in low pressure treatments. Repeated measures ANOVA was performed on pooled data for all six runs, normalized to time zero but not linearized. Subject matching was significant ($F = 8.1$, $p < 0.0001$, $n = 144$). The strongest effect was time ($F = 82$, $p < 0.0001$, $n = 144$), but both the pressure ($F = 10$, $p = 0.004$, $n = 144$) and pressure-time interaction ($F = 2.3$, $p = 0.008$, $n = 144$) were also significant.

Experiments with *N. designis* were performed for a longer period than for *C. roenbergensis* to obtain more data on the increase in cell abundance occasionally seen at the end of an experiment. *Neobodo designis* did exhibit net population growth in the latter part of some experiments (visually estimated from Fig. 18: run 1 low pressure and both treatments of run 3 appear to have maintained net population growth after ~5 days of incubation; both treatments of runs 2 and 4 and run 6 high pressure had net growth after ~5 days followed by a decline or leveling off; and run 1 high pressure, both treatments of run 5, and run 6 low pressure seem to level off without going through a period of net population growth). The growth rate, time of onset, and difference between high and low pressure treatments varied considerably among runs (Fig. 18). Oxygen declined throughout each run, with a minimum of 5% air saturation measured, though most runs ended at approximately 20% saturation.

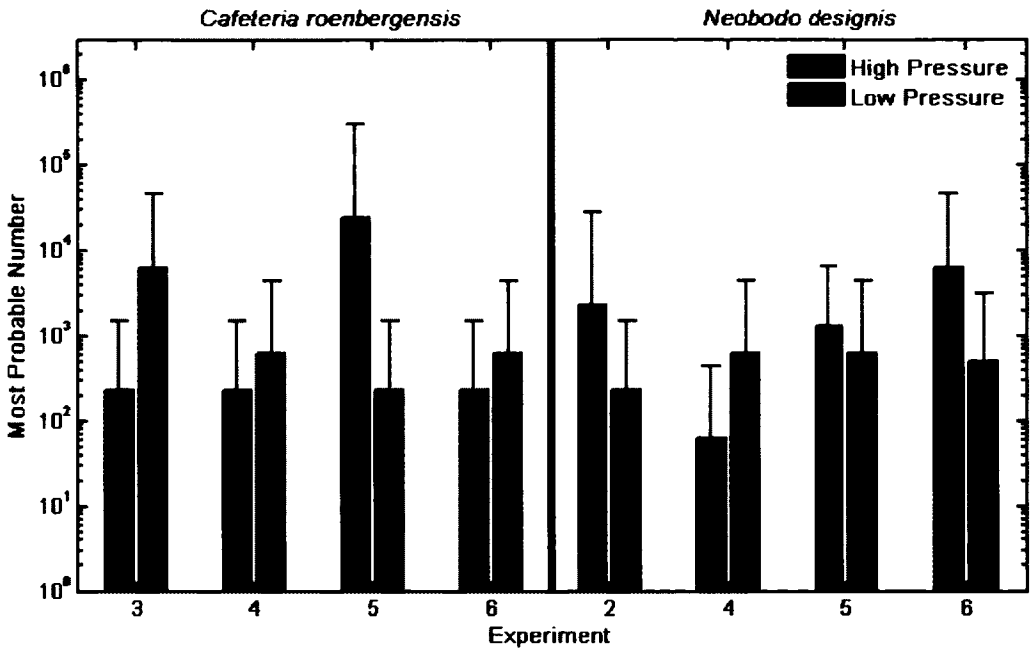

Fig. 17. Most probable number (MPN) estimates of flagellate cells remaining at the end of experiment based on dilution cultures. Each bar represents two replicate chambers from a single experiment. Error bars indicate high and low 95% confidence intervals for MPN. X axis corresponds to experimental run; dilution cultures were not prepared for all runs.

Using MPN estimates from dilution cultures, we found an average of 1203 (SD = 2029) cells ml^{-1} remained in high pressure treatments, and 4296 (SD = 8154) cells ml^{-1} in low pressure treatments at the termination of the experiments (Fig. 17). These numbers were not significantly higher than epifluorescence counts at the end of each experimental run, which were 61 (SD = 114) cells ml^{-1} in high pressure treatments (Student's t-test, t = -1.7, p = 0.10, n = 18) and 740 (SD = 1657) cells ml^{-1} in low pressure treatments

(Student's t-test, t = -0.56, p = 0.58, n = 19). MPN showed no difference between low and high pressure treatments (Student's paired t-test, n = 8, t = -1.46, p = 0.24; Fig. 17).

4.3.3 Comparison of organisms

Cafeteria roenbergensis and *N. designis* behaved differently both in terms of the initial decrease in cell abundance and the level at which abundance stabilized or grew at the end of an experiment. For *C. roenbergensis*, the initial decrease was more abrupt, with abundance dropping below the detection limit of our epifluorescence microscopy method after only two days in some cases (Fig. 15). Abundance of *N. designis,* by comparison, generally continued its exponential decrease until about day five, though generalizations are difficult due to the variability among experimental runs (Fig. 18). The ln-transformed cell abundance over days 0-5 was compared between the two organisms using ANCOVA homogeneity of slopes, and was significantly different (n = 430, F = 35,

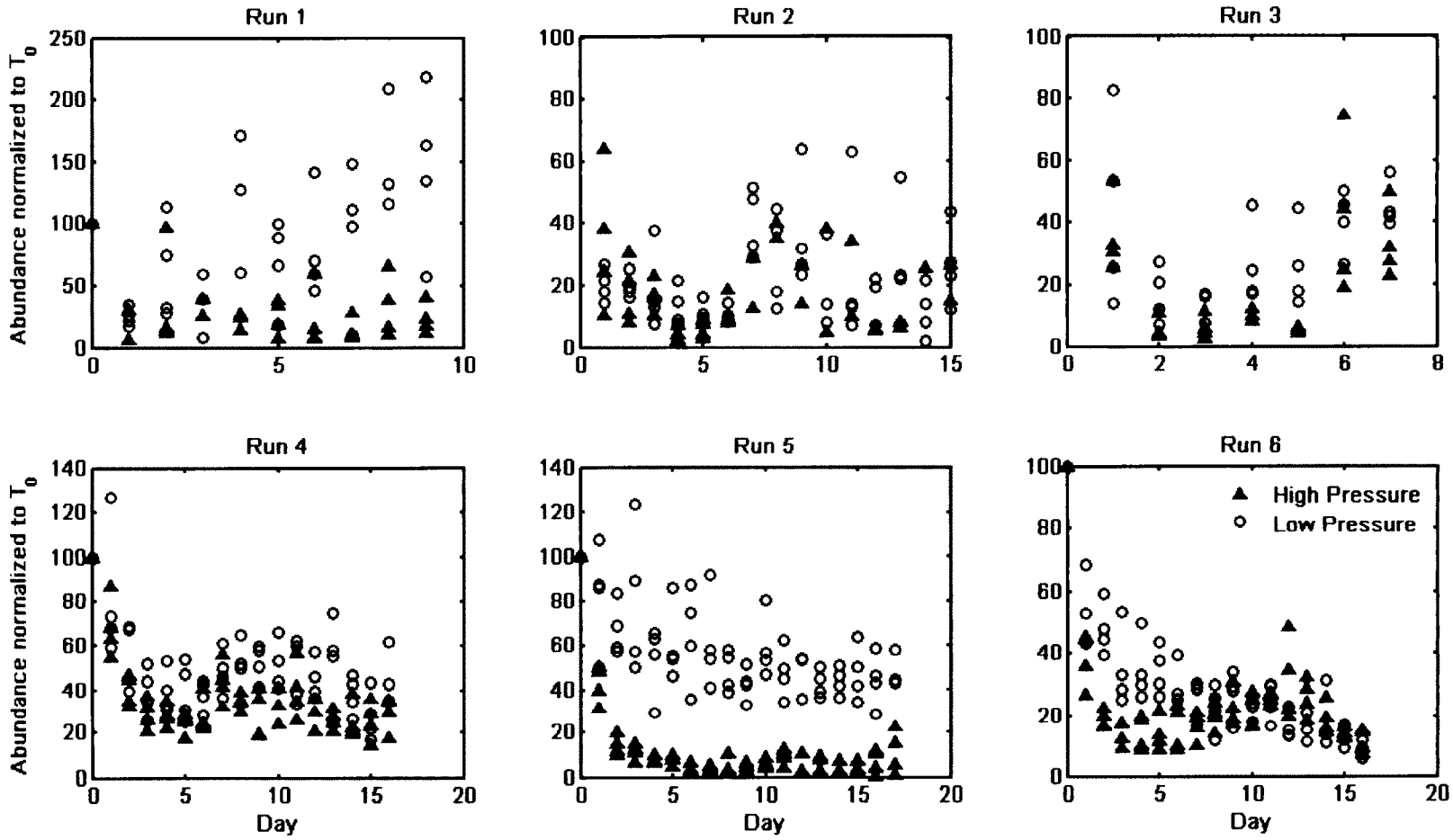

Fig. 18. *Neobodo designis* abundance normalized to time zero for six experiments.

Fig. 18 Continued. High-pressure treatments shown with red triangles, low pressure with blue circles. Each run consists of two high pressure and two low pressure chambers, with duplicate subsamples taken from each chamber daily.

$p < 0.0001$). Estimates of flagellate survival did not differ between organisms (Student's t-test, $n = 16$, $t = -0.85$, $p = 0.41$), based on dilution cultures inoculated at the end of most experiments using the MPN method (Cochran, 1950, Blodgett, 2010).

Oxygen concentration and cell abundance correlated significantly based on all data pooled (Pearson's linear correlation, $n = 744$, $r = 0.37$, $p < 0.0001$), as well as for *C. roenbergensis* (Pearson's linear correlation, $n = 264$, $r = 0.34$, $p < 0.0001$) and *N. designis* (Pearson's linear correlation, $n = 480$, $r = 0.46$, $p < 0.0001$) individually. These relationships are driven by both oxygen and cell abundance being strongly related to time. The lowest oxygen concentrations were measured in low pressure treatments where flagellate abundances were higher than in the corresponding high pressure chambers, indicating that oxygen did not compound the pressure effect as a major source of mortality.

4.4 Discussion

Abundance of both organisms generally decreased in the first days after inoculating HPS vessels (Fig. 15, 18), then stabilized at an abundance much lower than the initial value. The final abundance in each experiment was an average (SD) 1.6 (3.8)% of *C. roenbergensis* and 10.0 (6.1)% of *N. designis* cells in high pressure treatments, compared to 8.4% (SD = 21.3) of *C. roenbergensis* and 31.4 (31.2)% of *N. designis* in low pressure treatments. Around this overall pattern, however, interesting variability existed between high and low pressure treatments, experimental organisms, and among individual experiments. This variability points to the complexity of microbial systems, in

particular those involving heterotrophic flagellates which depend on bacterial prey for survival and growth.

Although flagellate abundance often fell below the counting threshold for epifluorescence microscopy, some organisms always survived. While epifluorescence counts often fell below detection limit (treated as zero for statistical analysis) later in the experiments and MPN estimates were always nonzero, the two methods were not significantly different across the entire data set due to high variability between sample runs and the very low precision of the MPN method.

Temperature and pressure effects existed, with the temperature drop being responsible for most of the mortality in these experiments. The two experimental organisms behaved differently in their response to temperature and pressure, however. *Cafeteria roenbergensis* decreased in abundance more rapidly at the beginning of each experiment than did *N. designis*, sometimes falling below the counting threshold after two to five days of incubation (Fig. 15, 18). This high mortality rate existed in both high and low pressure chambers, indicating that *C. roenbergensis* is more sensitive to low temperature than *N. designis*, or is affected more strongly by the incubation itself (i.e. bottle effect). *Cafeteria roenbergensis* is generally not abundant, despite being cultivable from deep-sea samples (Arndt et al., 2003). A single record of *Cafeteria* sp. in deep water came from a sample taken at 2500 m depth near a hydrothermal vent where water temperature was elevated (Atkins et al., 2000). In culture-based studies, *C. roenbergensis* survived and exhibited positive net population growth at temperatures as low as 1°C (Boenigk et al., 2007), so temperature alone is not sufficient to explain its low abundance in the deep ocean. *Neobodo* is regularly recorded in samples from the cold, deep sea

when live counts or cultures of flagellates are taken (Arndt et al., 2003, Patterson, 1993, Turley et al., 1988), indicating an ability to survive at low temperatures.

Cafeteria roenbergensis often fell to levels too low to count (Fig. 15), whereas *N. designis* never reached such low densities, stabilizing at cell abundances well above the counting threshold (Fig. 18). *Neobodo designis* was more likely to have positive growth in the latter portion of an experiment, with three out of six runs showing growth compared to only one of six using *C. roenbergensis*. However, *N. designis* experiments were run over a longer time, and in one of those cases, this growth only became apparent after more than eight days, the point at which *C. roenbergensis* experiments had already been terminated (Figs. 15, 18). Because of this difference in experimental design, it is difficult to discern whether a difference in recovery from the initial temperature shock existed between the two organisms.

A large amount of variability existed among experimental runs within each species (Figs. 15 and 18), even when differences in the initial abundance were accounted for by normalizing the data to abundance at time zero. One possible explanation of this variability is that the physiological conditions of the cells in the cultures were different (i.e. the flagellates were at different stages of their growth cycle) making them more or less susceptible to the experimental treatments. Bacterivorous protists depend on prokaryotic prey, and the abundance of prey greatly affects growth of flagellate cultures (Eccleston-Parry and Leadbeater, 1994). These variable starving or feeding conditions may provide them with different levels in resilience against other environmental stress factors. In our chemostat cultures, we often observed predator-prey oscillations wherein prokaryote abundance would increase, followed by an increase in flagellate abundance,

then a decrease in prokaryotes, followed by a decrease in flagellates (Fig. 14, see also Massana and Jürgens 2003). We suspect that if an experiment was started while flagellate abundance was high and still increasing, the culture would subsequently behave differently from an experiment that began with the same abundance but a negative growth rate. Unfortunately, these cycles did not have a predictable periodicity, so although effort was made to start each experiment at the same point (i.e. after prokaryote abundance had begun decreasing but before flagellate abundance reached its peak), there were certainly differences in the initial state of the culture among experiments. The variability among experiments was qualitatively greater with *N. designis* than with *C. roenbergensis*, with abundance during some runs decreasing steadily while others stabilized at a low abundance and some increased to levels as high as about 50% of the initial abundance (Fig. 18). In *C. roenbergensis* experiments, any positive growth was rare, and most experiments showed a decrease to undetectable levels (Fig. 15). Prokaryote abundances were apparently higher in *N. designis* cultures, indicating that the variability among experiments was not an effect of predator-prey cycling, because *N. designis* was never food limited (Eccleston-Parry and Leadbeater, 1994).

Prokaryote abundances (only measured during *C. roenbergensis* experiments) decreased steadily over the period of the experiment at a rate similar to the decrease due to daily sample removal (Fig. 16). This shows that the prokaryotes were not experiencing population growth, which is unsurprising given no new carbon source was added during experiments as well as the low temperature which slows growth for most organisms, or were growing at a rate balanced by mortality. The prokaryotic community in these flagellate cultures has not been characterized, but likely contains organisms which are

adapted to ~10-20 °C and atmospheric pressure, the conditions under which the stock cultures were maintained. The slow, steady decrease in abundance means that the prokaryotes were not being grazed at a high rate by the flagellates. Another possibility is that rather than a lack of growth and grazing, the two processes are occurring at higher rates but are tightly balanced. This latter explanation seems unlikely given the cyclic nature of both populations in chemostat culture (Fig. 14).

4.5 Conclusion

The effect of pressure is an important and poorly understood factor in the study of deep-sea microbial ecology. Microbes are constantly being carried to the deep ocean on particles and through mixing or advection of water, and must either acclimate to the high pressure and low temperature or die. In our experiments, flagellate cultures subjected to simulated deep-sea conditions experience a high mortality rate initially, and in all cases a small portion of the population remained and was able to reproduce once favorable temperature and pressure conditions returned. In some experiments, growth occurred in incubations after a period of acclimation even under these extreme temperature and pressure conditions. In contrast to flagellates, prokaryotes enumerated during the *C. roenbergensis* experiments did not experience great net mortality, and did not show the complexity of responses displayed by the eukaryotes. Instead they decreased in abundance exactly at the same rate as would be predicted by flushing due to the daily sampling routine. This study shows that at least some surface-water flagellates can survive the changes in temperature and pressure they experience when sinking on particles into the deep sea. In nature, subsets of these populations would have the

potential to colonize the deep ocean and to maintain slow-growing populations under the extreme pressure and low temperature conditions there. However, it is not clear how well these surface flagellates would ultimately survive in competition with resident deep-sea adapted organisms, as well as the predation pressure exerted by other protists and metazoans.

CHAPTER 5

CONCLUSION

5.1 Background

The deep sea environment is cold, high in pressure, and hostile to much of the life that thrives in the sunlit waters above (section 1.1). Prokaryotes exhibit shifts between epipelagic and deep waters in terms of their abundance, metabolism, and community structure, but less is known about microbial eukaryotes (section 1.2). High hydrostatic pressure affects many intracellular processes and structures (section 1.4, 4.1, see also reviews by Bartlett, 2002, Simonato et al., 2006), but its effects are poorly understood in protists as compared to bacteria.

In this dissertation, I combined *in situ* and experimental data to paint a broad picture of protist ecology in the deep sea, including studies on abundance (chapters 2, 3), broad-level diversity (chapter 3), interactions with environmental variables (chapters 2, 3), and the effect of conditions of the deep sea on cultured protists (chapter 4). In this chapter I will synthesize the findings based on the three main chapters, and demonstrate how they fit into the broader scientific spectrum of deep-sea protist ecology.

5.2 Abundance

In samples from the Archimedes I cruise (Fig. 1), from the depths of 1500 - 5000 m, average microbial eukaryote abundances of 0.45 cells ml^{-1} (range 0.04-1.8 cells ml^{-1})

were recorded (section 2.3), about an order of magnitude lower than previously reported (Tanaka and Rassoulzadegan, 2002, Fukuda et al., 2007, Sohrin et al., 2010). I undertook a thorough testing of the method I used (section 2.2.6.1 - 2.2.6.7) in comparison to a commonly used staining technique (Sherr and Sherr, 1983), during which I found several sources of discrepancy between abundance estimates using the two methods (section 2.3, 2.4, Table 2). When these error sources were multiplied, I found that only 39% as many protists could be expected in CARD-FISH counts as in DAPI-FITC staining. This discrepancy not only underlined the importance of using standard methods to verify the results of novel methods, but also provided a set of correction factors to allow comparisons between studies using traditional fluorochromes and those using FISH. These methodological corrections only accounted for about half of the difference between my estimates and those from previous studies (section 2.3), so I set out to investigate what other factors were influencing my measurements, using samples from the Archimedes 3 and 4 cruises (Fig. 6). For these cruises, I relied on DAPI-FITC enumeration to obtain estimates which were both accurate and directly comparable to the literature, and used CARD-FISH only to investigate relative taxonomic diversity. I found that areas of higher surface primary productivity had higher protist abundance at depth when a time lag was applied to account for the transit of particles from the surface to deep waters (section 3.4.3). Large differences in primary productivity, such as those among samples from the equatorial upwelling and the oligotrophic gyre, can exhibit 10-fold differences in protist abundance in deep water masses (section 3.4.3), though it was beyond the scope of this work to determine any causation in this relationship.

5.3 Diversity

I analyzed community shifts with depth and geography, based on broad taxonomic diversity, and also followed the distribution of an unusual morphotype, first seen in Archimedes I samples (section 2.2.4, Morgan-Smith et al., 2011). This "split nucleus" was an organism which, when stained with DAPI, appeared to have its nucleus divided into two equal halves by a dark central line (Fig. 2, section 2.2.4). Its abundance remained surprisingly unchanged with depth (section 2.3, 3.3.3), although abundance at all depths varied based on sampling location, with a link to sea-surface productivity (section 3.3.3). The taxonomic identification of this organism is not known. The split nucleus morphotype became a greater proportion of the total eukaryote community with increasing depth of sample collection, eventually making up about 30% of total eukaryotes in bottom water (section 2.3, 3.3.1, Figs. 4, 8).

Compared to studies based on 18S rRNA sequences (e.g. Countway et al., 2007; López-Garcia et al., 2001a; Massana et al., 2002), I found a higher proportion of kinetoplastids, fungi, and labyrinthulomycetes, and a lower proportion of alveolates and stramenopiles than expected (section 3.4.2). Some of this is likely due to real variability between samples, but much of it has to do with the different biases of the two methods (Kanagawa, 2003, section 2.3, 2.4, Table 2), reinforcing the conclusion that differences in methods must always be addressed. In the case of PCR-based and FISH-based methods for studying community composition at broad taxonomic levels, I propose that the two methods are complementary, and can be used to answer two different ecological questions: 1) which taxonomic groups make up most rRNA in a sample and 2) which

groups make up most of the cells in a sample. The discovery that up to 8% of microbial eukaryotes belonged to saprotrophic taxa (section 4.3.2.), together with finding these taxa in deep-sea clone libraries (López-Garcia et al., 2001a) or by culture-based methods (Raghukumar and Damare, 2008), affirms that deep-sea protists are a diverse group, not only in terms of taxonomy (section 3.4.2; López-Garcia et al., 2001a), but also in feeding strategies (section 3.4.2), which likely makes them important contributors to deep-sea carbon cycling.

One group of particular interest to me was the kinetoplastids, a deep branch taxon at the base of the eukaryotic phylogenetic tree. Due to their fast-evolving genome, the kinetoplastids were not labeled with general eukaryote FISH probes, leading to the recent development of a kinetoplastid-specific probe (Bochdansky and Huang, 2010). This dissertation is the largest application of this probe, and the largest kinetoplastid-specific sampling effort in the world ocean to date.

5.4 Pressure effects

When considering the depth distribution of microbial eukaryotes (Fig. 3, 7, sections 2.3, 3.3.1), it is clear that their abundance decreases at a greater rate than that of prokaryotes or viruses (Fig. 3, section 2.4, see also Parada et al., 2007). This greater-than-expected rate of decrease raised the question of which aspect of the deep-sea environment made it so inhospitable to microbial eukaryotes. I hypothesized that deep-sea physical conditions, i.e. low temperature and high hydrostatic pressure, had an antagonistic effect on microbial eukaryotes.

To test how microbial eukaryotes are affected by deep-sea temperature and pressure conditions, flagellate cultures were incubated at 2°C and 50 MPa for one to two weeks and sampled daily without pressure loss to the main culture vessel (section 4.2.1, Fig. 13). The cultures used were *Cafeteria roenbergensis*, which is cosmopolitan in surface waters but not in the deep sea, and *Neobodo designis,* which is common in both surface and deep waters. The initial experimental design involved longer (40+ day) incubations, with a gradual increase in pressure to mimic the descent of a particle through the water column at a rate of 1 MPa, or 100 m, per day, within the range of measured particle sinking speeds (Berelson, 2002, Ploug et al., 2008). However, these experiments resulted in hypoxic conditions due to a greater rate of microbial metabolism than could be supported by the dissolved oxygen in the medium (data not shown), a potentially confounding source of mortality which led to the development of the protocol presented in section 4.2.3. Although this model system is not a perfect replica of real-world conditions, it can be useful a useful step toward understanding basic protist ecology under high-pressure, low-temperature conditions.

From my incubations of flagellates under deep-sea conditions, I found that low temperature and high pressure both contributed to a high initial mortality rate of flagellate cultures, which then leveled off and sometimes showed net growth after several days. Up to a quarter of flagellates survived the incubation, and in every replicate a small population survived which was able to grow when returned to favorable conditions (section 4.3.1, 4.3.2). Since even surface-isolated flagellates always survived deep sea conditions, it is likely extreme prey limitation that determines their threshold abundances in nature, rather than solely effects of the physical environment.

The deep sea receives a constant flux of particles from the surface ocean, which can carry 10^3 flagellates per aggregate, equivalent to 10^4 - 10^6 flagellates ml^{-1} of aggregates (Simon, 2002, Herndl and Peduzzi, 1988, Turley and Mackie, 1994). Given the survival of at least a small flagellate population at the end of each high pressure incubation (section 4.3.1, 4.3.2), this constant rain of particles can provide a constant input of protists to the deep sea. My experiments did not address whether this influx of protists actually does survive in the deep sea, where in addition to temperature and pressure, the protists face stresses due to competition with an *in situ* community adapted to living and reproducing in the deep sea, predation by larger protists and small metazoans, and prey limitation, none of which were present in the incubations I performed.

5.5 Environmental impacts on microbial eukaryotes.

Total microbial eukaryote abundance, along with that of the split nucleus morphotype, were measured in samples from the North Atlantic Deep Water over three cruises covering 35° latitude, and 54 stations. I analyzed filters from 264 deep-water samples, representing several deep-sea basins, as well as two fracture zones, where deep water flows through the Mid-Atlantic Ridge (section 2.2.1, 3.2, Fig. 1, 6). This intensive sampling regimen led to true basin-scale coverage of this water mass, which is central to the flow of the global thermohaline circulation (Tomczak and Godfrey, 2003). Over this large study area, microbial eukaryote abundance was lag-correlated to surface primary productivity, but not strongly related to latitude or longitude (section 3.3.3, 3.4.3, Fig.10).

The time-lag relationship between surface and deep-sea conditions suggests a role of particles in energy transport between the two zones. However, no relationship was observed between particle abundance and microbial eukaryotes (section 3.3.3, 3.4.3), despite finding - using the same video measurements of particle abundance - that macroscopic particles drive oxygen consumption in the deep sea (Bochdansky et al., 2010).

5.6 Concluding remarks

Microbial eukaryotes in the surface ocean form an essential link in the cycling of carbon, keeping prokaryote abundances in check (Fenchel, 1986). In surface waters, protist abundance, diversity, and processes have been studied extensively (e.g. Eccleston-Parry and Leadbeater, 1994, Fenchel, 1986, Jürgens and Massana, 2008, López-Garcia et al., 2001a, Massana et al., 2002), but the literature on protists in the deep sea is much less abundant due to the difficulty of sampling this environment (Arístegui et al., 2009). For this dissertation, I characterized the abundance and broad-level diversity of microbial eukaryotes in the deep sea, on a basin scale, and over the full depth range of the ocean. Microbial eukaryote abundances decreased sharply in the upper 1000 m and then remained relatively constant below that.

Some of the most interesting questions in deep-sea biology revolve around organic aggregates or particles. The abundance of total microbial eukaryotes in deep water was lag-correlated with surface water productivity, indicating a possible relationship between the two variables via sinking particles, which bring organic matter,

prokaryotes, microbial eukaryotes, and even small metazoans (Kiørboe et al., 2003) to the deep sea. In experiments, I found that despite a sharp drop in abundance after deep-sea conditions were applied as an abrupt shock, flagellate cultures from the surface ocean could survive 1-2 weeks of incubation at 2°C and 50 MPa (equivalent to 5000 m depth) at low abundance, and were able to reproduce when returned to 15°C and atmospheric pressure. These findings combine to paint a picture of a deep-sea protist community that is more closely linked to the surface ocean than previously understood, and highlights the need for further studies to understand the processes surrounding this relationship.

REFERENCES

Adl, S.M., Simpson, A.G., Farmer, M.A., et al., 2005. The new higher level classification of eukaryotes with emphasis on the taxonomy of protists. J. Eukaryot. Microbiol. 52, 399-451.

Adl, S.M., Simpson, A.G.B., Lane, C.E., et al. 2005. The revised classification of eukaryotes. J. Eukaryot. Microbiol. 59, 429-514.

Agogue, H., Lamy, D., Neal, P. R., Sogin, M. L., and Herndl, G. J., 2011. Water mass-specificity of bacterial communities in the North Atlantic revealed by massively parallel sequencing, Mol. Ecol. 20, 258-274.

Alldredge A.L., Cohen, Y., 1987. Can microscale chemical patches persist in the sea? Microelectrode study of marine snow, fecal pellets. Science 235, 689-691.

Alldredge, A. L., Cole, J.J., Caron, D.A., 1986. Production of heterotrophic bacteria inhabiting macroscopic organic aggregates (marine snow) from surface waters. Limnol. Oceanogr. 31, 68-78.

Allen, E.E., Facciotti, D., Bartlett, D.H., 1999. Monounsaturated but not polyunsaturated fatty acids are required for growth of the deep-sea bacterium *Photobacterium profundum* SS9 at high pressure and low temperature. Appl. Environ. Microbiol. 65, 1710-1720.

Amann, R.I., Binder, B.J., Olson, R.J., Chisholm, S.W., Devereux, R., Stahl, D.A., 1990. Combination of 16S ribosomal-RNA-targeted oligonucleotide probes with flow-cytometry for analyzing mixed microbial-populations. Appl. Environ. Microbiol. 56, 1919-1925.

Andersen, P., Fenchel, T., 1985. Bacterivory by microheterotrophic flagellates in seawater samples. Limnol. Oceanogr. 30, 198-202.

Arístegui, J., Tett, P., Hernández-Guerra, A., Basterretxea, G., Montero, M.F., Wild, K., Sangrá, P., Hernández-Leon, S., Canton, M., García-Brau, J.A., Pacheco, M., Barton, E.D., 1997. The influence of island-generated eddies on chlorophyll distribution: a study of mesoscale variation around Gran Canaria. Deep-Sea Res. I 44, 71-96.

Arístegui, J., Agustí, S., Duarte, C.M., 2003. Respiration in the dark ocean. Geophys. Res. Lett. 30, 1041-1044.

Arístegui, J., Gasol, J.M., Duarte, C., Herndl, G.J., 2009. Microbial oceanography of the dark ocean's pelagic realm. Limnol. Oceanogr. 54, 1501-1529.

Arndt, H., Dietrich, D., Auer, B., Cleven, E.J., Gräfenhan, T., Wietere, M., Mylnikov, A.P., 2000. Functional diversity of heterotrophic flagellates in aquatic ecosystems. In: Leadbeater, B.S.C., Green, J.C. (Eds). The flagellates: unity, diversity and evolution. Taylor & Francis, London.

Arndt, H., Hausmann, K., Wolf, M., 2003. Deep-sea heterotrophic nanoflagellates of the Eastern Mediterranean Sea: qualitative and quantitative aspects of their pelagic and benthic occurrence. Mar. Ecol. Prog. Ser. 256, 45–56.

Artolozaga, I., Ayo, B., Latatu, A., Azúa, I., Unanue, M., Iriberri, J., 2000. Spatial distribution of protists in the presence of macroaggregates in a marine system. FEMS Microbiol. Ecol. 33, 191-196.

Artolozaga, I., Valcarcel, M., Ayo, B., Latatu, A., Iriberri, J., 2002. Grazing rates of bacterivorous protists inhabiting diverse marine planktonic microenvironments. Limnol. Oceanogr. 47, 142-150.

Atkins, M.S., Anderson, O.R., Wirsen, C.O., 1998. Effect of hydrostatic pressure on the growth rates and encystment of flagellated protozoa isolated from a deep-sea hydrothermal vent and a deep shelf. Mar. Ecol. Prog. Ser. 171, 85-95.

Atkins, M.S., Teske, A.P., Anderson, O.R., 2000. A survey of flagellate diversity at four deep-sea hydrothermal vents in the eastern Pacific Ocean using structural and molecular approaches. J. Eukaryot. Microbiol., 47, 400-411.

Balny, C., Mozhaev, V.V., Lange, R., 1997. Hydrostatic pressure and proteins: basic concepts and new data. Comp. Biochem. Physiol. 116A, 299-304.

Baltar, F., Arístegui, J., Gasol, J. M., Sintes, E., Herndl, G.J., 2009. Evidence of prokaryotic metabolism on suspended particulate organic matter in the dark waters of the subtropical North Atlantic. Limnol. Oceanogr. 54, 182-193.

Bartlett, D.H., 2002. Pressure effects on in vivo microbial processes. Biochim. et Biophys. Acta, 1595, 367-381.

Bauer, J.E., Williams, P.M., Druffel, R.M., 1992. ^{14}C activity of dissolved organic carbon fractions in the north-central Pacific and Sargasso Sea. Nature 357, 667-670.

Beardsley, C., Knittell, K., Amann, R., Pernthaler, J., 2005. Quantification and distinction of aplastidic and plastidic marine nanoplankton by fluorescence in situ hybridization. Aquat. Microb. Ecol. 41, 163-169.

Behrenfeld, M.J., Falkowski, P.G., 1997. Photosynthetic rates derived from satellite-based chlorophyll concentration. Limnol. Oceanogr. 42, 1-20.

Behrenfeld, M.J., Falkowski, P.G., 2010. Ocean Productivity. http://www.science.oregonstate.edu/ocean.productivity. Accessed May 8, 2012.

Berelson, W.M., 2002. Particle settling rates increase with depth in the ocean. Deep-Sea Res. II 49, 237-251.

Bianchi, A., Garcin, J., Tholosan, O., 1999. A high-pressure serial sampler to measure microbial activity in the deep sea. Deep-Sea Res. I 46, 2129-2142.

Blodgett, R., 2010. BAM Appendix 2: Most probable number from serial dilutions. US Food and Drug Administration Bacterial analytical manual. http://www.fda.gov/Food/ScienceResearch/ LaboratoryMethods/BacteriologicalAnalyticalManualBAM/ucm109656.htm Accessed June 10, 2012.

Bochdansky, A.B., Huang, L., 2010. Re-evaluation of the EUK516 probe for the domain Eukarya results in a suitable probe for the detection of Kinetoplastids, an important group of parasitic and free-living flagellates. J. Eukaryot. Microbiol. 57, 229-235.

Bochdansky, A.B., van Aken, H.M., Herndl, G.J., 2010. Role of macroscopic particles in deep-sea oxygen consumption. Proc. Natl. Acad. Sci. 107, 8287–8291.

Boenigk, J., Jost, S., Stoeck, T., Garstecki, T., 2007. Differential thermal adaptation of clonal strains of a protist morphospecies originating from different climatic zones. Environ. Microbiol. 9, 593-602.

Boyd, P., W., Newton, P., P., 1999. Does planktonic community structure determine downward particulate organic carbon flux in different oceanic provinces? Deep-Sea Res. I 46, 63-91.

Brul, S., Rommens, A.J.M., Verrips, C.T., 2000. Mechanistic studies on the inactivation of *Saccharomyces cerevisiae* by high pressure. Innovative Food Sci. & Emerging Tech., 1, 99- 108.

Caron, D.A., Davis, P.G., Madin, L.P., Sieburth, J.M., 1982. Heterotrophic Bacteria and Bacterivorous Protozoa in Oceanic Macroaggregates. Science, New Ser. 218, 795-797.

Cochran, W.G., 1950. Estimation of bacterial densities by means of the "most probable number". Biometrics 6, 105-116.

Corliss, J.O. 1992., Should there be a separate code of nomenclature for the protists? Biosystems 28, 1-14.

Countway, P. D., Gast, R. J., Savai, P. and Caron, D. A., 2005. Protistan Diversity Estimates Based on 18S rDNA from Seawater Incubations in the Western North Atlantic. J. Euk. Microbiol. 52, 95-106.

Countway, P.D., Gast, R.J., Dennett, M.R., Rose, J.M., Caron, D.A., 2007. Distinct protistan assemblages characterize the euphotic zone and deep sea (2500 m) of the western North Atlantic (Sargasso Sea and Gulf Stream). Environ. Microbiol. 9, 1219-1232.

Daims, H., Stoecker, K., Wagner, M., 2005. Fluorescence *in situ* hybridization for the detection of prokaryotes. In: Osborn, A.M., Smith C.J. (Eds.) Molecular microbial ecology. Taylor and Francis, New York, pp. 213–239.

Daniel, I., Oger, P., Winter, R., 2006. Origins of life and biochemistry under high-pressure conditions. Chem. Soc. Rev. 35, 858-875.

Davis, C.S., 2010. Statistical methods for the analysis of repeated measurements. Springer, New York.

DeLong, E.F., Yayanos, A.A., 1985. Adaptation of the membrane lipids of a deep-sea bacterium to changes in hydrostatic pressure. Science 228, 1101-1103.

DeLong, E.F., Franks, D.G., Alldredge, A.L., 1993. Phylogenetic diversity of aggregate-attached vs. free-living marine bacterial assemblages. Limnol. Oceanogr. 38, 924-934.

Dobell, C., 1932. Antony van Leeuwenhoek and his "Little animals": being some account of the father of protozoology and bacteriology and his multifarious discoveries in these disciplines. Dover, New York.

Dreyfus, G., Guimaraes-Motta, H., Silva, J.L., 1988. Effect of hydrostatic pressure on the mitochondrial ATP synthase. Biochem. 27, 6704-6710.

Eccleston-Parry, J.D., Leadbeater, B.S.C., 1994. A comparison of the growth kinetics of six marine heterotrophic nanoflagellates fed with one bacterial species. Mar. Ecol. Prog. Ser. 105, 167-177.

Edgcomb, V., Orsi, W., Bunge, J., Jeon, S., Christen, R., Leslin, C., Holder, M., Taylor, G.T., Suarez, P., Varela, R., Epstein, S. 2011. Protistan microbial observatory in the Cariaco Basin, Caribbean. I. Pyrosequencing vs Sanger insights into species richness. ISME J. 5, 1344–1356.

Egan, S.T., McCarthy, D.M., Patching, J.W., Fleming, G.T.A., 2012. An investigation of the physiology and potential role of components of the deep ocean bacterial community (of the NE Atlantic) by enrichments carried out under minimal environmental change. Deep Sea Res. I. 61, 11-20.

Eloe, E.A., Shulse, C.N., Fadrosh, D.W., Williamson, S.J., Eric E. Allen, E.E., Bartlett, D.H., 2011. Compositional differences in particle-associated and free-living microbial assemblages from an extreme deep-ocean environment. Env. Microbiol. 3, 449-458.

Fenchel, T., 1986. The ecology of heterotrophic microflagellates. Adv. Microb. Ecol. 9, 57-97.

Fenchel, T., Patterson, D.J., 1988. *Cafeteria roenbergensis* nov. et sp. nov. and the description of a new algal class, the Pelagophyceae classis nov. Mar. Microb. Food Webs 3, 9-19.

Finlay, B.J., 2002. Global dispersal of free-living microbial eukaryote species. Science 296, 1061-1063.

Fukuda, H., Sohrin, R., Nagata, T., Koike, I., 2007. Size distribution and biomass of nanoflagellates in meso- and bathypelagic layers of the subarctic Pacific. Aquat. Microb. Ecol. 46, 203-207.

Gasol, J.M., Vaqué, D., 1993. Lack of coupling between heterotrophic nanoflagellates and bacteria - a general phenomenon across aquatic systems. Limnol. Oceanogr. 38, 657-665.

Green, J.L., Holmes, A., H., Westoby, M., Oliver, I., Briscoe, D., Dangerfield, M., Gillings, M., Beattie, A.J., 2004. Spatial scaling of microbial eukaryote diversity. Nature 432, 747-750.

Gross, M., Jaenicke, R., 1994. Proteins under pressure. The influence of high hydrostatic pressure on structure, function and assembly of proteins and protein complexes. Eur. J. Biochem. 221, 617-630.

Grossart, H.-P., Gust, G., 2009. Hydrostatic pressure affects physiology and community structure of marine bacteria during settling to 4000 m: an experimental approach. Mar. Ecol. Prog. Ser. 390, 97-104.

Guillou, L., Viprey, M., Chambouvet, A., Welsh, R.M., Kirkham, A.R., Massana, R., Scanlan, D.J., Worden, A.Z., 2008. Widespread occurrence and genetic diversity of marine parasitoids belonging to Syndiniales (Alveolata). Env. Microbiol. 10, 3349-3365.

Hansman, R.L., Griffin, S., Watson, J.T., Druffel, E.R.M., Ingalls, A.E., Pearson, A., Aluwihare, L.I., 2009. The radiocarbon signature of microorganisms in the mesopelagic ocean. Proc. Natl. Acad. Sci. 106, 6513-6518.

Hemmingsen, E.A., Hemmingsen, B.B., 1979. Lack of intracellular bubble formation in microorganisms at very high gas supersaturations. J. Appl. Physiol. 47, 1270-1277.

Herndl, G. J., Peduzzi, P., 1988. The ecology of amorphous aggregations (marine snow) in the northern Adriatic Sea. Mar. Ecol. 9, 79-90.

Herndl, G.J., Reinthaler, T., Teira, E., van Aken, H., Veth, C., Pernthaler, A., Pernthaler, J., 2005. Contribution of Archaea to total prokaryotic production in the deep Atlantic Ocean. Appl. Environ. Microbiol. 71, 2303-2309.

Herndl, G.J., Agogue, H., Baltar, F., Reinthaler, T., Sintes, E., Varela, M.M., 2008. Regulation of aquatic microbial processes: the 'microbial loop' of the sunlit surface waters and the dark ocean dissected. Aquat. Microb. Ecol. 53, 59-68.

Hewson, I., Steele, J., Capone, D., and Fuhrman, J. A., 2006. Remarkable heterogeneity in meso- and bathypelagic bacterioplankton assemblage composition, Limnol. Oceanogr. 51, 1274-1283.

Jannasch, H.W., Wirsen, C.O., Winget, C.L., 1973. A bacteriological pressure-retaining deep-sea sampler and culture vessel. Deep-Sea Res. 20, 661-664.

Jürgens, K., Massana, R., 2008. Protistan grazing on marine bacterioplankton. In: Kirchman, D.L. (Ed.), Microbial ecology of the oceans, 2nd edn., John Wiley & Sons, Inc., Hoboken, NJ, USA.

Kanagawa, T., 2003. Bias and artifacts in multitemplate polymerase chain reactions (PCR). J. Biosci. Bioeng. 96, 317-323.

Kato, C., Qureshi, M.H., 1999. Pressure response in deep-sea piezophilic bacteria. J. Molec. Microbiol. Biotechnol. 1, 87-92.

Kelly, R.H., Yancey, P.H., 1999. High contents of trimethylamine oxide correlating with depth in deep-sea teleost fishes, skates, and decapod crustaceans. Biol. Bull. 196, 18-25.

Kempf, V.A.J., Trebesius, K., Autenrieth, I.B., 2000. Fluorescent *in situ* hybridization allows rapid identification of microorganisms in blood cultures. J. Clin. Microbiol. 38, 830-838.

Kimura, H., Sato, M., Sugiyama, C., Naganuma, T., 2001. Coupling of thraustochytrids and POM, and of bacterio- and phytoplankton in a semi-enclosed coastal area: implication for different substrate preference by the planktonic decomposers. Aquat. Microb. Ecol. 25, 293-300.

Kiørboe, T., Tang, K., Grossart, H.-P., Ploug, H., 2003. Dynamics of microbial communities on marine snow aggregates: colonization, growth, detachment, and grazing mortality of attached bacteria. Environ. Microbiol. 69, 3036-3047.

Lahr, D.J.G., Lara, E., Mitchell, E.A.D., 2012. Time to regulate microbial eukaryote nomenclature. Biol. J. Linnean Soc., in press.

Lara, E., Moreira, D., Vereshchaka, A., López-Garcia, P., 2009. Pan-oceanic distribution of new highly diverse clades of deep-sea diplonemids. Environ. Microbiol. 11, 47-55.

Lee, J.J., Leedale, G.F., Bradbury, P. (Eds.), 2000. Society of Protozoologists. Illustrated guide to the protozoa, 2nd edn. Allen Press, Lawrence, KS.

López-Garcia, P., López-López, A., Moreira, D., Rodríguez-Valera, F., 2001. Diversity of free-living prokaryotes from a deep-sea site at the Antarctic Polar Front. FEMS Microbiol. Ecol. 36, 193-202.

López-Garcia, P., Phillipe, H., Gail, F., Moreira, D., 2003. Autochthonous eukaryotic diversity in hydrothermal sediment and experimental microcolonizers at the Mid-Atlantic Ridge. Proc. Natl. Acad. Sci. 100, 697-702.

López-Garcia, P., Rodríguez-Valera, F., Pedros-Alio, C., Moreira, D., 2001. Unexpected diversity of small eukaryotes in deep-sea Antarctic plankton. Nature 409, 603-607.

Lukeš, J., Leander, B.S., Keeling, B.J., 2009. Cascades of convergent evolution: the corresponding evolutionary histories of euglenozoans and dinoflagellates. Proc. Natl. Acad. Sci. 106, 9963-9970.

Macdonald, A.G., 1997. Hydrostatic pressure as an environmental factor in life processes. Comp. Biochem. Physiol. 116A, 291–297.

Marx, G., Moody, A., Bermúdez-Aguirre, D., 2011. A comparative study on the structure of *Saccharomyces cerevisiae* under nonthermal technologies: High hydrostatic pressure, pulsed electric fields and thermo-sonication. Int. J. Food Microbiol. 151, 327-337.

Massana, R., 2011. Eukaryotic picoplankton in surface oceans. Ann. Rev. Microbiol. 65, 91-110.

Massana, R., Guillou, L., Diez, B., Pedros-Alio, C., 2002. Unveiling the organisms behind novel eukaryotic ribosomal DNA sequences from the ocean. Appl. Environ. Microbiol. 68, 4554-4558.

Massana, R., Jürgens, K., 2003. Composition and population dynamics of planktonic bacteria and bacterivorous flagellates in seawater chemostat cultures. Aquat. Microb. Ecol. 32, 11-22.

Massana, R., Terrado, R., Forn, I., Lovejoy, C., Pedros-Alio, C., 2006. Distribution and abundance of uncultured heterotrophic flagellates in the world oceans. Env. Microbiol. 8, 1515-1522.

Meganathan, R., Marquis, R.E., 1973. Loss of bacterial motility under pressure. Nature 246, 525-527.

Miura, T., Minegishi, H., Usami, R., Abe, F., 2006. Systematic analysis of HSP gene expression and effects on cell growth and survival at high hydrostatic pressure in *Saccharomyces cerevisiae*. Extremophiles 10, 279-284.

Moon-van der Staay, S.Y., De Wachter, R., Vaoulot, D., 2001. Oceanic 18S rDNA sequences from picoplankton reveal unsuspected eukaryotic diversity. Nature 409, 607-610.

Moreira, D., López-García, P., Vickerman, K., 2004. An updated view of kinetoplastid phylogeny using environmental sequences and a closer outgroup: proposal for a new classification of the class Kinetoplastea. Int. J. Syst. Evol. Microbiol. 54, 1861-1875.

Morgan-Smith, D., Herndl, G.J., van Aken, H.M., Bochdansky, A.B., 2011. Abundance of eukaryotic microbes in the deep subtropical North Atlantic. Aquat. Microb. Ecol. 65, 103-115.

Morita, R. Y., 1984. Feast or famine in the deep sea. Developments in industrial microbiology. Soc. Int. Microbiol. 25, 5-16.

Nagata, T., Tamburini, C., Arístegui, J., et al., 2010. Emerging concepts on microbial processes in the bathypelagic ocean - ecology, biogeochemistry, and genomics. Deep-Sea Res. II 57, 1519-1536.

Not, F., Gausling, R., Azam, F., Heidelberg, J.F., Worden, A.Z., 2007. Vertical distribution of picoeukaryotic diversity in the Sargasso Sea. Environ. Microbiol. 9, 1233-1252.

Not, F., Latasa, M., Scharek, R., Viprey, M., Karleskind, P., Balague, V., Ontoria-Oviedo, I., Cumino, A., Goetze, E., Vaulot, D., Massana, R., 2008. Protistan assemblages across the Indian Ocean, with a specific emphasis on the picoeukaryotes. Deep-Sea Res. I 55, 1456-1473.

Not, F., Simon, N., Biegala, I.C., Vaulot, D., 2002. Application of fluorescent in situ hybridization coupled with tyramide signal amplification (FISH-TSA) to assess eukaryotic picoplankton composition. Aquat. Microb. Ecol. 28, 157-166.

Oger, P.M., Daniel, I., Picard, A., 2010. *In situ* Raman and X-ray spectroscopies to monitor microbial activities under high hydrostatic pressure. Ann. N.Y. Acad. Sci. 1189, 113-120.

Paffenhöfer, G.A., Tzeng, M., Hristov, R., Smith, C.L., Mazzocchi, M.G., 2003. Abundance and distribution of nanoplankton in the epipelagic subtropical/tropical open Atlantic Ocean. J. Plankt. Res. 25, 1535-1549.

Parada, V., Sintes, E., van Aken, H., Weinbauer, M.G., Herndl, G.J., 2007. Viral abundance, decay, and diversity in the meso- and bathypelagic waters of the North Atlantic. Appl. Environ. Microbiol. 73, 4429-4438.

Patching, J.W., Eardly, D., 1997. Bacterial biomass and activity in the deep waters of the eastern Atlantic - evidence of a barophilic community. Deep Sea Res. I 44, 1655-1670.

Patterson, D.J., Nygaard, K., Steinberg, G., Turley, C.M., 1993. Heterotrophic flagellates and other protists associated with oceanic detritus throughout the water column in the mid North-Atlantic. J. Mar. Biol. Assoc. UK. 73, 67-95.

Patterson, D.J., 1993. The current status of the free-living heterotrophic flagellates. J. Euk. Microbiol. 40, 606-609.

Pernthaler, A., Pernthaler, J., Amann, R., 2002. Fluorescence *in situ* hybridization and catalyzed re-porter deposition for the identification of marine bacteria. Appl. Environ. Microbiol. 68, 3094-3101.

Picard, A., Daniel, I., Montagnac, G., Oger, P., 2007. *In situ* monitoring by quantitative Raman spectroscopy of alcoholic fermentation by *Saccharomyces cerevisiae* under high pressure. Extremophiles 11, 445-45.

Ploug, H., Grossart, H.-P., 2000. Bacterial growth and grazing on diatom aggregates: Respiratory carbon turnover as a function of aggregate size and sinking velocity. Limnol. Oceanogr. 45, 1467-1475.

Ploug, H., Iversen, M.H., Fischer, G., 2008. Ballast, sinking velocity, and apparent diffusivity within marine snow and zooplankton fecal pellets: Implications for substrate turnover by attached bacteria. Limnol. Oceanogr. 53, 1878-1886.

Raghukumar, C., Damare, S., 2008 Deep-sea fungi. In: Michiels, C., Bartlett, D.H., Aertsen, A. (Eds.), High-pressure microbiology. ASM Press, Washington, pp. 265-292.

Raghukumar, S., 1992. Bacterivory: a novel dual role for thraustochytrids in the sea. Mar. Biol. 113, 165-169.

Raghukumar, S., Ramaiah, N., Raghukumar, C., 2001. Dynamics of thraustochytrid protists in the water column of the Arabian Sea. Aquat. Microb. Ecol. 24, 175-186.

Ragukhumar, S., 2002. Ecology of the marine protists, the Labyrinthulomycetes (Thraustochytrids and Labyrinthulids). Eur. J. Protistology 38, 127-145.

Rivalain, N., Roquain, J., Demazeau, G., 2010. Development of high hydrostatic pressure in biosciences: Pressure effect on biological structures and potential applications in Biotechnologies. Biotechnol. Adv. 28, 659-672.

Rowe, G.T., 1983. Biomass and production of the deep-sea macrobenthos. In: Rowe, G.T. (Ed.), The sea, Vol 8. John Wiley & Sons, New York, NY.

Schlitzer, R., 2012. Ocean Data View, http://odv.awi.de. Accessed Feb. 1, 2012.

SeaDAS Development Group at NASA Goddard Space Flight Center, 2012. SeaDAS. http://oceancolor.gsfc.nasa.gov. Accessed May 4, 2012.

Sebert, P., 2002. Fish at high pressure: a hundred year history. Comp. Biochem. Physiol. A 131, 575-585.

Sharma, A., Scott, J.H., Cody, G.D., Fogel, M.L., Hazen, R.M., Hemley, R.J., Huntress, W.T., 2002. Microbial activity at gigapascal pressures. Science 295, 1514-1516.

Sherr, B., Sherr, E., 1983. Enumeration of heterotrophic micro-protozoa by epifluorescence microscopy. Estuar. Coast Shelf Sci. 16, 1–7.

Shimada, S., Andou, M., Naito, N., Yamada, N., Osumi, M., Hayashi, R., 1993. Effects of hydrostatic pressure on the ultrastructure and leakage of internal substances in the yeast *Saccharomyces cerevisiae*. Appl. Microbiol. Biotech. 40, 123-131.

Simon, M., Grossart, H.-P., Schweitzer, B., Ploug, H., 2002. Microbial ecology of organic aggregates in aquatic ecosystems. Aquat. Microb. Ecol. 28, 175-211.

Simonato, F., Campanaro, S., Lauro, F.M., Vezzi, A., D'Angelo, M., Vitlo, N., Valle, G., Bartlett, D.H., 2006. Piezophilic adaptation: a genomic point of view. J. Biotechnol. 126, 11-25.

Simpson, A.G.B., Stevens, J.R., Lukeš, J., 2006. The evolution and diversity of kinetoplastid flagellates. Trends Parasitol. 22, 168-174.

Sogin, M.L., Morrison, H.G., Huber, J.A., Welch, D.M. , Huse, S.M., Neal, P.R., Arrieta, J.M., Herndl, G. J., 2006. Microbial diversity in the deep sea and the underexplored "rare biosphere". Proc. Natl. Acad. Sci. 103, 12115-2120.

Sohrin, R., Imazawa, M., Fukuda, H., Suzuki, Y., 2010. Full-depth profiles of prokaryotes, heterotrophic nanoflagellates, and ciliates along a transect from the equatorial to the subarctic central Pacific Ocean. Deep-Sea Res. II 57, 1537–1550.

Souza, M.O., Creczynski-Pasa, T.B., Scofano, H.M., Graber, P., Mignaco, J.A., 2004. High hydrostatic pressure perturbs the interactions between CF_0F_1 subunits and induces a dual effect on activity. Int. J. Biochem. Cell. Biol. 36, 920-930.

Steinberg, D.K., Van Mooy, B.A.S., Buesseler, K.O., Boyd, P.W., Kobari, T., Karl, D.M., 2008. Bacterial vs. zooplankton control of sinking particle flux in the ocean's twilight zone. Limnol. Oceanogr. 53, 1327-1338.

Stoeck, T., Taylor, G.T., Epstein, S.S., 2003. Novel eukaryotes from the permanently anoxic Cariaco Basin (Caribbean Sea). Appl. Environ. Microbiol. 69, 5656-5663.

Stokes, N.A., Ragone Calvo, L.M., Reece, K.S., Burreson, E.M., 2002. Molecular diagnostics, field validation, and phylogenetic analysis of Quahog Parasite Unknown (QPX), a pathogen of the hard clam *Mercenaria mercenaria*. Dis. Aquat. Org. 52, 233-247.

Tamburini C., Goutx, M., Guigue, C., Garel, M., Lefèvre, D., Charrière, B., Sempéré, R., Pepa, S., Peterson, M.L., Wakeham, S., Lee, C., 2009. Effects of hydrostatic pressure on microbial alteration of sinking fecal pellets, Deep Sea Res. II 56,1533-1546.

Tamburini, C., Garcin, J., Bianchi, A., 2003. Role of deep-sea bacteria in organic matter mineralization and adaptation to hydrostatic pressure conditions in the NW Mediterranean Sea. Aquat. Microb. Ecol. 32, 209-218.

Tamburini, C., Garcin, J., Grégori, G., Leblanc, K., Rimmelin, P., Kirchman, D.L., 2006. Pressure effects on surface Mediterranean prokaryotes and biogenic silica dissolution during a diatom sinking experiment. Aquat. Microb. Ecol. 43, 267-276.

Tanaka, T., Rassoulzadegan, F., 2002. Full-depth profile (0-2000 m) of bacteria, heterotrophic nanoflagellates and ciliates in the NW Mediterranean Sea: vertical partitioning of microbial trophic structure. Deep-Sea Res. II 49, 2093–2107.

Teira, E., Reinthaler, T., Pernthaler, A., Pernthaler, J., Herndl, G.J., 2004. Combining catalyzed reporter deposition-fluorescence in situ hybridization and microautoradiography to detect substrate utilization by Bacteria and Archaea in the deep ocean. Appl. Environ. Microbiol. 70, 4411-4414.

Tomczak, M., Godfrey, J.S., 2003. Regional oceanography: an introduction, 2nd edn. Butterworth-Heinemann, Boston, MA.

Turley, C.M., and Mackie, P.J., 1994. Biogeochemical significance of attached and free-living bacteria and the flux of particles in the NE Atlantic Ocean. Mar. Ecol. Prog. Ser. 115, 191-203.

Turley, C.M., Carstens, M., 1991. Pressure tolerance of oceanic flagellates - implications for remineralization of organic-matter. Deep-Sea Res. A 38, 403-413.

Turley, C.M., Lochte, K., Patterson, D.J. 1988. A barophilic flagellate isolated from 4500 m in the mid-North Atlantic. Deep Sea Res. A 35, 1079-1092.

Vezzi, A., Campanaro, S., D'Angelo, M., Simonato, F., Vitulo, N., Lauro, F.M., Cestaro, A., Malacrida, G., Simionati, B., Cannata, N., Romualdi, C., Bartlett, D.H., Valle, G., 2005. Life at depth: *Photobacterium profundum* genome sequence and expression analysis. Science 307, 1459-1461.

Weber, F., del Campo, J., Wylezich, C., Massana, R., Jürgens, K., 2012. Unveiling trophic functions of uncultured protist taxa by incubation experiments in the brackish Baltic Sea. Plos One 7, e41970.

Welch, T.J., Farewell, A., Neidhardt, F.C., Bartlett, D.H., 1993. Stress response of *Escherichia coli* to elevated hydrostatic pressure. J. Bacteriol. 175, 7170-7177.

Wikner, J., Hagström, Å., 1991. Annual study of bacterioplankton community dynamics. Limnol. Oceanogr. 36, 1313-1324 .

Winter, C., Kerros, M.E., Weinbauer, M.G., 2009. Seasonal changes of bacterial and archaeal communities in the dark ocean: evidence from the Mediterranean Sea. Limnol. Oceanogr. 54, 160-170.

Woese, C.R., Kandler, O., Wheelis, M.L., 1990. Towards a natural system of organisms: proposal for the domains Archaea, Bacteria, and Eucarya. Proc. Natl. Acad. Sci. 87, 4576-4579.

Yano, Y., Nakayama, A., Ishihara, K., Saito, H., 1998. Adaptive changes in membrane lipids of barophilic bacteria in response to changes in growth pressure. Appl. Environ. Microbiol. 64, 479.

ZoBell C.E., Oppenheimer, C.H., 1950. Some effects of hydrostatic pressure on the multiplication and morphology of marine bacteria. J. Bacteriol. 60, 771-781.

Zuendorf, A., Bunge, J., Behnke, A., Barger, K. J.-A., Stoeck, T., 2006. Diversity estimates of microeukaryotes below the chemocline of the anoxic Mariager Fjord, Denmark. FEMS Microbiol. Ecol., 58, 476-491.

VITA

Danielle Morgan-Smith
Old Dominion University
Department of Ocean, Earth and Atmospheric Sciences
4600 Elkhorn Ave
Norfolk, VA 23529

Education

PhD in Oceanography, Old Dominion University, pending
Concentration: Biological Oceanography
Advisor: Dr. Alexander Bochdansky
Master of Science in Earth and Ocean Sciences, Old Dominion University, May 2008
Concentration: Biological Oceanography
Advisor: Dr. Alexander Bochdansky
Bachelor of Science, College of William and Mary, December 2005, Cum Laude
Majors: Biology, Environmental Science

Publications

Morgan-Smith, D., Herndl, G.J., van Aken, H.M., Bochdansky, A.B., 2011. Abundance of eukaryotic microbes in the deep subtropical North Atlantic. Aquat. Microb. Ecol. 65, 103-115.

Selected conference contributions

American Society of Limnology and Oceanography 2011 Aquatic Sciences Meeting
"High pressure, low-temperature incubations of the flagellate *Cafeteria roenbergensis* (Chromista, Bicosoecales)", Morgan-Smith, D., Garrison, C., Bochdansky, A.B., February 14, 2011 (Oral)
American Society of Limnology and Oceanography 2009 Aquatic Sciences Meeting
"Basin-scale distribution of certain bacterivorous and saprotrophic eukaryotic microbes in the deep tropical Atlantic", Morgan-Smith, D., Bochdansky, A.B., van Aken, H.M., Herndl, G.J. January 29, 2009. (Oral)
American Society of Limnology and Oceanography 2008 Ocean Sciences Meeting
"Quantification and characterization of deep-sea eukaryotic communities based on morphology and fluorescence in situ hybridization with a robotic microscope", Morgan-Smith, D., Bochdansky, A.B., Herndl, G.J., Van Aken, H.M.. March 7, 2008. (Oral)
International Symposium on Microbial Ecology 2010 "Abundance and diversity of eukaryotic microbes in the deep Atlantic including the Romanche Fracture Zone", Morgan-Smith, D., Clouse, M., Bochdansky, A.B., Herndl, G J, Van Aken, H.M. August 22 - 27 2010. (Poster)